IS FGF1 ACTING AS A PROMOTER OF REMYELINATION IN PERIPHERAL NERVOUS SYSTEM?

by

Nazmiye Özkan

B.S., Molecular Biology and Genetics, Boğaziçi University, 2015

Submitted to the Institute for Graduate Studies in
Science and Engineering in partial fulfilment of
the requirements for the degrees of
Master of Science

Graduate Program in Molecular Biology and Genetics
Boğaziçi University
2018

To my family …

ACKNOWLEDGEMENTS

I would like to express my sincere gratitude to my thesis supervisor Esra Battaloğlu for her great support, guidance, encouragement and patience throughout the study. She is very kind and insightful and I feel very lucky for being her student. I would like to thank Assoc. Prof. Arzu Çelik and Assist. Prof. Aslı Kumbasar for allocating their time to evaluate my thesis.

I am very grateful to my lab members Burçak Özeş and Ayşe Candayan for helping me to survive in this department. Though they focused on different projects, they were always ready to help when I have a problem or question in my project. I am thankful to them for sharing their precious experiences and knowledge with me. I am very grateful to Aslı Uğurlu for her valuable friendship and great guidance. She devoted her time to teach me almost every laboratory techniques I know and she was always ready to help when I have a problem. I am very lucky to have great friends Ceren Saygı, Seden Tezel, Harun Niron, Beren Aylan, Tuğberk Kaya and Oğuz Arı. I would like to thank to my best friends Yunus Altunocak, Merve Peker, Sıla Rızalar, Dicle Söylemez, Olcay Kırdemir, Maral Budak for their support and helps that pushed me to go on every time I was in trouble. I am thankful to Arzu Temizyürek, Leyla Dikmedaş and Ersin Eruz for taking care of my animals and helping me during the injections.

I would like to express my deepest appreciation to Carla Taveggia and her precious lab members for sharing their facility with me to perform my experiments. I am grateful to Marta Pellegatta for her helps, guidance and patience during my stay in Italy. I am glad that I have a chance to take her opinion about my project and her valuable guidance for Co-IP. I feel very lucky to have my dear friend Maria Concetta Cariello who devoted her time to help me in almost every experiments. I am also thankful to her for her great support and valuable friendship. I would like to thank Maria Grazie Forese for her great friendship and guidance during my study. I am also grateful to Rosa La Marca, Chiara Raffaele, Paolo Canevazzi and Amelia Trimarco for their great support.

I would like to express my deepest gratitude to my beloved family for their support and encouragement during my life. I am grateful to have such wonderful and amazing niece Duru Ilgın Elçin.

This study was supported by Boğaziçi University Research Fund (BAP11940). I would like to thank The Scientific and Technological Research Council of Turkey (TÜBİTAK-215S883) to support me financially during my study.

ABSTRACT

IS FGF1 ACTING AS A PROMOTER OF REMYELINATION IN PERIPHERAL NERVOUS SYSTEM?

Bidirectional and continuous communication between Schwann cells (SCs) and axons are crucial for peripheral nervous system (PNS) myelin development, maintenance, and repair after injury. Disruption of SCs-axon interaction leads to peripheral neuropathies, therefore, elucidating the molecular mechanisms underlying this interaction is highly important for understanding the etiology of these disorders. FGF1 was suggested to act in peripheral myelination and remyelination by our previous findings. To study remyelination in mouse sciatic nerve, 'LPC induced demyelination' model was optimized in another study. In this study, myelin sheath was visualized by immuno-staining and the expression of myelin proteins were analyzed by western blot analysis at different time periods up to three months after LPC injections. The recovery of myelin sheath was shown at three months and accordingly, the level of myelin proteins, MAG and MBP, reached to that of the control group. In the second part of the study, FGF1 involvement in remyelination was further confirmed by FGF1 injections after LPC induced demyelination. The expression of myelin proteins increased significantly 30 minutes after FGF1 injection and reached to the same level with that of the control group in seven days' time. This observation showed that FGF1 has short term and rapid effects on remyelination, in accordance with the literature. In the last part of the study, the possible interaction partners of FGF1 during peripheral myelination was investigated using dorsal root ganglia co-cultures and precipitating their lysates with Co-IP method. After confirmation of expression of FGF1 protein in DRG co-cultures, its interaction with FGFR1 and MPZ was investigated. FGFR1-FGF1 and MPZ-FGF1 interactions were observed when the precipitates were analyzed by western blot. However, results remained inconclusive due to weak signals that were also observed in control groups. In summary, we have shown that 'LPC induced demyelination' model can be used for further analysis as a PNS demyelinating disease model. FGF1 involvement in remyelination was also confirmed. The results from analysis of Co-IP remained elusive that needs of further investigation.

ÖZET

FGF1 PERİFERİK SİNİR SİSTEMİ'NİN REMİYELİZASYONUNDA PROMOTOR OLARAK GÖREV ALIYOR MU?

Schwann hücreleri (SH) ve aksonlar arasındaki çift yönlü ve sürekli iletişim periferik sinir sistemindeki (PSS) miyelin tabakasının gelişimi, bakımı ve yaralanma sonrası onarımı için önemlidir. SH-akson etkileşiminin bozulması periferik nöropatilere yol açar ve bu etkileşimin altında yatan moleküler mekanizmaların aydınlatılması demiyelizan hastalıkların etiyolojisinin anlaşılması için önemlidir. Daha önceki bulgularımız ışığında FGF1'in PSS'de miyelizasyonda ve LPC ile indüklenen demiyelizasyon sonrası gerçekleşen remiyelizasyonda rol alabileceği savlandı. Bu çalışmada, remyelinasyon sürecini *in vivo* inceleyebilmek amacıyla fare siyatik sinirinde "LPC enjeksiyonu ile indüklenen demiyelizasyon" modeli optimize edildi. LPC enjeksiyonlarından sonra farklı zaman aralıklarında myelin kılıf immün-boyama ile ve myelin proteinlerinin anlatımı western yöntemi ile incelendi. Üçüncü ayda myelin kılıfın geri kazanıldığı ve miyelin protein düzeylerinin normale yaklaştığı gösterildi. Çalışmamızın ikinci kısmında, LPC ile indüklenen demiyelizasyon sonrasında yapılan FGF1 enjeksiyon deneyleri ile FGF1'in remiyelizasyonda görev aldığı bulgusu doğrulandı. Miyelin proteinlerinin anlatımı, FGF1 enjeksiyonundan 30 dakika sonra önemli ölçüde arttı ve yedi gün içerisinde kontrol grubu ile eşitlendi. Bu sonuçlar, literatür ile uyumlu olarak FGF1'in remiyelizasyon üzerinde hızlı ve geçici bir etkisi olduğunu gösterdi. Çalışmanın son aşamasında, periferik miyelizasyon sırasında FGF1 ile etkileşebilecek olası proteinleri belirleyebilmek amacıyla, dorsal kök gangliyon ko-kültürü oluşturuldu ve lizatları Co-IP yöntemi kullanılarak incelendi. Öncelikle FGF1 protein üretimi DRG lizatlarında doğrulandı ve FGFR1 ve MPZ ile olası etkileşimi incelendi. Co-IP lizatları western blot ile incelendiğinde, FGF1'in FGFR1 ve MPZ ile etkileştiği gözlendi. Ancak kontrol gruplarında etkileşimin zayıf da olsa görülmesi nedeni ile bu etkileşimler doğrulanamadı. Bu sonuçlar "LPC kaynaklı demiyelizasyon" modelinin bir PSS demiyelizan hastalık modeli olarak kullanılabileceğini gösterdi ve FGF1'in remiyelizasyonda rol alabileceğine dair ileri kanıt sağladı. Bu süreçte FGF1'in, FGFR1 ve MPZ ile etkileştiğinin doğrulanması için ileri analizlerin gerekliliği gösterildi.

TABLE OF CONTENTS

LIST OF FIGURES

LIST OF TABLES

LIST OF ACRONYMS/ABBREVIATIONS

7TM	Seven Transmembrane
ADAM	Disintegrin and Metalloproteinase Domain-Containing Protein
AKT	Serine/Threonine Kinase 1
APS	Ammonium Peroxodisulphate
ATP	Adenosine Triphosphate
BACE-1	Beta-secretase 1
Brn-2	Brain-2
BSA	Bovine Serum Albumin
cAMP	Cyclic Adenosine Monophosphate
CCP	Caudal Cerebellar Peduncle
CMT	Charcot Marie Tooth
CNS	Central Nervous System
Co-IP	Co-immunoprecipitation
DABCO	1,4-Diazabicyclo[2.2.2]octane, 98%
DAPI	Diaminophenylindolamine
DM-20	Myelin Proteolipid Protein
DMEM	Dulbecco's Modified Eagle's Medium
DOC	Deoxycholic Acid
DRG	Dorsal Root Ganglion
DTT	1,4-Dithiothreitol
E13.5	Embryonic day 13.5
EAN	Experimental Allergic Neuritis
ECM	Extracellular Matrix
EDTA	Ethylenediaminetetraacetic Acid
EGF like	Early Growth Factor Like
ErbB2/3	Huma Epidermal Growth Factor Receptor 2/3
ERK	Extracellular Regulated Kinase
EtBr	Ethidium Bromide
FBS	Fetal Bovine Serum

FGF	Fibroblast Growth Factor
FGFR	Fibroblast Growth Factor Receptor
ga	Gauge
GPCR	G Protein Coupled Receptor
GPR126	G Protein 126
HBSS	Hank's Balanced Salt Solution
HCl	Hydrochloric Acid
HDAC	Histone deacetylase
HNPP	Hereditary Neuropathy with Liability to Pressure Palsies
HPSG	Heparan Sulfate Proteoglycans
HRP	Horseradish Peroxidase
Ig like	Immunoglobulin like
Jnk	c-Jun N-terminal Kinase
kD	Kilodalton
Krox-20	Early Growth Response Protein 2
Lgi4	Leucine-rich Repeat LGI Family Member 4
LPC	Lysolecithin
MAG	Myelin Associated Glycoprotein
MAPK	Mitogen-Activated Protein Kinase
MBP	Myelin Basic Protein
Mek	MAPK/ERK Kinase
MEM	Minimum Essential Medium
mg	Milligram
ml	Milliliter
MOG	Myelin Oligodendrocyte Glycoprotein
MPZ	Myelin Protein Zero
MS	Multiple Sclerosis
mTOR	Mechanistic Target Of Rapamycin Kinase
mTORC1	Mammalian Target of Rapamycin Complex 1
NaCl	Sodium Chloride
NB	Neurobasal
NF-200	Neurofilament 200
NFkB	Nuclear Factor NF-kappa-B

NGF	Nerve Growth Factor
NICD	Intracellular Component- Notch Intracellular Domain
NMJ	Neuromuscular Junction
Notch1	Neurogenic Locus Notch Homolog Protein 1
NP-40	Nonidet P40
NRG-1	Neuregulin-1
Oct-6	Octamer Binding Factor 6
OPC	Oligodendrocyte Precursor
P0	Myelin Protein Zero
P2	Protein 2
PBS	Phosphate Buffered Saline
PDK1	Pyruvate Dehydrogenase Kinase 1
PFA	Paraformaldehyde
PGD2	Prostaglandin D2 Synthase
PI-3 kinase	Phosphoinositide 3-kinase
PKA	Protein Kinase A
PLL	Poly-L-lysine
PLP	Proteolipid Protein
PMP-22	Peripheral Myelin Protein-22
PNS	Peripheral Nervous System
Ptdlns	Phosphatidylinositol
PTEN	Phosphatase and Tensin Homolog
Raf	Raf-1 Proto-Oncogene, Serine/Threonine Kinase
RIPA buffer	Radioimmunoprecipitation Assay Buffer
RNA	Ribo Nucleic Acid
SC	Schwann Cell
SCP	Schwann Cell Precursor
SDS	Sodium Dodecyl Sulfate
Sox	SRY-related HMG-box Gene
STAT3	Signal Transducer and Activator of Transcription 3
TACE	ADAM 14-like Protease
TAM receptor	Tyro3, Axl, Mer Receptor
TBS	Tris-buffered Saline

TBS-T	Tris-buffered Saline with Tween-20
TEMED	Tetramethylethylenediamine
µg	Microgram
µl	Microliter
µm	Micrometer

1. INTRODUCTION

1.1. Myelin Sheath

Myelination is a remarkable process which is one of the evolutionary trademarks of the nervous system. Insulating axons with myelin enables the nervous system to perform its motor, cognitive, and sensory functions which require fast and rapid impulse conduction (Taveggia, 2016).

1.1.1. Function of Myelin Sheath

In unmyelinated axons, the impulse can be transmitted through the fiber in a way of continuous sequential manner which means action potential can depolarize the adjacent plasma membrane with a local circuit of an ion flow. High lipid containing myelin sheath can act as an electrical insulator which directs the propagation of action potentials to the Nodes of Ranvier (Morell *et al.*, 1999). Myelin sheath restrict the excitable plasma membrane only at the Node of Ranvier where myelin is absent and ionic channels and Na^+/K^+ pumps are enriched (Waxmann *et al.*, 1993). When an impulse depolarizes the membrane at the Node of Ranvier, the ion flow cannot be propagated and the adjacent myelinated plasma membrane cannot be depolarized. The ion conduction should be carried into the next node that is about 1 mm away. This allows for rapid and fast transmission of impulses known as saltatory conduction. Saltatory conduction in the presence of myelin sheath is an outstanding adaptation for vertebrates. Spiral wrapping of axons with myelin increases the velocity of current through the axons since the current jumps from one node to the next. Since axons of peripheral neurons are long the nerve conduction velocity is highly important. This phenomenon is depicted in Figure 1.1.

The myelin sheath can also provide trophic support for the axon that it enwraps. It can mechanically protect the axons from environmental stress and damage. Also, it can provide nutritional support to the axon-specifically to axonal parts distant from their neuronal body.

Myelin sheath may also help to reduce the energy consumption during the maintenance of resting potentials. The myelin sheath reduces energy consumption by restricting the action potentials to the Node of Ranvier. In the presence of myelin sheath a small number of ATP dependent Na^+/K^+ pumps can maintain ionic balance across the membrane. However, the energy required for myelin production and its maintenance is much higher than the amount of the energy saved by myelin during resting potential (Nave *et al.*, 2014).

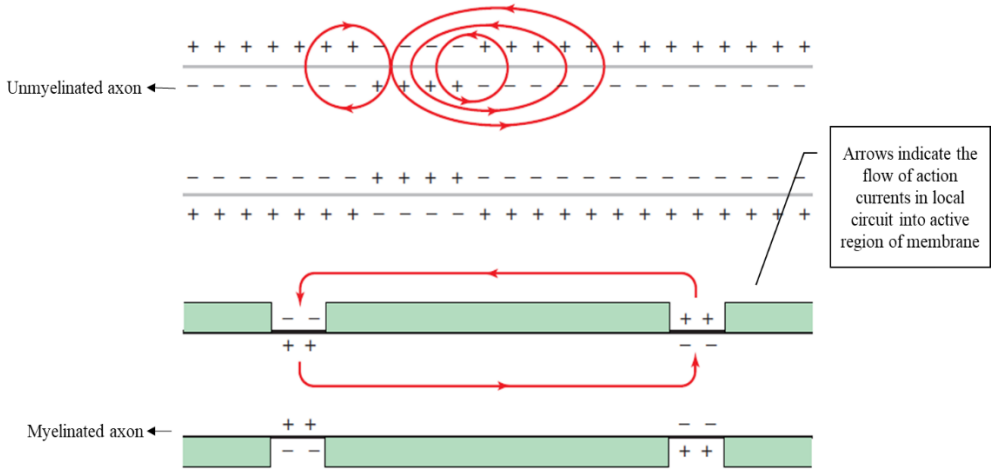

Figure 1.1. Conduction of electrical impulses in unmyelinated versus myelinated fiber (modified from Morell *et al.*, 1999).

1.1.2. Structure of The Myelin Sheath

Unlike other biological membranes, the myelin sheath contains a high lipid to protein ratio. Lipids constitute 70 to 75% of myelin sheath which has an unusual ratio of 2:2:1:1 for cholesterol, phospholipids, galactolipids and plasmogens (Norton *et al.*, 1973; Morell *et al.*, 1996). Cerebroside is one of the core lipids of myelin for which the amount is proportional to that of myelin. It was thought to be an essential lipid for myelin formation, however, knock out mice that lack cerebroside show normal myelin with minor changes in structure and reduced conduction velocity. This observation implicates that cerebroside is not a core unit for myelin formation, but plays important roles in stability and insulation (Jahn *et al.*, 2009).

Cholesterol is another major lipid found in myelin. Lipids of myelin sheath have high lateral mobility; however, high cholesterol content become a limitation factor for the membrane fluidity that eventually, influence intracellular trafficking and compartmentalization. The lipid composition of peripheral myelin and central myelin are qualitatively similar, but vary quantitatively.

CNS myelin proteins are composed of proteolipid protein (PLP) and DM-20 that are produced by alternative splicing of RNA encoded by the PLP gene, myelin oligodendrocyte glycoprotein (MOG), myelin basic protein (MBP) and myelin associated glycoprotein (MAG). While MOG, PLP and DM-20 proteins are unique to CNS myelin, MBP and MAG are common proteins for both CNS and PNS myelin (Gardinier *et al.*, 1992).

In PNS myelin, P_0 protein is the core unit that constitutes more than half of the PNS myelin protein. The molecular weight of P_0 is 30 kDa and it is composed of 220 amino acids. It has one intracellular domain, one hydrophobic transmembrane domain and one Ig like extracellular domain. The N terminal extracellular domain has signal sequences for its insertion to the membrane and a site for glycosylation. P_0 has other posttranslational modifications such as phosphorylation, sulfation and acylation. It undergoes homophilic binding with extracellular domains of other P_0 proteins and projects as a tetramer from the membrane that is responsible for cell-cell interaction. The transfection of this protein into non-neuronal cells increases their ability of adhesion and cell-cell interactions (D'Urso *et al.*, 1990; Filbin *et al.*, 1990). When PLP and P_0 proteins are compared, they show differences in sequences, structures and posttranslational modifications. However, PLP and P_0 proteins have similar roles in the formation of myelin in CNS and PNS, respectively.

Myelin basic protein (MBP) is another major protein for PNS myelin. The amount of MBP can vary among species from 5% to 18%. As in CNS myelin, MBP has 4 different isoforms in PNS that are produced by alternative splicing. Rodents have 14 kDa, 17 kDa, 18.5 kDa and 21.5 kDa MBP isoforms while in human the 17.2 kDa isoform replaces the 17 kDa MBP. MBP is located in the major dense lines that occupy the cytoplasmic face of the myelin (DesJardins *et al.*, 1983). The most prominent form of MBP in adult rodent is the 14 kDa isoform that is referred as 'P_r' in the PNS nomenclature. MBP has an important function in both production of the PNS myelin and its maintenance.

Another positively charged PNS myelin component is P_2 protein. The amount of this protein varies among species. Thicker myelin sheath seems to have more P_2 protein than thinner myelin sheath within species. The role of P_2 in myelin is still in question. There is a similarity in structure of P_2 protein with cytoplasmic binding protein. Therefore, P_2 may have a function in lipid assembly and lipid turnover of myelin. It is considered as one of the PNS myelin components, but P_2 is also expressed in CNS in small quantities. P_2 is an antigen which is injected to induce experimental allergic neuritis (EAN).

Peripheral myelin protein-22 (PMP-22) is a glycoprotein that constitute 5% of PNS myelin. It is named after its molecular weight and found in minor quantities in myelin. It is suggested that PMP-22 doesn't have a major structural role but may affect myelin assembly or maintenance. Its duplication and nucleotide changes cause Charcot Marie Tooth (CMT) disease. CMT is a genetically heterogeneous inherited neuropathy that is associated with at least 80 genes. The symptoms vary among patients but it is characterized by distal muscle weakness, sensory loss and atrophy. PMP-22 gene duplication can cause CMT1A while its deletion causes Hereditary Neuropathy with Liability to Pressure Palsies (HNPP). Point mutation of PMP-22 gene can lead to both CMT1A or HNPP.

MAG that is a 100 kDa protein with a single transmembrane domain is an essential protein for PNS myelin with a role in transmitting signals from axons to Schwann cells and vice versa to maintain the myelin sheath. N terminal domain that is heavily glycosylated is separated from the C terminal domain by a single transmembrane domain. L-MAG and S-MAG are two known isoform of MAG that are produced by alternative splicing. The protein is localized in the periaxonal membrane of myelinating Schwann cells like in CNS (Eichberg *et al.*, 1996; Quarles, 1997). But, it is also found in Schwann cell membranes at Schmidt-Lantermann incisures, paranodal loops and outer mesaxon. Its localization suggests that MAG may be required for interaction between adjacent Schwann cells. Although S-MAG and L-MAG are found in PNS myelin, the most common isoform is S-MAG (Morell *et al.*, 1999).

Schmidt-Lentermann clefts that contain cytoplasm of Schwann cells or glial cells are localized at the cytoplasmic face of the myelin sheath. The myelin sheath does not produce a major dense line in these regions. Schmidt-Lantermann clefts are common in PNS myelin,

but are rarely seen in CNS. The summary of the protein composition of the myelin sheath in CNS and PNS is given in Figure 1.2.

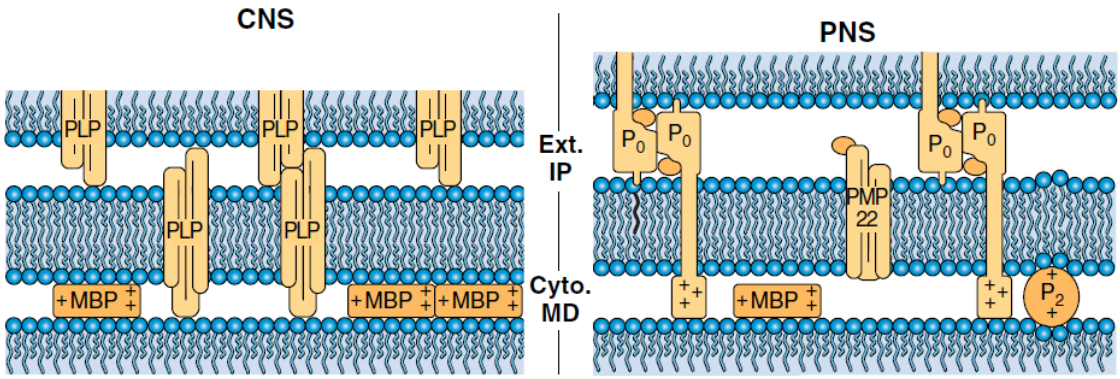

Figure 1.2. Protein composition of myelin sheath in CNS and PNS (Morell *et al.*, 1999).

1.1.3. Myelinating Cells

Glial cells are non-neuronal cells that outnumber the nerve cells with a ratio of 3:1. Myelin sheath are produced by Schwann cells in PNS and oligodendrocytes in CNS. In CNS, oligodendrocyte can produce myelin sheath for 30-40 axons while in PNS, each Schwann cell can wrap around and form myelin for only one segment of an axon. Therefore, mechanisms that oligodendrocyte and Schwann cells use to insulate the axon differ (Jessen *et al.*, 2004).

In the following sections, Schwann cells and their development will be mentioned explicitly.

1.2. Schwann Cells and Their Development

The SC lineage during development is summarized in Figure 1.3.

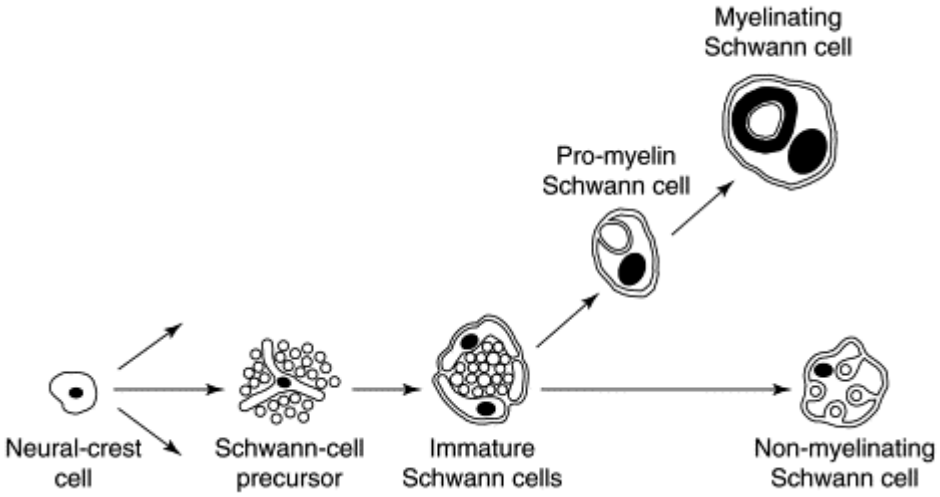

Figure 1.3. Schwann cells lineage (Jessen *et al.*, 1999).

Schwann cells (SCs) are derived from neural crest cells that arise from the dorsal region of the neural tube. They become highly migratory and proliferative when they scatter throughout the embryo after stratification. The multipotent nature of neural crest cells allows them to produce an outstanding variety of cell types such as melanocytes, glial cells and neurons of PNS (Theveneau *et al.*, 2012, Dong *et al.*, 1995, Ledouari *et al.*, 1974).

Neural crest cells are transformed to Schwann cell precursors that are also proliferative and migratory like their ancestors (Smith *et al.*, 1993). Sox10 is expressed by neural crest cells and is an important transcription factor that is involved in this transition. Its expression ceases in neurons while PNS glia persist to express Sox10 (Woodhoo *et al.*, 2009). Neuregulin-1 (NRG-1) is another molecule that restrain neuronal differentiation and improve glial specification (Shah *et al.*, 1994).

SC precursors co-migrate with axons to provide axonal survival signals. When SC precursors stop migrating, they develop into immature SCs that are proliferative but not migratory (Newbern, 2015). Notch signaling has been considered as an important regulator for this transition even though the exact underlying molecular mechanism has not been elucidated so far (Woodhoo *et al.*, 2009).

Immature SCs have two important roles in nerve biogenesis; they are required for radial sorting and signaling to their surrounding perineurial cells and others for their differentiation. Radial sorting helps immature SCs to establish proper relationship with axons for further differentiation. Immature SCs can be associated with large caliber axons that are myelinated or with small diameter axons that will remain as non-myelinated Remak bundles. This process starts perinatally and persists until post-natal day 10 in rodents.

Radial sorting enables immature SCs to form proper 1:1 axon- SC interaction that is the ultimate way for transition of promyelinating SCs to myelinating SCs. The molecular mechanisms that govern SC proliferation, SC development, radial sorting, axon-SC interaction and myelination have been investigated for centuries to reveal the most important regulators and their action mode. Studies after the middle of 1970s showed the importance of axonal and glial factors in these processes. These factors are explained explicitly under the following sections.

Motor nerve terminals at neuromuscular junctions (NMJs), C fiber nociceptors, post-ganglionic parasympathetic and sympathetic fibers are non-myelinated fibers in PNS. Remak SCs can gather more than one axon together into a fiber and form basal lamina, thus, ensheath more than one axon to form Remak bundles. Unlike myelinating SCs, Remak bundles reside along the axon very closely. Recent exciting studies propose that Remak SCs may have a role in sustaining trophic support for axon (Monk *et al.*, 2015).

1.3. Peripheral Neuropathy Related to Myelin Sheath and Regeneration

Myelin sheath holds an essential task for the nervous system to transmit both sensory and motor impulses in a rapid fashion. Damage to myelin sheath lead to enormous destruction in maintenance of both peripheral and central nervous system which in turn lead to various severe symptoms in patients. Demyelinating and dysmyelinating diseases are common peripheral neuropathies caused by trauma in the myelin sheath.

1.3.1. Dysmyelinating Disease- Leukodystrophy

In dysmyelinating diseases, there is a failure to generate myelin normally. It is associated with a genetic defect that impairs stability or turnover of the myelin sheath. Leukodystrophy is an inherited dysmyelinating disease caused by a lysosomal or perixosomal enzyme deficiency. Abnormal myelin production, turnover and maintenance caused by enzymatic deficiency lead to destruction of white matter with or without involvement of peripheral nerves. This progressive and lethal disease has early onset (Vanderver *et al.*, 2014).

1.3.2. Demyelinating Disease- Multiple Sclerosis (MS) in CNS and Charcot Marie Tooth (CMT) in PNS

Demyelinating disease is defined as destruction of myelinating cells-oligodendrocytes and Schwann cells in CNS and PNS respectively- or damage to the myelin sheath itself. Demyelinating disease should be distinguished from dysmyelinating disease that is caused by a damage during formation of the myelin sheath. Though it is hard to differentiate these diseases for clinicians.

Myelin loss results in axonal atrophy since the axon loses its protective shield. In those cases, myelin is lost primarily and axonal loss occurs secondarily. In some diseases, however, myelin loss is secondary to axonal loss (Mehndiratta *et al.*, 2014).

Demyelination has two important effects on nerves; it slows down the conduction velocity through the nerve and blocks conduction because of mismatch in resistance between unmyelinated and myelinated regions. In the absence of the myelin sheath, conduction area gets larger and hinders the conduction velocity.

The second effect of demyelination is conduction blockage. Demyelination increases the area for current flow which in turn lower current density and resistance. After all, capacitance increases and impairs membrane potential.

The most common CNS demyelinating disease is Multiple Sclerosis (MS) which is characterized by white matter lesions where myelin is damaged. The disease falls into a category of autoimmune neuropathy in which multiple genetic and environmental factors are involved. Autoimmune dysregulation targets myelin sheath that leads to demyelination. In the early phase of MS, remyelination takes place where the myelin sheath is recovered by repair cells, however, myelin break down takes place faster than the recovery. It is followed by axonal loss.

The most common PNS demyelinating disease in Charcot Marie Tooth (CMT) which is defined by chronic motor and sensory loss. CMT is a genetically heterogenous disease for which more than 80 causative genes have been identified. CMT can be inherited in autosomal recessive, autosomal dominant or X-linked manner. CMT1 is the demyelinating form while CMT2 is the axonal form (Love, 2006).

1.3.3. Myelin Recovery After Demyelination

Bidirectional and continuous communication between Schwann cells and axon is essential for myelin formation, PNS maintenance, and repair after injury. The extrinsic and intrinsic factors involved in this remarkable interaction were explained in Section 1.4.

When there is a damage to the myelin sheath, it causes demyelination. At this stage, signals that are secreted from SCs and axons to maintain the stability of myelin should be silenced to achieve successful regeneration. After nerve injury, mature SCs form repair cells in order to remove myelin debris and form regenerative tracks which in turn guide axons for successful regeneration. These repair cells have some common abilities with immature SCs in the developmental lineage and start to activate the expression of immature SC genes. But, they also start to express some injury related genes to promote successful nerve repair. In older reviews, these SCs have been called de-differentiated SCs. However, the mechanism that governs this transition is not passive induction of injury related genes. That is why these cells are now called trans-differentiated SCs (Jessen *et al.,* 2015). One of the injury related genes that is expressed by trans-differentiated SCs is c-jun. Activation of c-jun opposes the activity of Krox20 and inhibits myelination. It is indispensable for the repair SCs to form Bands of Büngner and provides efficient support to the neurons after injury. The inhibition

of myelination at the early phase of remyelination is needed for proper regeneration (Quintes *et al.*, 2017).

The morphological changes during transition of Schwann cells to repair cells have been shown by Jose and his colleagues. Remak and mature myelinating SCs become elongated and extend their branches to form Büngner bands which guide axon during regeneration. Morphological analysis show that during regeneration, repair SCs become shortened to become mature SCs and induce myelination successfully (Gomez-Sanchez *et al.*, 2017). During recovery, SCs recruit macrophages that mediate autophagy to remove myelin debris. Rapid clearance of myelin debris is part of the remarkable regeneration capacity of PNS. A recent study showed that SCs not only use the autophagy to remove myelin debris, but also recruit TAM receptor-mediated phagocytosis pathway molecules (Brosius Lutz *et al.*, 2017). The mechanism of myelin removal is important to design a possible therapy for both CNS and PNS neuropathy associated with myelin damage.

1.4. Schwann Cells-Axon Interaction

During development, maintenance of PNS myelin, and recovery after injury, myelinating SCs and axons generate a solid assembly in which they talk to each other by reciprocal exchange of signals to organize each other's phenotype.

Throughout SC lineage, axons send signals to SCs to promote their proliferation, survival, differentiation and myelin formation. During development, SCs send signals to their target axons to provide trophic support and to control components of axolemma and diameter of axons. In the course of adulthood, mature myelinating SCs enable myelin maintenance and axolemmal organization stability while axons preserve glial differentiation and myelin integrity.

1.4.1. Axonal Signals in Developmental Myelination and Repair after Injury

In 1970s, cross-anastomosis studies revealed that neurons provide signals for myelination. In these studies, when myelinating neurons were cross anastomosed to non-

myelinating conditions, they became myelinated (Aguayo *et al.*, 1976; Weinberg *et al.*, 1975). Axonal signals that govern myelination and repair after injury are explained below.

Conditional ablation studies discovered one of the most essential pathways for myelination which is NRG1-ErbB2/3 signaling. The NRG1 family of growth factors are expressed in axons as transmembrane protein which can be cleaved from the membrane by α and β secretases. NRG1 has 3 different isoforms- Nrg1 type I-III and all have epidermal growth factor (EGF)-like signalling domains in their extracellular part. The EGF-like domain enables NRG1 isoforms to bind their heteromeric ErbB2-3 receptors which are located in SCs membrane. The N terminal part of the EGF like signaling domain, however, shows some differences between isoforms and there is an additional extracellular domain in NRG1 type III. Therefore, proteolytic cleavage of NRG1 type I and type II enable these isoforms to become independent from the axonal membrane and act as soluble proteins, but NRG1 type III remains membrane bound and acts in a contact dependent pathway (Syed *et al.*, 2010, Newbern *et al.*, 2010). Carla and her colleagues revealed that the key axonal molecule that control PNS myelination is NRG1 type III. It regulates the amount of myelin that will be generated and determines the ensheatment fate of the axons. The fact that atypical expression of NRG1 type III in non-myelinated superior cervical ganglia neurons rescues the non-myelinating phenotype and induces myelination for those cells revealed that NRG1 type III is the core unit for PNS myelination. This growth factor is also involved in the formation of Remak bundles and Remak SCs. NRG1 is the main contributor for all the developmental stages in the SC lineage- neural crest cell migration, SCP differentiation, immature SC proliferation, mature myelinating SC and non-myelinating SC formation, and myelination. Post-translational modification is a way to regulate the activity of NRG1 protein family. The extracellular domains of the NRG1 proteins are cleaved by secretases. BACE-1 is a β secretase which is a positive regulator for myelination. The null mice in which BACE-1 is knocked out show hypomyelination and inability to recover myelin after injury. On the other hand, the cleavage by α secretase TACE or ADAM 17 which is a member of ADAM protein family inhibit myelination by acting as a negative regulator. BACE-1 and TACE secretases compete for the cleavage of NRG1 type III which balances the myelin formation and maintenance during the development and adulthood. ADAM 19 is another secretase that cleaves NRG1 type I which is upregulated upon axonal injury suggesting that NRG1 type I is involved in remyelination after injury. Although ADAM 19 can cleave

NRG1 type III too, the effect of this cleavage is not known. ADAM 10 can also cleave NRG1 type III which has been suggested as an indispensable positive regulator of PNS myelination. ADAM10 may induce the outgrowth of small fibers after injury. Γ secretases regulate the intra-membrane cleavage of NRG1 type III upon extracellular cleavage. It promotes the expression of prostaglandin D2 synthase in neurons. This enzyme catalyses the generation of PGD2 which in turn activates G protein coupled receptors (GPCRs) and downstream cascade. This signaling pathway eventually promotes myelination (Taveggia, 2016). NRG1 type II was always considered as an inhibitor of myelination unlike other isoforms. Soluble NRG1 type II binds and activates its cognate receptors as the positive regulators of myelination like NRG1 type III. The mechanisms that govern these differences have been under investigation. Recent study by Neeraja and her colleagues revealed that soluble form of NRG1 can act in a concentration dependent manner and has a bifunctional effect on SC myelination; high doses of soluble NRG1 type II and III inhibit myelination while their low doses promote myelination (Syed *et al.*, 2010).

Analysis to identify the claw paw mouse mutant genotype in that delayed onset of myelination of PNS was observed revealed an essential regulatory pathway in Schwann cell-axon interaction that involves Lgi4 and ADAM22. Lgi4 is a ligand expressed and secreted by Schwann cells that in turn acts on its cognate receptor- ADAM22 at the axonal membrane. ADAM22 does not have a secretase function but acts as a receptor for Lgi4 ligand. The conditional mutation or full ablation of ADAM22 and mutations in Lgi4 gene lead to a severe PNS phenotype- impaired axonal sorting and hypomyelination. The interaction between ADAM22 and Lgi4 ligand serve an important function in PNS myelination but, the action mechanism is not known (Monk *et al.*, 2015).

Notch1 is an essential regulator involved in Schwann cell-axon interaction that has a vital role in PNS myelin development and remyelination. Notch1 expressed on Schwann cells surface has four members. All of the members are type I transmembrane proteins that are cleaved by secretases. Intracellular cleavage by γ secretases produces an intracellular component- Notch intracellular domain (NICD) which in turn translocates to nucleus to promote gene expression. Notch1 can act in a canonical or non-canonical pathway depending on the type of ligands. In rodents, Nfiotch1 is located on Schwann cells while its ligand Jagged-1 can be found in both axons and Schwann cells. During SC development, Notch1

acts in canonical pathway to promote immature SC differentiation from SCPs. However, Notch1 acts as a negative regulator for the PNS myelination in the non-canonical pathway. Overexpression of Notch1 leads to a delay in onset of myelination and hypomyelination. It is vital to downregulate Notch1 expression with a transcription factor-EGR2 to promote the activity of the myelinating program. Interestingly, Notch1 is reactivated upon injury to cease myelination and allow for the production of repair SCs via the canonical pathway associated with RBPJ signals. The Notch1 signaling pathway is active during SC development and gets downregulated during myelination by a transcription factor. When there is an injury, the signaling pathway is reactivated in the repair SCs to stop myelination and allow for the process in demyelination. Regulation of Notch1 activity is therefore essential to drive developmental myelination and repair upon injury in PNS (Taveggia *et al.*, 2010). SC and axon interaction is summarized in Figure 1.4.

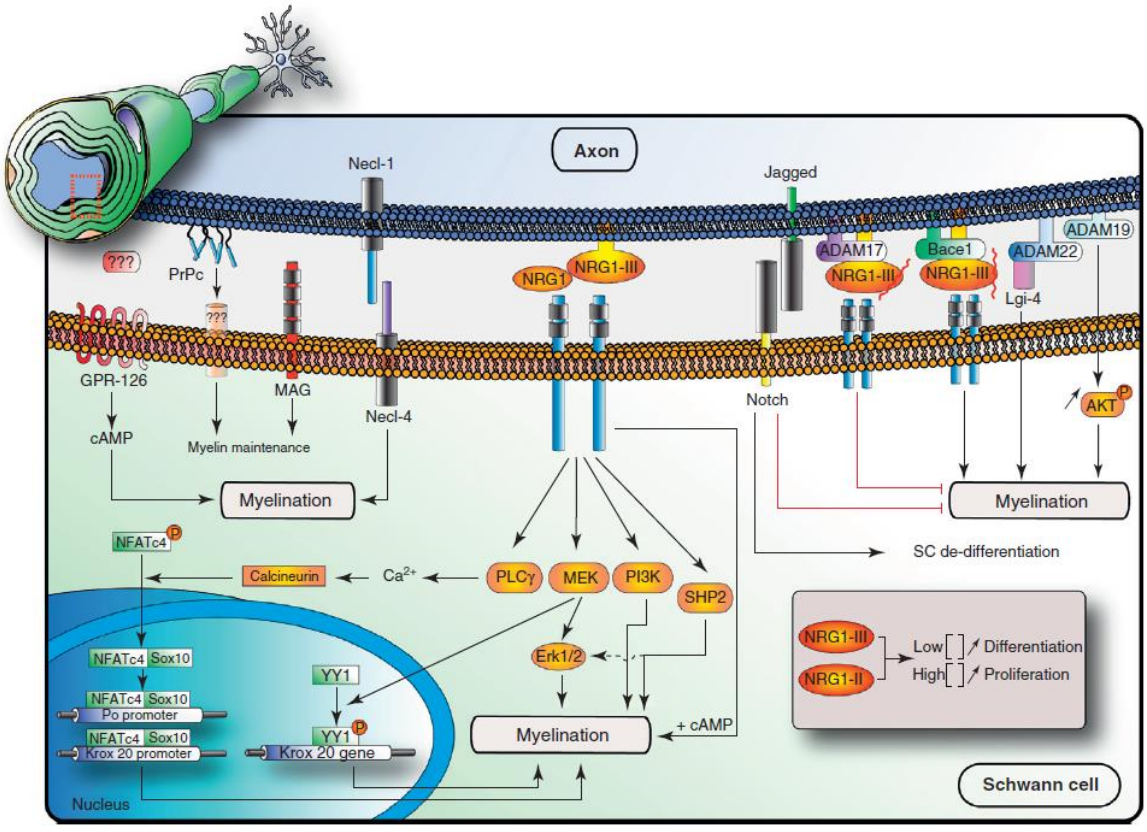

Figure 1.4. Continuous bidirectional communication between SCs and axon (Pereira *et al.*, 2012).

1.4.2. Glial Signals in Developmental Myelination and Repair After Injury

Extracellular matrix (ECM) components are essential regulators for radial sorting which enable SCs to segregate to axons destined to be myelinated. By governing radial sorting, ECM components enable SCs to make proper interactions with axons and in turn to myelinate. Mutations in Laminin 211,411 and Collagen XV lead to impairment in radial sorting which in turn impairs the myelination process. G protein coupled receptors also regulate radial sorting and act as a regulator for myelination as well as regeneration. GPCRs have conserved seven transmembrane (7TM) domain that can transduce signals via their heterotrimeric assembly. GPR126 is a positive regulator for PNS myelination which is needed to initiate myelination, but not necessary for myelin maintenance. GPR126 can integrate signals from abaxonal layer and increase cAMP levels in SCs that in turn elevate PKA levels (Taveggia, 2016).

1.4.3. Transcription Factors Involved in SC Myelination and Remyelination

The cascade of positive and negative transcriptional regulators involved in SC myelination and remyelination are well defined. Sox10 is the main transcriptional factor that is involved in both SC lineage development and myelination. Its expression starts in neural crest cells that in turn act in SCP differentiation and SC maturation. Sox10 can bind to a SC-specific enhancer which in turn activates octamer binding factor-6 (Oct-6). Sox 10, Oct-6, and related transcription factor brain-2 (Brn-2) form complexes and promote Krox20 gene expression. Krox20 is the master transcription factor required for PNS myelination. Sox2 is a negative regulator for PNS myelination and suppresses Krox20 to inhibit myelination (Parkinson *et al.*, 2008). Surprisingly, it was shown that Sox2 and Sox10 work together to activate myelin gene expression in SCs (Arter *et al.*, 2015).

NFkB is another positive transcription factor which is an indispensable regulator for developmental myelination. NRG1 activates this transcription factor that in turn stimulates Oct-6 and eventually Krox20.

The hippo signaling pathway has a conserved structure during evolution that has been indicated as a significant regulator for PNS myelination and regeneration upon injury (Parmantier *et al.*, 1993).

In addition to transcription factors, epigenetic regulators have roles in myelination and regeneration. Chromatin-remodeling complexes- HDAC1 and HDAC2 - are recruited by Sox10 via Oct6 activation. HDAC2 act as a positive factor to promote myelination while HDAC1 is responsible for SC survival (Jacob *et al.*, 2014). Transcriptional and epigenetic regulation mechanisms of SC-axon interactions during developmental myelination and repair after injury are summarized in Figure 1.5.

1.4.4. Signaling Pathways Involved in SC Myelination and Remyelination

Signaling pathways that govern the myelination and remyelination processes have been studied and well characterized. The majority of signaling pathways are induced upon NRG1 type III activation. The PI-3 kinase/AKT/mTOR pathway is one of the important signaling cascades involved in regulation of myelination and its maintenance. It can be activated by two different ligands; NRG1 type III and laminin. Laminin acts as a negative regulator of myelination. NRG1 promotes myelination via this pathway. PI-3 kinase phosphorylate PDK1 that in turn phosphorylates Ptdlns (4,5) to activate myelin formation. PDK1 activity was opposed by the action of PTEN which is a negative regulator of myelination. PTEN dephosphorylates Ptdlns(3,4,5)P3 to preserve the myelin sheath thickness at the correct rate. MTORC1 that acts as a downstream element of Ptdlns(3,4,5)P3 has been indicated as a positive regulator of PNS myelination by mutational analysis.

MAPK/ERK signaling is a regulator for both developmental myelination and remyelination after injury. Conditional ablation of ERK leads to hypomyelination and its overexpression causes hypermyelination. Recent studies revealed that constitutive activation of ERK can overcome the myelin growth arrest caused by ablation in NRG1/ErbB signaling. On the other hand, P38 MAPK acts as a negative regulator for PNS myelination. An imbalance between PI3 kinase and Map kinase signaling has been shown by using rat model of CMT1A.

Elevation of cAMP levels upon GPCR activation is another regulatory pathway for PNS myelination. Increased levels lead to SC myelination phenotype while low level is sustained in immature SCs. Downstream factors of cAMP signaling in SCs are Oct-6 and Krox20 that are the main transcription factors in PNS myelination (Monk *et al.*, 2015).

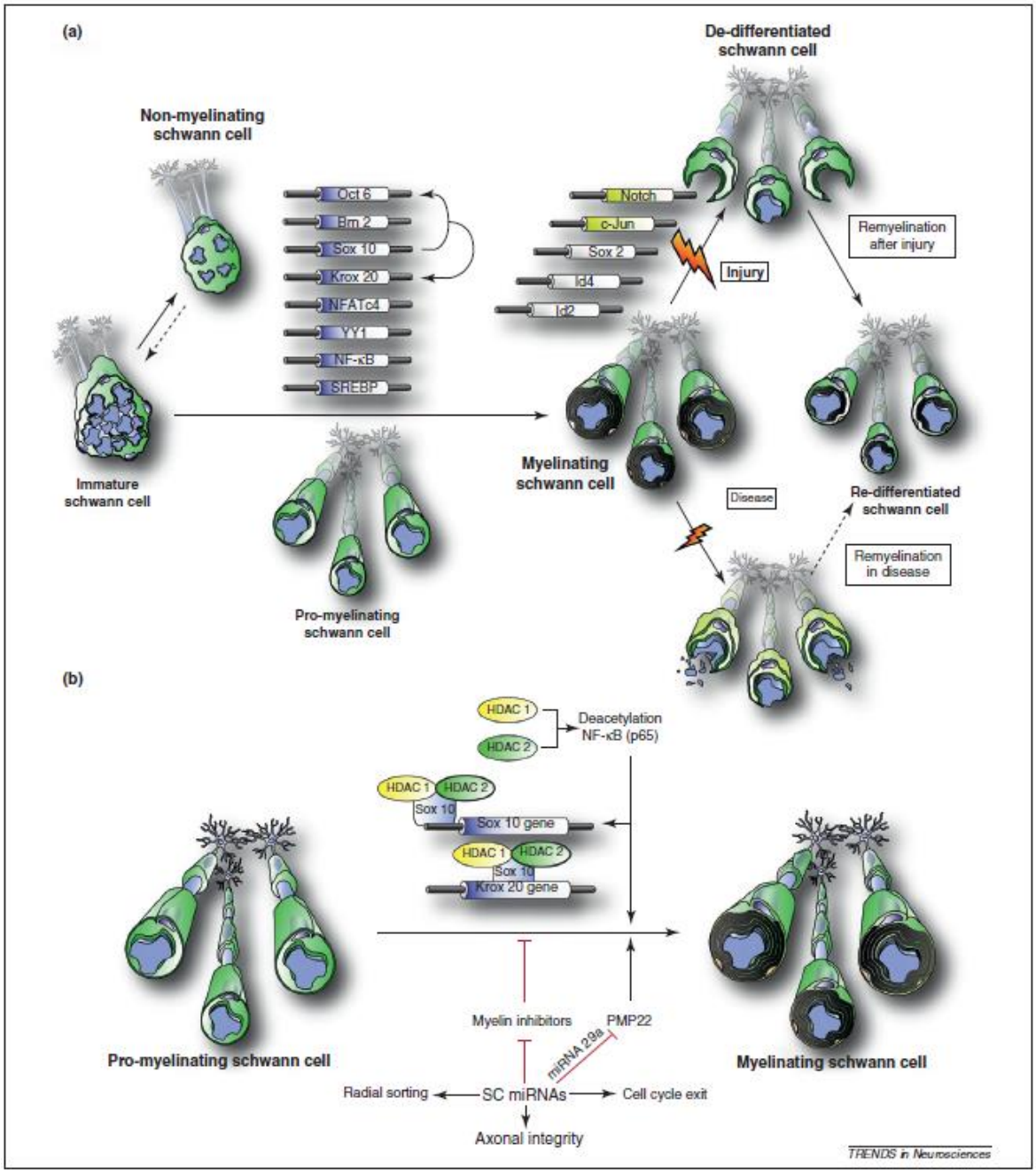

Figure 1.5. (a) Transcriptional regulation and (b) epigenetic involvement in SC-axon interaction during normal myelination and remyelination (Pereira *et al.*, 2012).

1.5. Chemically Induced Demyelination

There are several chemically induced demyelination models that have been used in pharmaceutical studies of demyelinating diseases. Cuprizone (bis-cyclohexanone oxaldihydrazone) has been widely used to induce central demyelination in mice and rats. Young adult mice can show demyelinating lesions throughout the white matter when they are exposed to cuprizone. Demyelination starts within 3 weeks after exposure to cuprizone diet and is completed within 5 weeks. Remyelination can be assessed within 4 weeks after replacing cuprizone with a normal diet. The time interval required for induction of demyelination and remyelination is very long for this chemical. The second chemical used to induce demyelination is ethidium bromide (EtBr). Demyelination can be induced by injecting 1% of EtBr into the spinal cord or the caudal cerebellar peduncle (CCP) of adult mice or rats. Even though demyelination starts within 48 hours upon injection, it may not be completed after 2 weeks based on the concentration of EtBr. Remyelination depends on the macrophages and microglia recruitment to digest myelin debris. The third chemical is lysolecithin (lysophosphatidylcholine) that was also used in our study and will be described in more detail in the next section.

1.5.1. Lysolecithin Induced Demyelination

Lysolecithin (LPC) is a derivative of phosphatidylcholine and a detergent that causes membrane solubilisation. It can induce demyelination upon injection. LPC is a widely used chemical to assess demyelinating lesions particularly in CNS. Demyelination is completed within 48 hours upon 1% LPC injection into the spinal cord or CCP. Generally axonal loss is at very low level after its injection. Macrophage and microglial cell recruitment is essential for remyelination as in case of other chemically induced demyelination models. Complete myelin debris removal and remyelination take place in seven days after injection and remyelination can be completed in one month after LPC injection into the spinal cord of adult mice or rat. Depending on the injected area, demyelination can still exist one month after injection. For CCP, remyelination takes place at a slower rate. LPC induced demyelination has been an extensively applied method in CNS since the time interval for demyelination and remyelination can be observed and the level of axonal damage is at low level while myelin damage and removal can be completely achieved (Merrill, 2008).

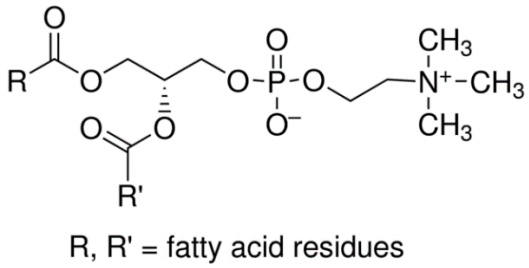

Figure 1.6. Chemical structure of LPC- R indicates fatty acid chain.

In PNS models, on the other hand, nerve transection or nerve crush methods are widely used to induce nerve degeneration. Unfortunately, in these models, not only myelin but also axonal damage has been observed. Besides, axonal damage is not primarily observed in most of the CMT cases, thus, nerve transection or crush method were not suitable for our studies that focus on understanding the role of FGFs and their receptors in myelin maintenance. We established the use of LPC, instead, to generate a PNS demyelination model.

1.6. Fibroblast Growth Factor

Fibroblast growth factor (FGF) family is composed of 22 structurally related polypeptides that can act through FGF receptors (FGFRs). FGFs are revealed to be involved in various cellular processes including cell proliferation, differentiation, normal development, wound healing, repair, tumorigenesis and metastasis. They have high binding affinity for heparan sulfate proteoglycans (HPSGs) and their analog heparin. This binding leads to a conformation change in FGF that affects the stability of the protein in the extracellular matrix (ECM). This interaction controls their binding to and activation of FGFRs. Either FGFRs can be attracted by multiple FGFs or they have affinity for only one specific FGF. This phenomena determines a cell's affinity for FGFs depending on the receptor type on it. FGFs are 30-50% similar on the amino acid sequence level and two cysteine residues are conserved among them (Galzie *et al.*, 1997). They have a N terminal signal peptide that helps FGF to be released from a certain cell and act on its receptors. FGF1 and FGF2 are also known as acidic and basic FGFs, respectively and do not have this N terminal signaling peptide. Therefore, they cannot be released from cells under normal physiological conditions. Damaged cells can secrete FGF1 and FGF2 under stress conditions

such as hypoxia, heat shock, serum starvation, or they can be released in a Golgi-endoplasmic reticulum independent fashion (Raju *et al.*, 2014). FGF1 was the protein of interest in our study since it has the highest RNA among other FGFs in PNS and our preliminary studies implicated its involvement in PNS myelination.

1.6.1. Fibroblast Growth Factor 1 (FGF1) and FGF1/FGFR Signaling System

Both *in vivo* and *in vitro* studies suggest involvement of FGF1 in neuronal differentiation and survival. FGF1 is widely expressed in the adult PNS and in CNS. It shows an increased expression during neuronal development. For example, neuronal layers of retina have different amount of FGF1 which shed light into the role of FGF1 in retinal development (Rodriguez-Enfedaque *et al.*, 2009). FGF1 can act through one of its four receptors-FGFR1, FGFR2, FGFR3 and FGFR4 in various cellular functions in autocrine, paracrine fashion or intacrine fashion. The binding of FGF1 to its receptor leads to activation and phosphorylation of these receptors which in turn activate downstream cascades in Ras/Raf/Mek/Erk, pi3k/Akt, Jnk and p38 Mapk and STAT3/Nf-kb pathways (Figure 1.7). FGF1 can also act as an intacrine factor in which it binds to FGFR1 or FGFR3 which in turn are translocated into cytosol and then into nucleus. Nuclear translocation of FGF1 is revealed to be essential for its neurotrophic activity and p53-dependent apoptosis (Rodriguez-Enfedaque *et al.*, 2009).

1.6.2. Involvement of FGF Proteins in Developmental Myelination and Regeneration

The role of FGF family members in myelination and repair after injury in CNS have been extensively studied for decades. FGF2 has emerged as a potential therapeutic target for myelin disorders. Although FGF2 has been previously considered as a negative regulator of myelination in CNS, major differences appeared to exist between the results of *in vivo* and *in vitro* studies. Expression of FGF2 is increased as a response to demyelination which in turn promotes proliferation of oligodendrocyte precursors (OPCs), but inhibit differentiation of OPCs. Therefore, it inhibits remyelination in CNS (Armstrong *et al.*, 2002). However, Schwann cells were found to overexpress different isoforms of FGF2 when it was analyzed *in vivo* upon PNS injury by using a nerve graft model. When nerve graft was transplanted into a complete nerve transection area, different isoforms have been shown to exert different

effects on peripheral nerve regeneration. While 18 kDa FGF2 acts as a negative regulator, 21/23 kDa FGF2 facilitates early recovery of sensory functions (Haastert *et al.*, 2006).

FGF9 in glial cells of MS patients has an increased expression in active demyelinating lesions. Mariko and her colleagues found out that vascular barrier breakage resulted from demyelination of CNS, can help to recover of the injury. Peripherally derived FGF21 which is secreted from the pancreas and circulates into PNS and later enters CNS due to disruption of vascular barriers has been shown to promote remyelination (Kuroda *et al.*, 2017). FGFR1 was suggested to act as an inhibitor of myelination since its conditional ablation leads to increase in remyelination of mature oligodendrocytes (Mierzwa *et al.*, 2013). It was also suggested that FGF1 may act as a promoter of remyelination in CNS after regeneration studies (Mohan *et al.*, 2014).

1.7. Previously Performed Studies in Our Laboratory

Analysis performed by our previous laboratory member Dr. Duygu Dağlıkoca showed that FGF1 is the most abundant FGF in PNS among others. Localization studies also showed that while FGF1 is localized both in neurons and Schwann cells, FGFR1-3 were found only in Schwann cells. FGFR4 was not expressed at RNA level in PNS. When lysates from mouse sciatic nerve were analysed during different developmental time periods, expression of FGF1 was shown to increase during myelination. Blockage of FGF1 in DRG co-cultures was shown to have an inhibitory effect on myelination (Dağlıkoca, 2014). Büşra Şimşek, from our lab, established and optimized LPC induced demyelination in the mouse sciatic nerve to study the effect of FGF1 in remyelination. She found that FGF1 was downregulated during demyelination and upregulated during remyelination. When FGF1 was blocked after demyelination, myelin protein expression was downregulated (Şimşek, 2015). From all the data obtained in our laboratory, we suggest that FGF1 might have a role in both developmental myelination and may act as a promoter of remyelination after demyelination induced by LPC.

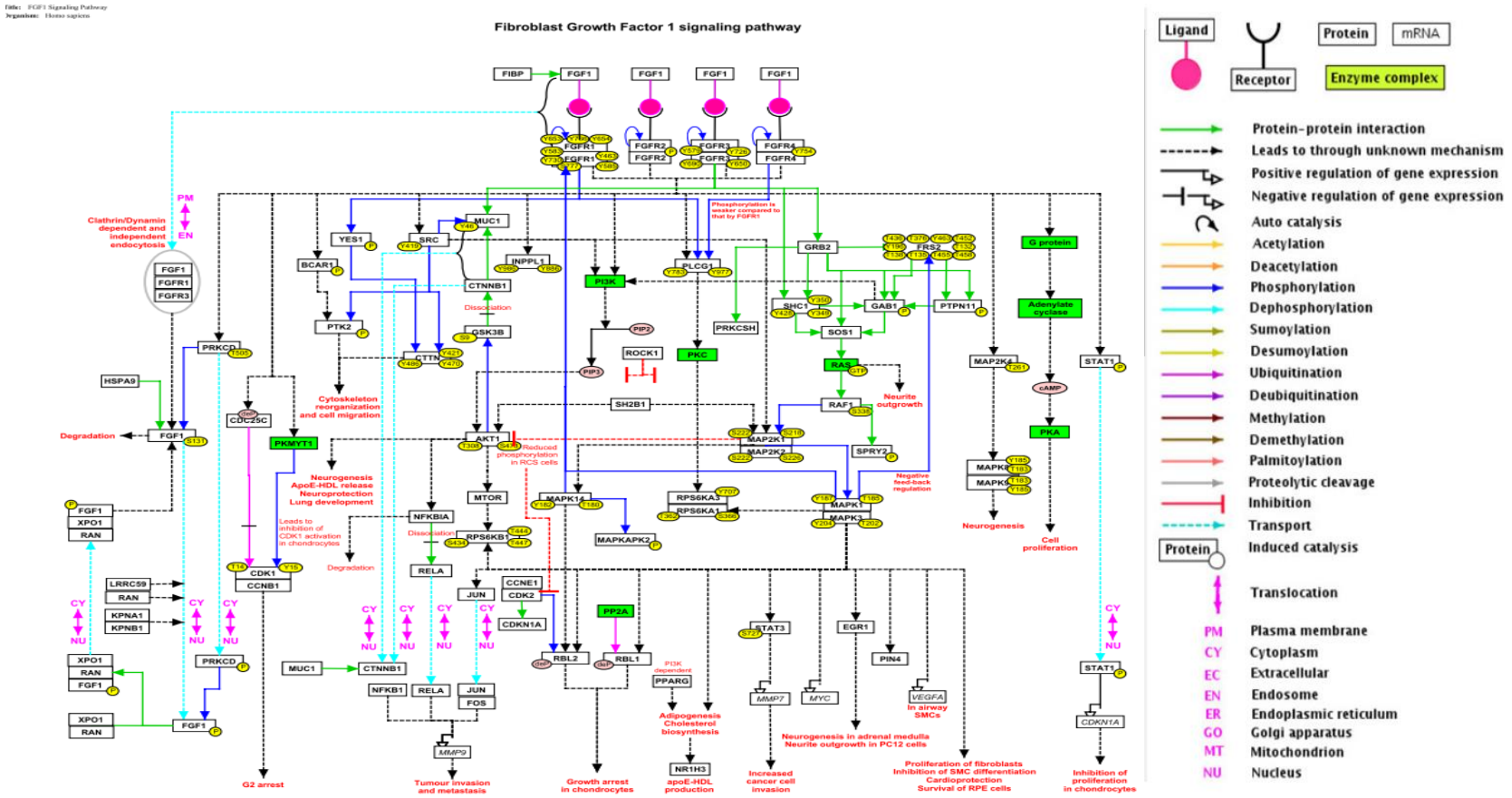

Figure 1.7. FGF1/FGFR signaling pathway. FGF1 can act through FGFR1-4 in paracrine and autocrine pathway which in turn activate Ras/Raf/Mek/Erk, pi3k/Akt, Jnk and p38 Mapk, and STAT3/Nf-kb pathways and involved in various cellular functions. FGF1 can also translocate into nucleus where it interacts with different proteins (Raju *et al.*, 2014).

2. PURPOSE

The first aim in this study is to optimize an ‘LPC induced demyelination model’ in the mouse sciatic nerve to use it as a demyelinating disease model of PNS and to monitor remyelination in long term. For this purpose, LPC injected nerves are visualized by immunohistochemistry after a month, two and three months after injection and expression of myelin proteins are investigated by western blotting.

The second aim is to further confirm the role of FGF1 in remyelination after demyelination induced by LPC injection since *in vitro* and *in vivo* analyses performed previously in our laboratory implicated that FGF1 may act as a promoter of remyelination. The concentration of FGF1 to be injected to nerve was optimized and its effect on remyelination is investigated by western blot analysis of myelin proteins.

The last aim is to investigate the possible proteins that interact with FGF1 during peripheral myelination by co-immuno-precipitation method of the mouse DRG co-culture lysates.

3. MATERIALS

3.1. Mice Strains

For our *in vivo* studies, C57BL/6J mice were kindly provided by Bogazici University Animal Facility. Mice were kept and maintained at appropriate conditions. All the procedures performed on animals properly followed the instructions indicated by Bogazici University Ethical Committee.

For our DRG co-culture studies, C57BL/6J type pregnant mice were kindly provided by San Raffaele Scientific Institute. Mice were held under 12 h dark/12 h light cycle and kept at 24 ℃. The experiments were carried out by following the regulation of San Raffaele Scientific Institute Ethical Committee.

3.2. Buffers and Solutions

Buffers and solutions used for the western blot analysis are given in Table 3.1.

Table 3.1. Buffers and solutions used for western blot analysis.

Buffer or Solution	Content
10% SDS polyacrylamide gel (Resolving gel)	375 mM Tris-HCl (pH 8.8)
	10% Acrylamide:Bisacrylamide (30:0.8)
	0.1% SDS
	0.1% APS
	0.1% TEMED
12% SDS polyacrylamide gel (Resolving gel)	375 mM Tris-HCl (pH 8.8)
	12% Acrylamide:Bisacrylamide (30:0.8)
	0.1% SDS
	0.1% APS
	0.1% TEMED

Table 3.1. Buffers and solutions used for western blot analysis. (cont.)

Buffer or Solution	**Content**
2x Protein Sample Buffer	100 mM Tris-HCl (pH 6.8)
	4% SDS
	0.2% bromophenol blue
	20% glycerol
	200 mM β-mercaptoethanol
4.5% SDS polyacrylamide gel (Stacking gel)	125 mM Tris-HCl (pH 6.8)
	4.5% Acrylamide:Bisacrylamide (30:0.8)
	0.1% SDS
	0.1% APS
	0.1% TEMED
5% SDS polyacrylamide gel (Stacking gel)	125 mM Tris-HCl (pH 6.8)
	5% Acrylamide:Bisacrylamide (30:0.8)
	0.1% SDS
	0.1% APS
	0.1% TEMED
6x Protein Sample Buffer	300 mM Tris-HCl (pH 6.8)
	12 mM EDTA
	60% glycerol
	12% SDS
	6% β-mercaptoethanol
	0.04% bromophenol blue
Blocking Solution	1% or 5% skim milk powder in TBST
Lysis Buffer 2%SDS	95 mM NaCl
	25 mM Tris-HCl (pH 7.4)
	10 mM EDTA
	2% SDS
	Protease inhibitor cocktail
	Phosphatase inhibitor cocktail

Table 3.1. Buffers and solutions used for western blot analysis. (cont.)

Buffer or Solution	**Content**
Radioimmunoprecipitation assay Buffer (RIPA Buffer)	1 M NaCl
	1% Triton X-100
	0.1% Na-deoxycholate
	50 mM Tris-HCl (pH 7.4)
	2 mM EDTA
	0.1% SDS
	Protease inhibitor cocktail
	Phosphatase inhibitor cocktail
Running Buffer	25 mM Tris
	250 mM Glycine
	0.2% SDS
Stripping Solution	62.5 mM Tris-HCl (pH 6.8)
	2% SDS
	0.7% β-mercaptoethanol
TBS with Tween-20 (TBST)	0.1% or 0.2% Tween-20 in 1x TBS
Transfer Buffer	25 mM Tris
	200 mM Glycine
	20% Methanol
Tris Buffer Saline (TBS)	20 mM Tris-HCl (pH 8.0)
	150 mM NaCl

Buffers and solutions used for immunohistochemistry and immunocytochemistry and their contents are given in Table 3.2. Phosphate buffered saline (PBS) was used as a buffer for immunostainings. PBS was commercially available and purchased from GIBCO.

Table 3.2. Buffers and solutions used for immunostainings.

Buffer or Solution	**Content**
Blocking solution	5% BSA or 0.1% BSA in 1x PBS
Blocking solution (cont.)	0.25% Triton X-100
	1% Donkey serum
DABCO mounting medium	50 mM Tris-HCl (pH 8.6)
	90% Glycerol
	2.5 % DABCO solution
DAPI	0.02 µg/ml in 1x TBS
Paraformaldehyde Solution	4% PFA in 1x PBS
Sucrose Solution	20% sucrose in 1x PBS
Washing Solution	0.25% Triton X-100 in 1x PBS

Buffers and solutions used for co-immunoprecipitation are given in Table 3.3.

Table 3.3. Buffers and solutions for co-immunoprecipitation.

Buffer or Solution	**Content**
2x SDS PAGE Sample Buffer	100 mM Tris-HCl (pH 6.8)
	40 mM DTT
	2% SDS
	20% Glycerol
	0.2% Bromophenol blue
Co-IP Lysis Buffer	50 mM Tris-HCl (pH 7.4)
	150 mM NaCl
	1 mM EDTA
	Protease inhibitor cocktail
	Phosphatase inhibitor cocktail
	1% NP40
	0.25% DOC
	0.1% SDS

Table 3.3. Buffers and solutions for co-immunoprecipitation. (cont.)

Buffer or Solution	Content
Washing Solution	50 mM Tris-HCl (pH 7.4)
Washing Solution (cont.)	150 mM NaCl
	1 mM EDTA
	Protease inhibitor cocktail
	Phosphatase inhibitor cocktail

3.3. Cell Culture Mediums

Mediums that were used for DRG co-culture growth and maintenance are given in Table 3.4.

Table 3.4. Cell Culture Mediums and their ingredients.

Medium	Content
C medium	Minimum Essential Medium (MEM)
	10% FBS
	200 mM Glutamine
	0.2 g/ml Glucose
	50 ng/ml Nerve Growth Factor (NGF)
NB medium	Neurobasal (NB) medium
	B27
	0.2 g/ml Glucose
	200 mM Glutamine
	50 ng/ml Nerve Growth Factor (NGF)
C+C medium	C medium
	50 μg/ml Ascorbic acid

3.4. Antibodies

In Table 3.5, primary antibodies which were used for western blot analysis and their usage information are given. In Table 3.6, secondary antibodies used for western blot analysis and product information are given.

Table 3.5. List of primary antibodies used for western blot and their usage information

Antibody	Brand	Product Code	Host	Dilution	Blocking
FGF1	R&D System	AF-4686	Sheep	1:100	5% MP in 1x TBS-0.1% Tween 20
FGFR1	Santa Cruz Biotechnology	sc-121	Rabbit	1:100	5% MP in 1x TBS-0.1% Tween 20
MAG	Santa Cruz Biotechnology	sc-15324	Rabbit	1:1000	5% MP in 1x TBS-0.1% Tween 20
MBP	Biolegend	SMI-99	Mouse	1:1000	5% MP in 1x TBS-0.2% Tween 20
β-actin	Santa Cruz Biotechnology	sc-47778	HRP tagged	1:1000	1% MP in 1x TBS-0.1% Tween 20

Table 3.6. List of secondary antibodies used for western blot and product information

Target	Brand	Product Code	Host	Dilution	Tag
Mouse	Cell Signaling	7076	-	1:1000	Horseradish Peroxidase
Rabbit	Santa Cruz Biotechnology	sc-2004	Goat	1:5000	Horseradish Peroxidase
Sheep	R&D System	HAF-016	Donkey	1:1000	Horseradish Peroxidase

Primary and secondary antibodies that were used for immunostainings are given in Table 3.7 and Table 3.8 respectively.

Table 3.7. List of primary antibodies used for immunostaining.

Antigen	Brand	Product Code	Host	Dilution
MBP	Biolegend	SMI-99	Mouse	1:1000
MBP	Biolegend	SMI-99P	Mouse	1:1000
NF-200	Sigma Aldrich	N4142	Rabbit	1:1000

Table 3.8. List of secondary antibodies used for immunostaining.

Target	Brand	Product Code	Host	Dilution	Fluorescence Tag
Mouse	Molecular Probes	A21202	Donkey	1:500	Alexa 488
Rabbit	Molecular Probes	A31572	Donkey	1:500	Alexa 555

Antibodies which are used for co-immunoprecipitation experiments are given in Table 3.9.

Table 3.9. List of antibodies used for Co-IP method.

Target	Brand	Product Code	Host	Dilution	Conjugated
Mouse FGF1	Santa Cruz Biotechnology	sc-7910	Rabbit	1:400	-
Mouse FGF1	LifeSpan Biosciences	LS-C171982	Rabbit	1:1000	Sepharose Bead
Mouse FGF1	R&D System	AF-4686	Sheep	1:100	-
Rabbit	Santa Cruz Biotechnology	sc-2004	Goat	1:5000	Horseradish Peroxidase
Sheep	R&D System	HAF-016	Donkey	1:1000	Horseradish Peroxidase

3.5. Chemicals

Chemicals which were used for this study are given in Table 3.10.

Table 3.10. Chemicals used in this study.

Chemical	Brand	Product Number
1,4-Diazabicyclo[2.2.2]octane, 98% (DABCO)	Sigma-Aldrich	D2 780-2
2-Mercaptoethanol	Merck Millipore	805740
30% Acrylamide/bis solution, 29:1	Bio-Rad	1610156
Acrylamide	Sigma	A3553
Ammonia	Merck	K47969723
Ammonium peroxodisulphate (APS)	Fluka	09914
Ascorbic Acid	Sigma-Aldrich	A4544
Protein A-Agarose	Roche	70439221
B27 Supplement	Thermo Scientific	17504044

Table 3.10. Chemicals used in this study. (cont.)

Chemical	Brand	Product Number
BCA protein assay kit	Thermo Scientific	23227
Bovine Serum Albumin (BSA)	Sigma-Aldrich	A2153
Collagen R solution 0.2	Pan Biotech	P06-20166
DAPI	Roche	10 236 276 001
Dulbecco's Modified Eagle's Medium (DMEM)	Gibco	1858686
DMEM	Sigma-Aldrich	D5671
EDTA	Riedel-de Haen	34549
Ethanol	Sigma-Aldrich	32221
Fast Green FCF	Sigma-Aldrich	F7252
Fetal Bovine Serum (FBS)	Gibco	10500056
Glucose	Sigma-Aldrich	G8270
Glycerol	Sigma-Aldrich	G5516
Glycine	Sigma-Aldrich	G8898
Hank's Balanced Salt Solution (HBSS)	Gibco	1830696
HCl	Merck	1003172500
IGEPAL	Sigma-Aldrich	CA-630
Leibovitz's L-15	Gibco	1895885
L-Glutamine	Thermo Scientific	21051040
L-α-Lysophosphatidylcholine	Sigma-Aldrich	L4129
Minimum Essential Media	Gibco	1880324
Methanol	Sigma-Aldrich	32213
Neurobasal Medium (NB)	Gibco	1894793
Neutral Membrane	Appligene	130302
Nerve Growth Factor (NGF)	Sigma Aldrich	N8133
Nitrocellulose membrane	Amersham Protran	1060002

Table 3.10. Chemicals used in this study. (cont.)

Chemical	Brand	Product Number
N,N,N',N'-tetramethylethlenediamine (TEMED)	Sigma-Aldrich	T7024
N,N'-Methylenebisacrylamide	Sigma-Aldrich	M7279
PageRuler Prestained Protein Ladder	Thermo Fisher	26616
Paraformaldehyde (PFA)	Sigma-Aldrich	15812-7
Penicillin-Streptomycin	Thermo Scientific	15070063
Phosphatase inhibitor cocktail tablets	Roche	04 906 845 001
Poly-L-lysine (PLL)	Sigma-Aldrich	P5899
Protease inhibitor cocktail tablets	Roche	11 873 580 001
Protein A Sepharose	Abcam	Ab193256
Recombinant Mouse FGF acidic Protein	R&D System	4686-FA
Sodium chloride	Merck Millipore	106404
Sodium deoxycholate	Merck	6504
Sodium dodecyl sulphate (SDS)	Sigma-Aldrich	L3771
Sodium hydroxide	Sigma-Aldrich	06203
Sucrose	Sigma-Aldrich	S0389
SuperSignal West Femto Maximum Sensitivity Substrate	Thermo Scientific	34095
Trisma base	Sigma-Aldrich	T1503
Triton X-100	Sigma-Aldrich	T8787
Tween-20	Riedel-de Haen	63158
Western blotting luminol reagent	Santa Cruz	sc-2048

3.6. Disposable Materials

In Table 3.11, disposable materials used in this study are given.

Table 3.11. List of the disposable materials used in this study.

Product	Supplier
4 well plates	Falcon- a corning brand
6 well plates	Falcon- a corning brand
Centrifuge tubes, 15 ml	CAPP-Denmark
Centrifuge tubes, 50 ml	CAPP-Denmark
Filtered tips	Axygen Scientific
Microcentrifuge tubes, 0.5 ml	Axygen Scientific
Microcentrifuge tubes, 1.5 ml	Axygen Scientific
Microcentrifuge tubes, 2 ml	Axygen Scientific
Microscope cover glass	Isolab
Pasteur pipettes	Isolab
Pipette tips	Axygen Scientific
Positively charged slides	Thermo Scientific
White Pestel	Argos Technologies

3.7. Equipment

Devices that were used in this study are given in Table 3.12.

Table 3.12. List of laboratory equipment used in this project.

Equipment	Supplier
Autoclave	Astell Scientific
Blotting Apparatus	Mini Trans-Blot Cell, Bio-Rad
Centrifuge	Centrifuge 5415-R, Eppendorf Spectrafuge 16 M, Labnet
Confocal microscopy system	TCS SP5, Leica Microsystems
Cryostat	Leica CM3050 S
Deep Freezers	-20 C^0 Arçelik

Table 3.12. List of laboratory equipment used in this project. (cont.)

Equipment	**Supplier**
Documentation System	Raystella, Bio-Rad Syngene
Electrophoresis	Mini-Protean III Cell, Bio-Rad
Fluorescence microscopy	MZ16FA, Leica Microsystems
Hamilton injector	Hamilton CO
Heat blocks	DRI-Block BD-20, Techne
Isoflurane inhalation anesthesia	Unitest
Magnetic Stirrer	Hanna Instruments
Micropipettes	Gilson
Light Microscope	S2026, Prion
Microwave oven	Arçelik
Power supplies	PowerPac Basic, Bio-Rad
Refrigerator	Arçelik
Shaker	SL 350 Nüve
Spectrophotometer	Nanodrop ND-1000 Nanodrop
Ultra Low Temperature Freezer	Thermo Forma
Vortex	NM110 Nüve

4. METHODS

4.1. Sciatic Nerve Injections

'*Lysolecithin induced demyelination*' model has been used to mimic demyelination in this study. This model is optimized and widely used to study central nervous system, especially in Multiple Sclerosis research, but very rarely used to examine peripheral nervous system. In our laboratory, the model was optimized to be used as a demyelinating disease model and to unravel the roles of FGFs in PNS.

For mouse sciatic nerve injections, the instruments used were cleaned and sterilized by autoclaving to eliminate possible inflammation. They were performed on adult mice that were two-three months old.

Isofluorane inhalation apparatus was used for anesthesia since recovery of mice is better than other anesthetic methods. The oxygen and the isofluorane levels were adjusted to 1% liters/min and 5% (volume/volume), respectively. Mice were taken out of the cage and isofluorane flux was provided through their noses. After 5-10 minutes, respiration of the mice decelerated. The paw reflexes were checked to be sure that mice become unconscious. During the surgery, the isofluorane level was maintained at 1.5% (volume/volume). The skin at the posterior thigh level of a mice lying on face down was shaved by razor blade and cleaned with baticon applied on cotton swabs. Upper layer of the skin was lifted by forceps and cut parallel to the nerve with a scissor. After the connective layer was exposed, it was gently lifted and a small cut was introduced. The scissors was put inside closed and then opened in the connective layer to cut it completely. Forceps was used to raise the sciatic nerve gently. After it was exposed, the tip of the Hamilton syringe 33 ga was inserted inside of the nerve very slowly. The chemical inside of the syringe was injected at a rate of 1 ul per minute. The nerve was placed back after the injection was finished. In case where the muscle was damaged, it was sutured. The skin was also stitched up by surgery needles and fibres. After surgery, mice were taken out of the anesthetic device and put face down onto a piece of napkin inside of the cage.

4.1.1. Monitoring Remyelination upon L-α-Lysophosphatidylcholine Induced Demyelination

From previous studies performed in our laboratory, 2% of L-α-Lysophosphatidylcholine has been found to be the optimal concentration to induce demyelination in mouse sciatic nerve. This concentration was used for all the injections performed in this study. In order to track the injection, Fast Green FCF dye was used as 0.05% in total solution. Each nerve was injected with around 5 μl of L-α-Lysophosphatidylcholine – Fast Green FCF mixture.

In our all injections, left sciatic nerve was used as an experimental group while right sciatic nerve was used as a control group. In order to track remyelination, different time points were chosen after demyelination was induced. First group of mice were sacrificed after one month, two or three months from the injections, total protein was extracted from the sciatic nerve and the level of myelin marker proteins were analyzed by western blot. Experimental and biological repeats were done for three times.

Second group of mice were sacrificed after a month, two or three months from the injections and tissues were preserved for immunohistochemistry to visualize myelin sheath as explained in Section 4.1.5.

4.1.2. Injection of Recombinant Mouse Acidic FGF

FGF acidic protein was injected after L-α-Lysophosphatidylcholine injection to analyze its role in remyelination. Recombinant mouse FGF acidic protein was obtained from R&D and dissolved in sterile PBS to get 250 μg/ml stock solution. For the optimization of the concentration of FGF1 that should be injected to mouse sciatic nerve, 50, 100, and 200 μg/ml was used. After literature survey and analysis of the results of different concentrations of FGF1 injections, 100 μg/ml was chosen as the concentration for further injections (Ooto *et al.*, 2004). In this part of our study, L-α-Lysophosphatidylcholine was injected as described above to both nerves and considered as the first injection. After 7 days from the first injection, recombinant FGF1 was injected to the left nerve and referred as the

experimental group. Isotonic saline solution was injected to right nerve as the control group. In order to track the injection through nerve, Fast Green FCF was mixed with FGF1.

First group of mice were sacrificed after 15 days from the first injection and whole protein lysate was obtained from the nerves. Expression level of myelin protein markers in control and experimental groups were analyzed by western blot. For the first group of mice, three mice were injected with 100 µg/ml FGF1 for statistical analysis. One mouse was injected with 200 µg/ml FGF1 to check whether different concentration of FGF1 can change the myelin protein expression.

Second group of mice were sacrificed instantly after FGF1 injection and protein was extracted from the nerves. Myelin protein levels were analyzed by western blot. The timeline of the injections were given in Figure 4.1. For second group of mice, three mice were injected with 100 µg/ml FGF1 for statistical analysis. Two mice were injected with 50 µg/ml FGF1 to check whether different concentration of FGF1 can change the myelin protein expression.

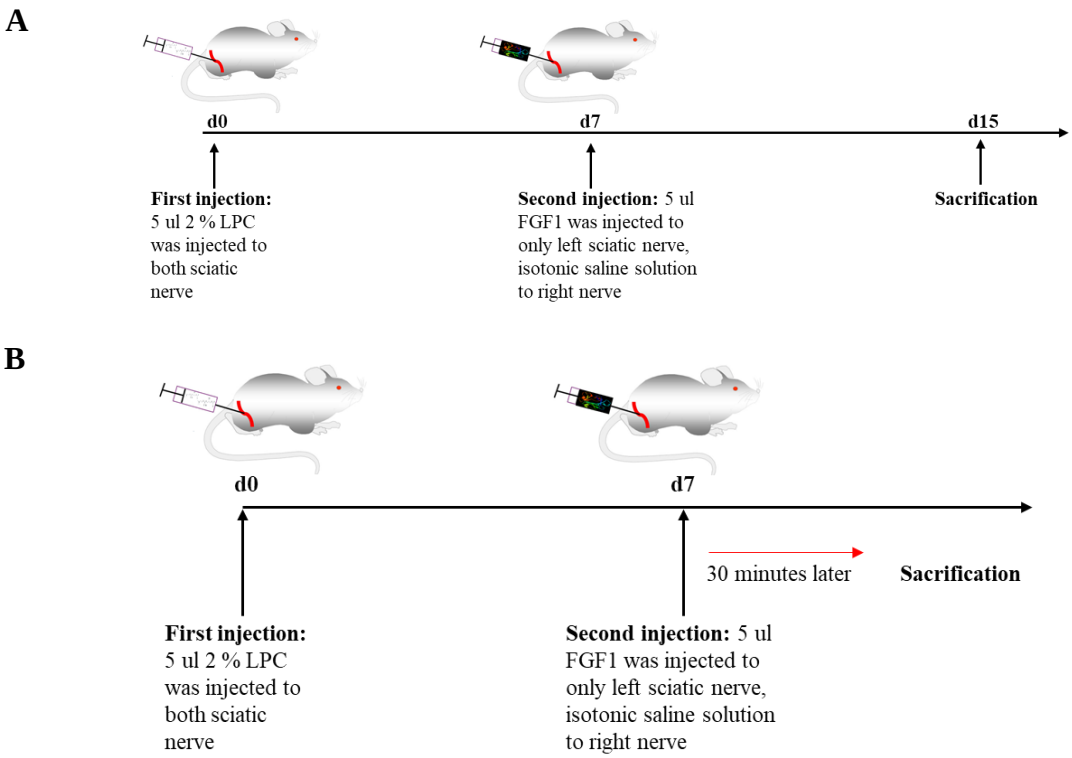

Figure 4.1. Time table of injections. (A) First group and (B) Second group of mice.

4.1.3. Protein Extraction from Sciatic Nerve and Determination of Protein Concentration

Mice were sacrificed and sciatic nerve was dissected by sterile scissors and forceps. The samples were placed onto ice and after this point, all steps were performed on ice. First, 60-70 µl RIPA buffer was added to each nerve sample and then mixed with 8-10 MagnaLyser ceramide beads. The nerves were lysed with MagnaLyser homogenizer for 60 seconds at 6500 rpm and were incubated on ice for 1 hour by shaking. The samples were centrifuged at 13.200 rpm for 30 minutes at 4 ℃. The supernatant that was final protein lysate was transferred to a new eppendorf tube and stored at -80 ℃.

In order to determine total protein concentration, BCA protein assay kit was used. Two mg/ml bovine serum albumin was diluted to create a series of concentrations from 0.025 to 2 mg/ml. Working solution was diluted with a ratio of 50:1 and mixed with known and unknown concentrations. After 30 minutes of incubation at 37 ℃, absorbance was recorded for OD_{595}. The concentration of the unknown samples were calculated from the reference curve that was obtained from known BSA concentrations.

4.1.4. Western Blot Analysis

The protein lysates were prepared for western analysis by mixing with 2X or 6X protein sample buffer to a total amount of 20 µg to examine myelin proteins or 50 µg to investigate other proteins. Samples were boiled for 5 minutes at 95 ℃ to denature the proteins. Depending on the molecular weight, proteins were separated on 10% or 12% polyacrylamide gel. The gels were run at 80 V until proteins reached at resolving gel and proceeded at 100 V for around 2 hours. The proteins were transferred to PVDF membrane at 100 V for 100 minutes by blotting machine. After transfer, membrane was washed with 1X TBST for 3 times and 5 minutes. Blocking of membrane was performed for 1 hour rotating at room temperature with blocking buffer that contains 1% or 5% milk powder in TBST. Then, membrane was left overnight at 4 ℃ with primary antibody diluted at appropriate concentration in the blocking solution. Next day, antibody containing solution was removed and membrane was washed with 3 times and 5 minutes with 1X TBST at room temperature. Membrane was rotated with horseradish peroxidase (HRP)-conjugated

secondary antibody diluted at appropriate concentration in blocking solution for 1 hour at room temperature. Membrane was washed with 1X TBST for 3 times and 5 minutes and then incubated with Immunocruz western blotting luminol reagent for a time specific to proteins of interest. The proteins on the membrane were visualized and photographed with Stella or Syngene imaging systems.

4.1.5. Immunohistochemistry

Sciatic nerve tissues dissected and placed into ice were fixed with 4% paraformaldehyde (PFA) for 1 hour at 4 ℃. It was washed with ice cold 1X PBS for 3 times and 10 minutes at 4 ℃ and left for overnight incubation with 20% sucrose in 1X PBS at 4 ℃. Next day, tissue was placed into mold with OCT embedding medium and frozen at -80 ℃. Using a Cryostat sectioning machine, 12 μm sections were taken from the frozen tissue that were left at room temperature for 30 minutes for adherence to the positively charged glass slides. The sections were stored at -20 ℃ for further analysis or -80 ℃ for long term.

Slides washed with 1X PBS for 3 times and 10 minutes were blocked with 2% donkey serum, 0.1% Triton X-100 and 0.1% BSA in 1X PBST for 1 hour. After blocking, slides were left for overnight incubation with primary antibodies diluted in blocking solution at 4 ℃ to mark myelin sheath. Next day, slides were rinsed with washing solution for 3 times and 10 minutes and incubated with fluoresence tagged secondary antibodies diluted in blocking solution for 1 hour at room temperature in dark. In order to stain nucleus, incubation was performed with 0.02 μg/ml DAPI in 1X TBS for 5 minutes. Slides rinsed with washing solution were mounted with DABCO mounting medium. The samples were visualized by using fluoresence or confocal microscopes. They were stored at -20 ℃.

4.2. Dorsal Root Ganglion (DRG) Co-culture

In order to reveal the interaction partner or partners of FGF1 in myelinating cultures, dorsal root ganglion (DRG) co-culture technique was used. For our analysis, 6 well plates were used to seed and grow DRGs.

4.2.1. Collagen Coated Plate Preparation

To prepare collagen covered slides, autoclaved coverslips were placed into 6 well plates. Collagen was diluted to a ratio of 1:1000 by acetic acid in water (1:10) and dropped on top of the coverslips. After 10 minutes, the collagen was removed and a piece of napkin was placed onto the plates with 1 ml of ammonia to dry the plates. After 30 minutes, napkin was removed and plates were left open under the hood for 6 hours. They were stored at 4 ℃.

Plastic covered plates were also prepared to catalyze the attachment of DRGs. For this preparation, 1 ml of poly-L-lysine (PLL) was added onto 6 well plates and left for 5 minutes. After 2 times of washing with distilled water for 5 minutes, 1 ml of collagen was placed onto the wells and incubated for 5 minutes. Collagen was removed and napkin with ammonia was placed onto 6 well plates. After 30 minutes of incubation, napkin was removed and plates were left open for 6 hours. They were stored at 4 ℃.

4.2.2. Dorsal Root Ganglion (DRG) Dissection

Pregnant C57BL/6J mice were sacrificed by CO_2 at embryonic day 13.5. Mice were placed in supine position and abdomen part was cleaned with 70% ethanol. The skin in the lower part of abdomen was lifted and cut with a scissors to expose the embryos. By using forceps, uterus laden with embryos were separated gently from the peritoneal cavity and the ends were cut. Uterus were then transferred to Falcon tube containing Leibovitz's L-15 medium. For dissection under the hood, uterus was transferred to 10 cm plate with Leibovitz's L-15 medium and washed for 2 times with L-15 medium. By scissors and forceps, single embryo was cut from the others. Amniotic fluid and the tissue that surrounded the amniotic fluid were removed to expose the embryo. Embryo was transferred to 6 cm plate with L-15 medium and placed under a dissection microscope. After cutting off the head and tail of the embryo, it was placed in supine position and the organs were removed by forceps. Bones on the dorsal part are removed next so that the spinal cord was exposed and removed from the body gently. The dissected spinal cord was transferred to a fresh 6 cm plate with L-15 medium. The root part that connect dorsal root ganglions (DRG) to spinal cord was cut off to dissect DRGs. Dissected DRGs were then placed into 6 well plates and each well was filled with about 35-40 DRGs. Approximately 500 µl C medium was added

to each well with antibiotics. Penicillin-Streptomycin (P/S) was used as antibiotics to eliminate the mother's residuals. They were added to C medium with a ratio of 1:100. The plates were left for overnight at 37 ℃ with 5% CO_2 to enable DRGs to attach to the collagens. The day that dissection was performed was considered as Day 0.

4.2.3. DRG Co-culture

One day after DRG seeding, DRGs were supposed to be attached but they were still fragile and ready to detach so the medium was changed to C medium without P/S very gently. The timeline of the process and medium changes were given at Table 4.1. Usually myelination were stimulated nine days after the dissection by adding ascorbic acid (Vitamin C) to medium and in eight days' time myelin sheath appears around the neurofilaments. The culture was stopped approximately 20 days after dissection. DRG co-culture was very sensitive to environmental factors like CO_2 levels of the hoods or handling and they were naïve. Some DRG co-cultures may be very healthy upon dissection while some others may have tendency to detach easily several days after DRG dissections because of some environmental factors or their nature. Therefore, the time table that were followed for medium changes were slightly different from one DRG co-culture to other depending on physical appearance. Since C+C medium helps DRGs to recover and allow them to grow better, unhealthy looking DRGs were sustained in C+C medium for 25-26 days while healthy ones were stayed in C+C medium for 20 days. At the end, all DRGs were guaranteed to have similar amount of myelin sheath before ceasing the co-culture.

Table 4.1. The type of medium that was used at a given time point of DRG co-culture.

DRG co-culture day	**Medium type**
Day 0	C+ P/S medium
Day 1	C medium
Day 3	NB medium
Day 5	NB medium
Day 7	C medium

Table 4.1. The type of medium that was used at a given time point of DRG co-culture. (cont.)

DRG co-culture day	**Medium type**
Day 9	C+C medium
Day 11	C+ C medium

4.2.4. Immunocytochemistry

DRGs are dissected and plated onto collagen coated coverslips as explained in Section 4.2.2. Nine days after dissection, ascorbic acid was added to medium to induce myelination. After myelin sheath was observed by using bright field microscope, the medium was removed and cells were washed with 1X PBS for 2 times and 5 minutes at room temperature.

For immunocytochemical analysis, 200 µl 4% PFA was added to each well to fix the cells. After 15 minutes of incubation with 4% PFA at room temperature, cells were rinsed with 1X PBS for 2 times and 5 minutes. They were incubated with 200 µl methanol (-20 ^{0}C) for 20 minutes at -20 ℃ to allow permeabilization. This was an important step since it allowed antibodies to bind their targets efficiently. Cells were washed with 1X PBS for 2 times and 5 minutes. Coverslips were transferred to the humidified chamber from 6 well plates. Eighty µl blocking solution was added to coverslip slowly and incubated for 1 hour at room temperature. Cells were then left for overnight incubation at 4 ℃ with blocking solution containing appropriate amount of primary antibody. Next day, cells were rinsed with 1X PBS for 2 times and 5 minutes. Cells were incubated with blocking solution containing secondary antibody diluted at an appropriate concentration for 1 hour at room temperature in the dark. For nuclei staining, cells were incubated with 1X Hoescht dye for 5 minutes. After they were washed with 1X PBS for once for 5 minutes, cells were rinsed with distilled water again for once. One drop of vectoshield mounting medium was put onto slides and then a coverslip was laid on top. The images were captured by both confocal and fluoresence microscopy.

4.2.5. Determining the Expression Level of FGF1 in DRG co-culture and Coimmunoprecipitation

After myelin sheath was observed, the cells were lysed in order to examine the expression level of FGF1 in DRG co-culture. They were rinsed with ice cold 1X PBS for 2 times and 5 minutes gently to avoid detachment. 150 µl lysis buffer containing 2% SDS was added to each well and cells were scraped out of the wells. After transferring the cells to eppendorf tubes, they were broken down by mechanic forces; pushing the cells up and down to lyse. After samples were boiled at 100 ℃ for 5 minutes, they were centrifuged at 16 ℃ for 10 minutes at 14000 g. Supernatant was transferred to a new tube. To avoid precipitation of SDS, samples were kept at room temperature after addition of the lysis buffer. Samples were stored at -80 ℃ for further use. Protein concentration was determined by BCA assay as explained above in Section 4.1.3.

Western blot was used to determine the level of expression of FGF1 in myelinating co-culture as explained above in Section 4.1.4. The concentration of samples that were loaded to polyacrylamide gel were in between 20-50 µg.

To identify the interaction partner/s of FGF1 in myelinating co-culture, co-immunoprecipitation (Co-IP) method was preferred. After myelin sheath was observed, cells were rinsed once with ice cold 1X PBS. 200 µl ice cold Co-IP lysis buffer was added to each well. They were incubated on ice for 5 minutes. Cells were scraped and transferred to a new tube. Mechanical forces were used to lyse the cells with up and down movement. The samples were centrifuged for 20 minutes at 4 ℃ and 14000 g. Supernatant was transferred into a new tube and stored at -80 ℃ for further analysis.

Before Co-IP was performed, cells were defrosted and protein concentration was determined by applying BCA assay. Then, lysate were centrifuged for 1 minute at 14000 and vortexed gently. Commercially available sepharose bead conjugated mouse FGF1 antibody was added to cell lysate at 1mg/ml and left for overnight with gentle rocking at 4 ℃. Next day, samples were centrifuged for 30 seconds at 4 ℃. After supernatant was removed, pellet was washed with lysis buffer with detergent for 3 times and 5 minutes and

washed with lysis buffer without detergent for 3 times and 5 minutes on ice. Pellet was stored at -80 ℃ for further analysis.

Pellet was resuspended with 20 µl 3X SDS sample buffer, vortexed, and centrifuged for 30 seconds. Samples were boiled at 95 ℃ for 5 minutes and centrifuged for 1 minute and 14000g. Then they were analyzed by SDS-PAGE and Coomassie blue staining and western blotting approaches.

For negative control, unconjugated sepharose bead was used to test for unspecific protein binding to the bead itself. Besides, to be used as a negative control for FGF1 activity, a tissue which doesn't express FGF1 was searched from appropriate websites. Liver of embryonic mice from E13.5 were found not to express FGF1. Therefore, liver of embryonic mice from E13.5 was dissected before the spinal cord was removed and frosted by dried ice. Livers were stored at -80 ℃ for further analysis. First, the tissue was lysed with lysis buffer for western blot analysis to check the FGF1 expression level and to confirm its absence. The lysis procedure was similar with the cell culture and sciatic nerve lysis. Frozen liver was splintered with a metal pestel on dried ice and turned into powder. The powder was dissolved in lysis buffer which contains 2% SDS. After this point, samples were handled at room temperature to avoid precipitation of SDS. Mechanical forces was applied to break up the tissue. When the sample became viscous, syringe was used to make it completely transparent. It was boiled at 100 ℃ for 5 minutes and then were centrifuged at 14000 g for 20 minutes at room temperature. The supernatant was transferred to a new tube and the total protein concentration was calculated by BCA assay. The samples were stored at -80 ℃ for further analysis. For liver and only unconjugated sepharose bead controls, the Co-IP was applied as explained before and results were analyzed by Coomassie blue staining and western blot.

Co-IP was performed also with unconjugated bead and FGF1 antibody. For this part, Protein A-agarose beads were washed with Co-IP lysis buffer for 3 times and 5 minutes. Preclearance of the samples were performed by incubating the sample with beads for 3 minutes. Samples were isolated from the beads by centifugation for 15 minutes at 10.000 g at 4 ℃.

Protein A-agarose beads were incubated with sc-7910 Rabbit anti FGF1 at 1:400 dilution for 4 hours on ice by shaking gently. After antibody-agarose binding, beads were precipitated and precleared samples were added to antibody-bead complex at 1mg/ml and incubated for overnight at 4 ℃. Next day, samples were precipitated and dissolved in 2X protein samples which contain 50 mM DTT. Then samples were analyzed with Coomassie Blue staining and western blotting.

4.2.6. Coomassie Blue Staining

After FGF1 and its possible interaction partner was pulled down, the samples were loaded on 12.5% polyacrylamide gel and run at 100 volt for 2 hours. The gel was stained with 0.1% Coomassie Blue R250 in 10% acetic acid, 50% methanol and 40% distilled water by rotating for 1 hour at room temperature. The gel was washed with 10% acetic acid and 50% methanol for 3 hours with two changes of this solvent. In order to de-stain the gel, it was soaked into a 10% acetic acid, 50% methanol and 40% distilled water by rotating for 2 hours with at least three changes of this solvent. The proteins on the gel were visualized by naked eyes.

5. RESULTS

FGF1 involvement in developmental myelination and in remyelination was suggested by previous studies performed by Dr. Dağlıkoca and Büşra Şimşek, respectively. For *in vivo* analysis, an 'LPC induced demyelination model' was optimized for sciatic nerve. The previous findings in our laboratory can be summarized as follows: demyelination was observed after LPC injection and it continued for 7 days after LPC injection; remyelination was initiated at around 7-8 days after LPC injections, however, total recovery couldn't be achieved even at 21 days after LPC injections: blockage of FGF1 by a neutralizing antibody leads to a decrease in the expression of myelin proteins during remyelination. Unfortunately, we could not get results for FGFR1-3 blockage by neutralizing antibody during remyelination. To further use the LPC model as a demyelinating disease model and to provide further evidence for involvement of FGF1 in remyelination, in this study, the LPC model was optimized further by monitoring the total recovery of myelin proteins after LPC injections. After that, mouse recombinant FGF1 was injected into the sciatic nerve during remyelination-7 days after LPC injections and recovery of myelin proteins were investigated. To further investigate FGF1 involvement in developmental myelination, FGF1 and its possible interaction partners were precipitated from myelinating mouse DRG-rat SCs co-cultures.

5.1. Sciatic Nerve Injection

Nerve crush and nerve transection methods are widely applied techniques to induce nerve degeneration in PNS, however, they also cause axonal damage. Since most of the CMT patients do not show primary axonal damage and present myelin maintenance defects, we preferred to induce demyelination in the sciatic nerve of mice using an 'LPC induced demyelination model'. This method has been widely used to mimic demyelinating disease in CNS but very rarely in PNS. The concentration of LPC required to induce demyelination, the starting time of demyelination and remyelination after injections were already investigated and determined by Büşra Şimşek. In the first part of this project, remyelination was monitored 1-3 months after LPC injections to provide evidence for maximum recovery of myelin after LPC induced remyelination.

5.1.1. Confirmation of 0.2 mg/µl LPC injections was enough to induce demyelination

Initially, before further analysis with LPC injections, the concentration of LPC that is required to induce demyelination was confirmed. For this purpose, 0.2 mg/µl LPC in 0.09% NaCl with 0.05% Fast Green FCF solution was injected to the left sciatic nerve of mice. The right sciatic nerve was used as a control and was injected with only saline solution. Mice were sacrified seven days after injections and proteins were extracted from the sciatic nerves. Expression of MAG was analysed as the early myelination marker. Western blot analysis showed that MAG protein levels were decreased on the LPC compared to NaCl injections, confirming that 2% or 0.2 mg/µl LPC was enough to induce demyelination. This LPC concentration was used in further analysis (Figure 5.1).

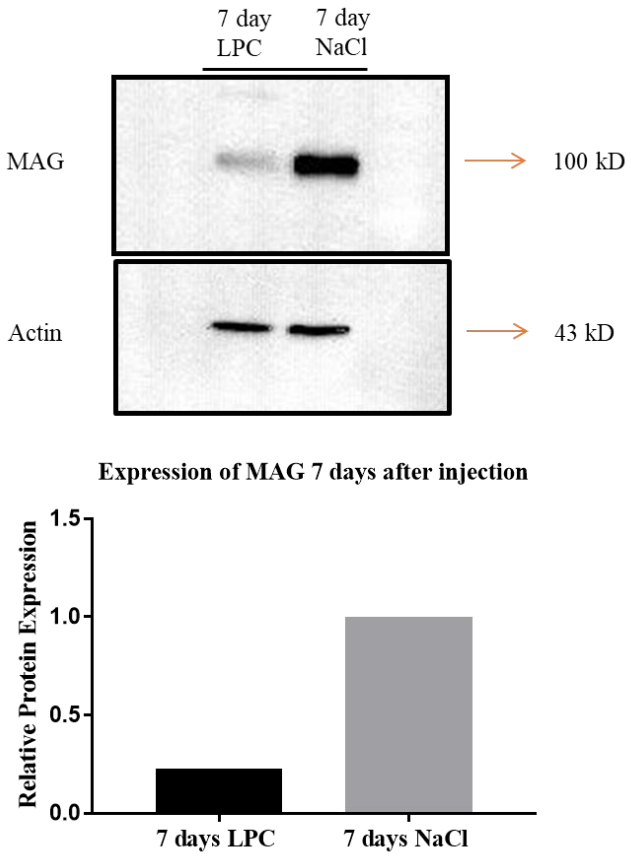

Figure 5.1. Western blot analysis of relative expression of MAG (to β-actin) 7 days after LPC and NaCl injections to left and right sciatic nerves, respectively.

5.1.2. Long Term Monitoring of Remyelination

Sciatic nerves were dissected and remyelination was traced by western blot analysis and immunohistochemistry at different time points; 7 days, 14 days, 1 month, 2 months and 3 months after 2% LPC injection.

5.1.2.1. Western analysis. For western blot analysis, three independent experiments were conducted and Student t-test and one-way ANOVA was applied for statistical analyses. The right sciatic nerve injected with isotonic saline solution was used as the control. MAG which is an early myelination marker was downregulated 7 days after LPC injection during demyelination. That downregulation at 7 days was statistically significant compared to control that has a p value less than 0.0001. Expression of MAG was upregulated at 14 days after LPC injection that has a p value of 0.003 compared to negative control. After that point, the expression of MAG persists to remain upregulated during remyelination at a steady state for months 1-2. In the third month, on the other hand, the change was statistically significant compared to control. While the changes between 7 days and 14 days; 14 days and 1 month; 1 month and 2 month; 2 month and 3 month were not statistically significant, One-way ANOVA analysis showed 0.0025 p value. The results of western analysis and relative expression of MAG to actin is given at Figure 5.2.

MBP expression was monitored as a late myelination marker using the same approach with three biological replicates. The results were evaluated statistically with t-test and presented in Figure 5.3. The antibody used for MBP was able to detect only three isoforms which are 21.5, 18.5 and 17.2 kD but it has four different isoforms in mouse and rats. The expression MBP was also reduced with LPC injection until the time point of 14 days and almost reaches to its normal levels in 1-3 months (Figure 5.3). MBP seemed to be increased at 7 days after LPC injections in some samples which were excluded from our analysis.

5.1.2.2. Immunohistochemical analysis. Horizontal sections were obtained at time points of 7 days, 14 days, 1 month, 2 months and 3 months after LPC injections. The myelin sheath was visualized with MBP marker, neurofilaments were labelled with NF-200, and nuclei of Schwann cells were stained with DAPI.

The structure of the myelin sheath of control sciatic nerve that was injected with 0.09% NaCl was well preserved and did not get affected by NaCl injection as expected (Figure 5.4). They revealed normal myelin appearance with wrapping around neurons and establishment in a decent shape. NF-200 stained neurofilaments were in shape of smooth tubules. Nuclei of Schwann cells showed normal appearance with their elongated form and their localization around myelin sheath.

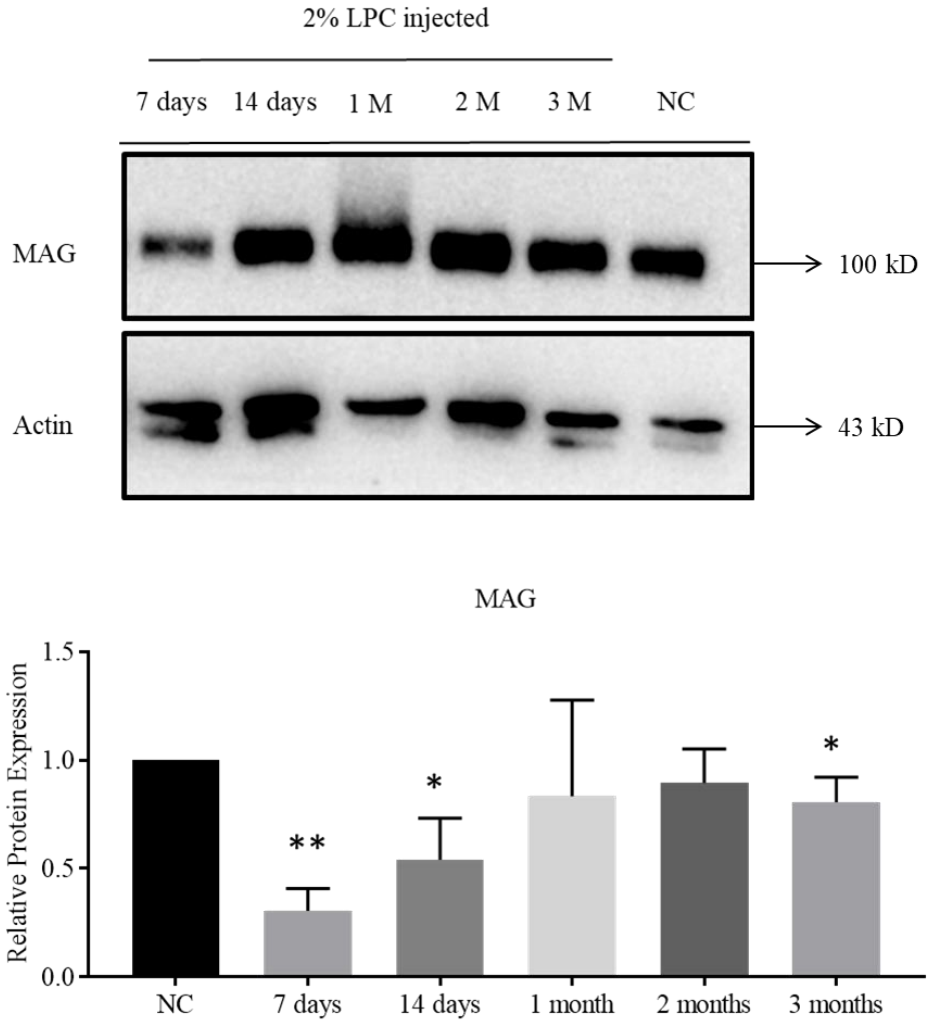

Figure 5.2. Western blot analysis of MAG levels at different time points after LPC injection. NC is control that represent the nerve injected with isotonic saline solution. MAG was normalized to actin and mean values of 3 independent experiments were graphically depicted, * $p < 0.05$ and ** $p < 0.01$.

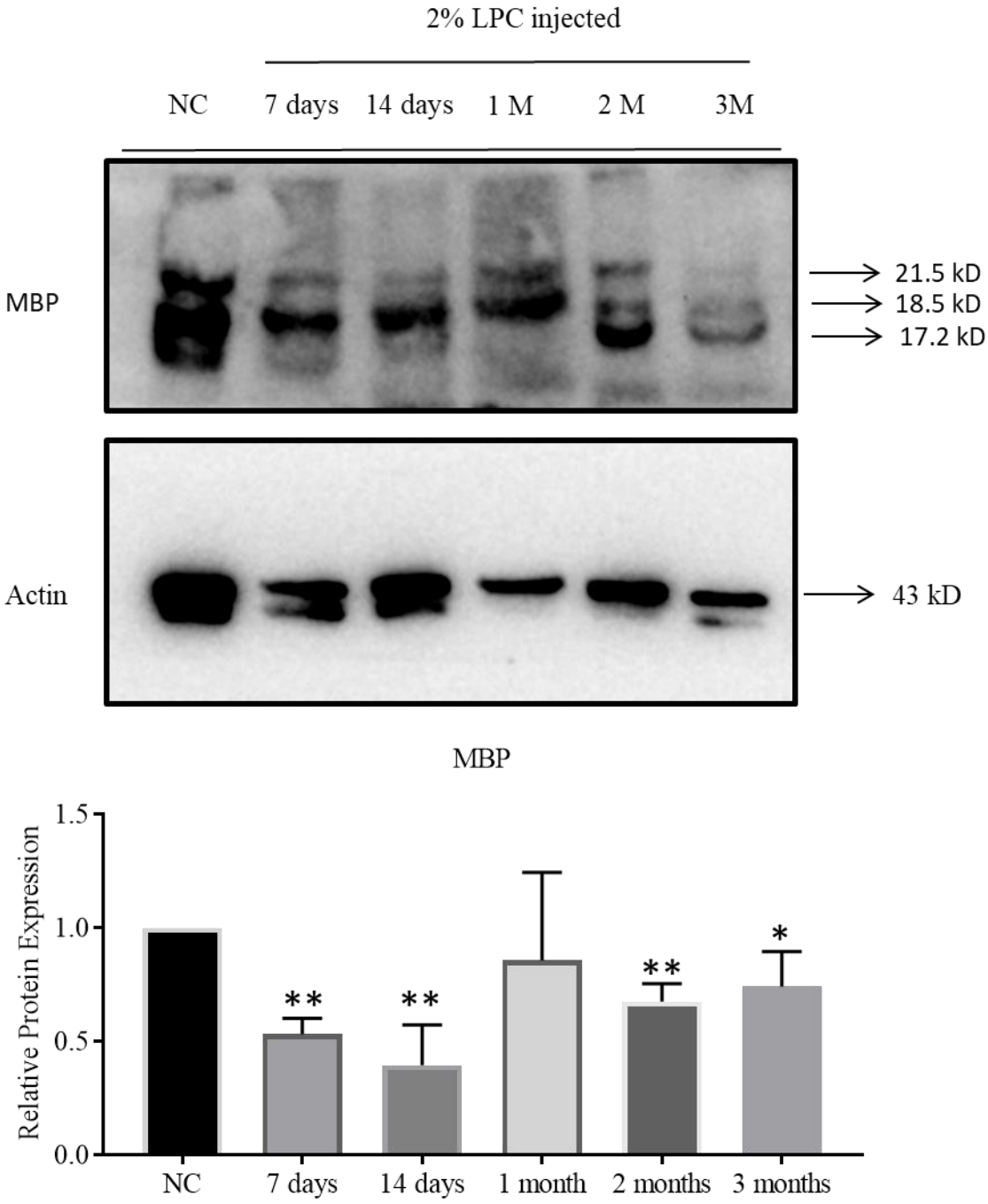

Figure 5.3. Western blot analysis of MBP levels at different time points after LPC injection. NC is control that represent the nerve injected with isotonic saline solution. MBP was normalized to actin and mean values of 3 independent experiments were graphically depicted, * $p < 0.05$ and ** $p < 0.01$.

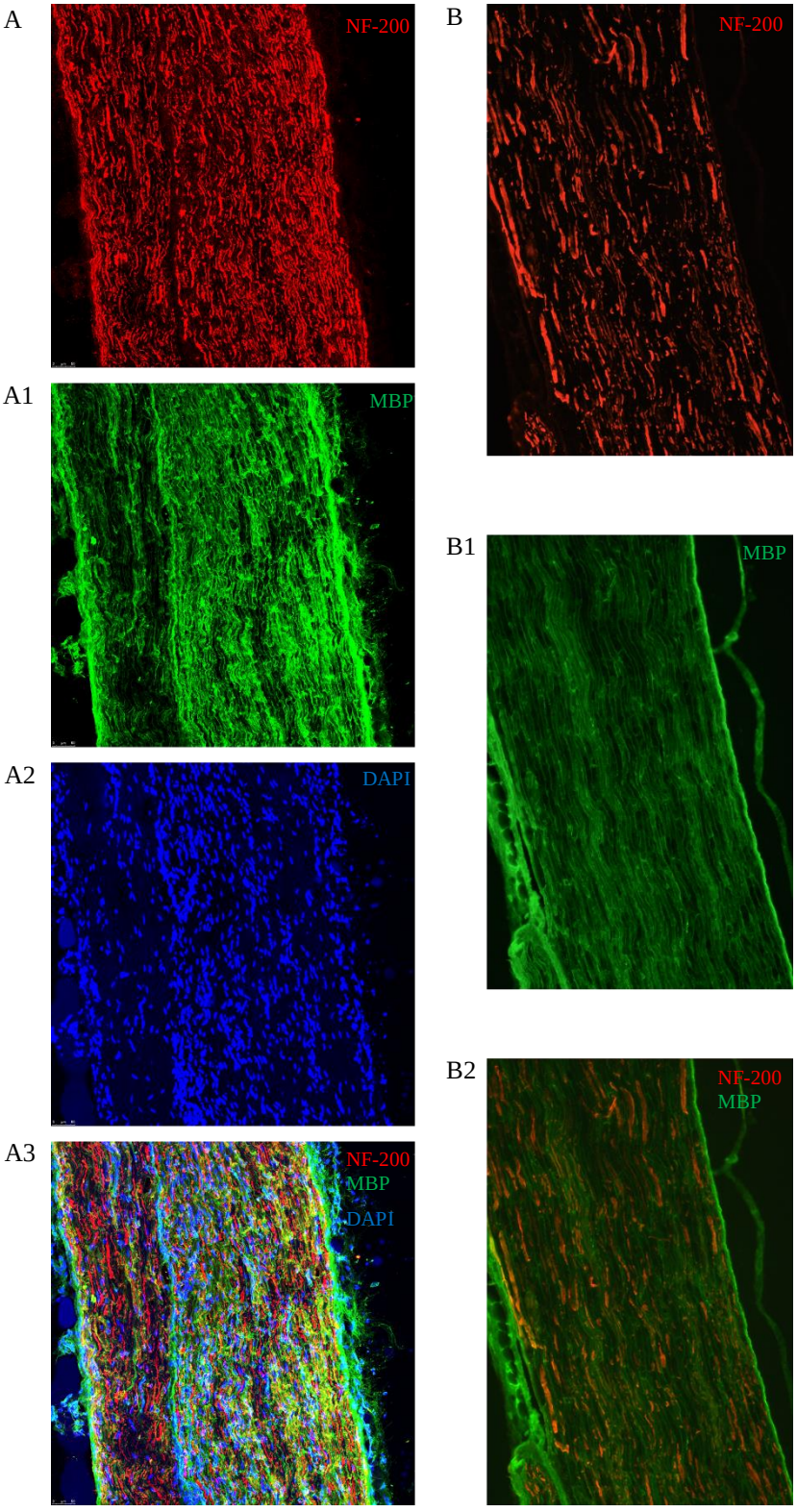

Figure 5.4. Immunostainings of horizontal sections of sciatic nerve which was injected with isotonic saline solution. A, confocal images of controls. B, fluoresence images of controls. MBP in green, NF-200 in red and DAPI in blue.

Immune analysis showed that LPC injection induced demyelination that lasted for 7 days as previously described in the literature. As shown in Figure 5.5, when the nerve was visualized at 7 days after LPC injection the myelin sheath was partly lost as a result of demyelination and became disorganized. Neurofilaments were also affected and they appeared like shuffled tubular assemblies. Some of Schwann cells' nuclei seemed to become rounded and got smaller while some others were still elongated.

As stated in literature and in our previous studies, remyelination started around 7 days after LPC induced demyelination. At 14 days after injection the myelin sheath appeared still disturbed and partly disorganized (Figure 5.6).

At 1 month after LPC injection, recovery of myelin sheath could be visualized very briefly. It was partly reconstructed and still disorganized and partly lost. Neurofilaments appeared also still disorganized (Figure 5.7).

Myelin sheath stained with anti MBP seemed to be more organized at 2 months after LPC injections indicating successful remyelination at this period. Neurofilaments were more organized compared to those at 1 month (Figure 5.8).

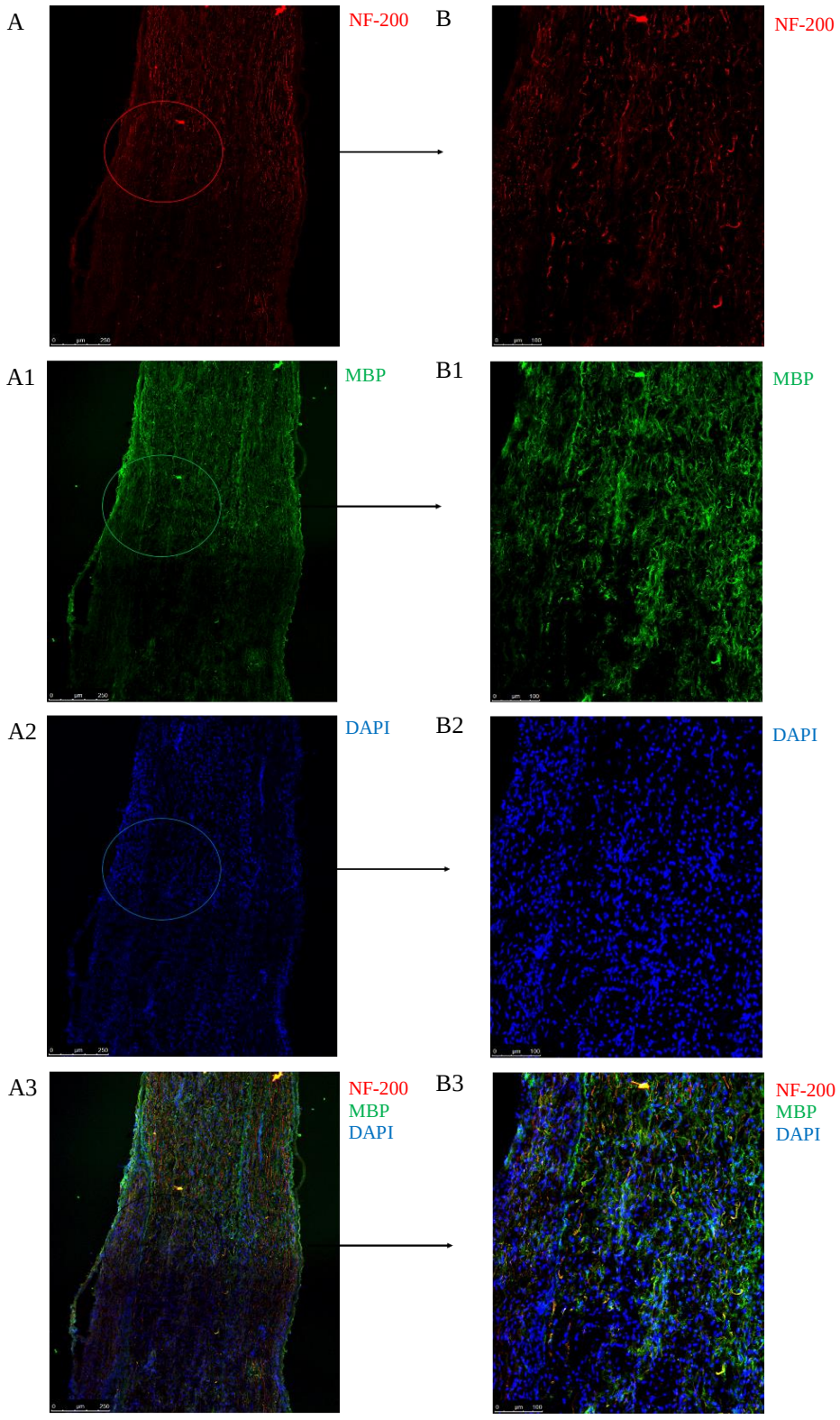

Figure 5.5. Immunostainings of horizontal sections of sciatic nerve dissected 7 days after LPC injection. A. 10x magnification. B. 20x magnification. MBP in green, NF-200 in red and DAPI in blue.

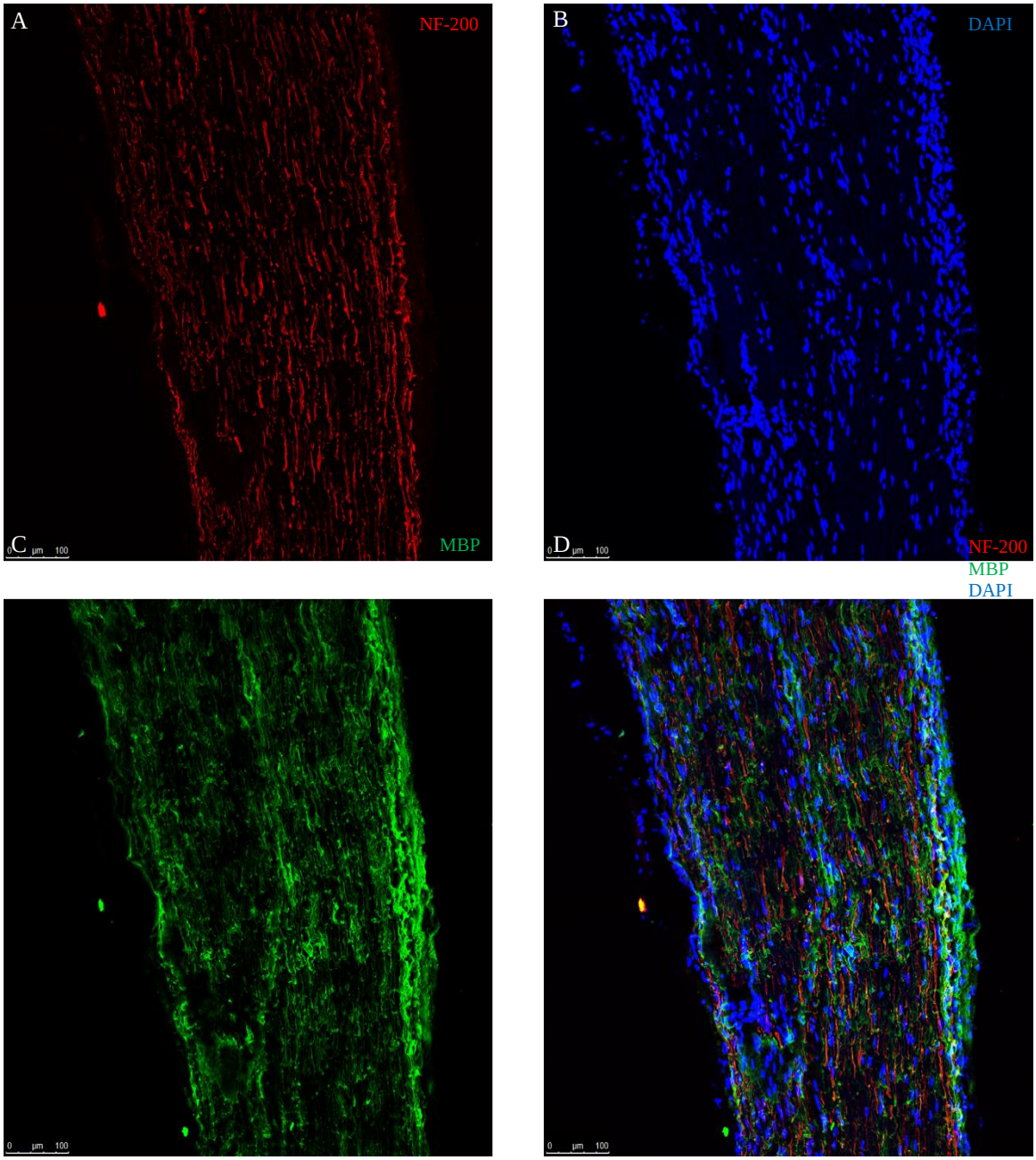

Figure 5.6. Immunostainings of horizontal sections of sciatic nerve dissected 14 days after LPC injection. A. 10x magnification. MBP in green. B. DAPI in blue. C. NF-200 in red. D. Merged image.

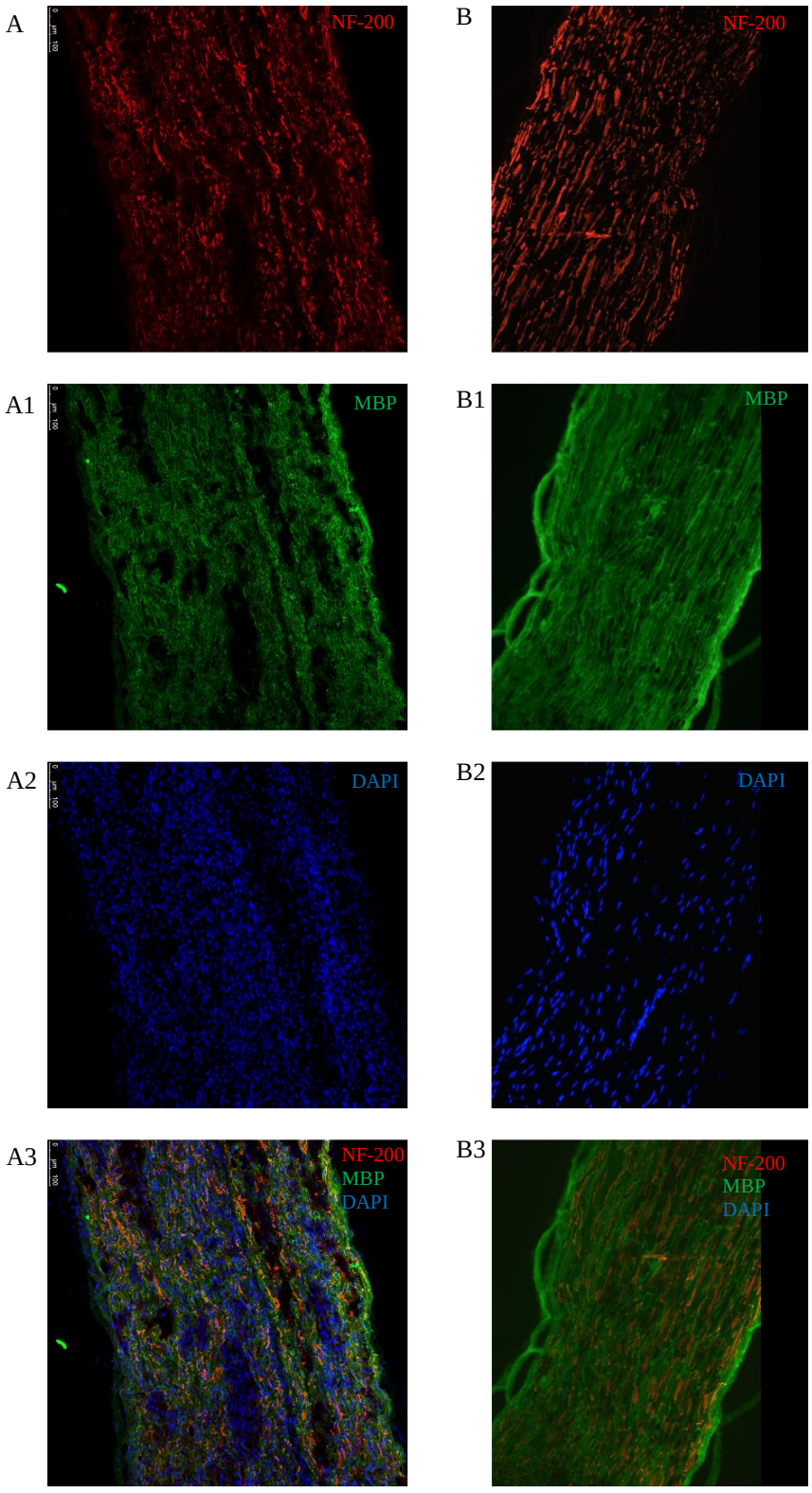

Figure 5.7. A. Immunostainings of horizontal sections of sciatic nerve 1 month after LPC injection. B. control group injected with isotonic saline solution. MBP in green, NF-200 in red and DAPI in blue.

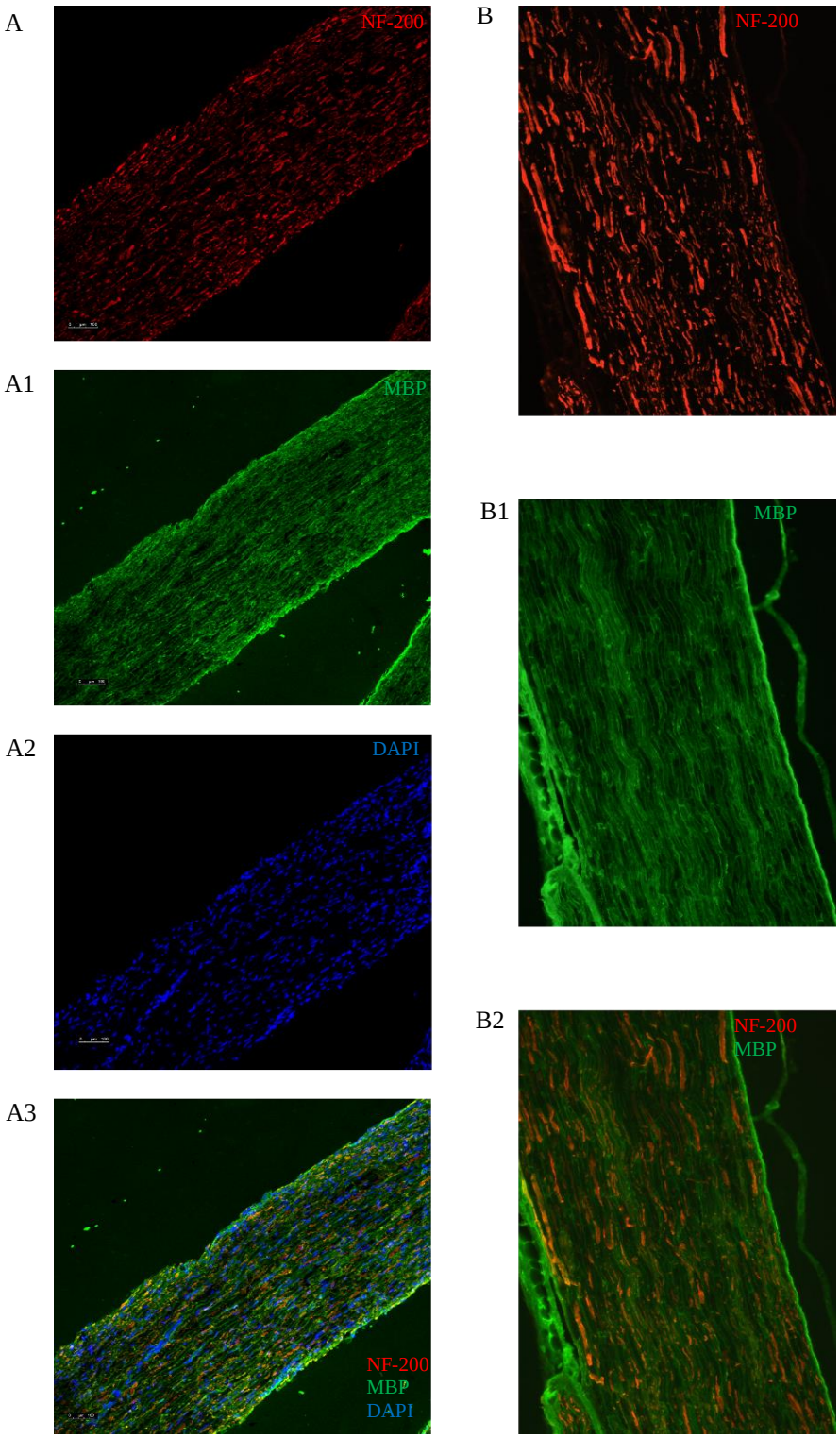

Figure 5.8. Immunostaining of horizontal sections of sciatic nerve which was dissected 2 months after LPC injections. Myelin sheath was stained with MBP in green, neurofilaments were stained with NF-200 and nuclei of Schwann cells were labelled with DAPI. A. LPC treated nerve. B. 0.09% NaCl treated nerve.

Eventually, the myelin sheath was highly organized and recovered at 3 months after LPC injections compared to 1-2 months. Neurofilaments were also in finely organized appearance (Figure 5.9).

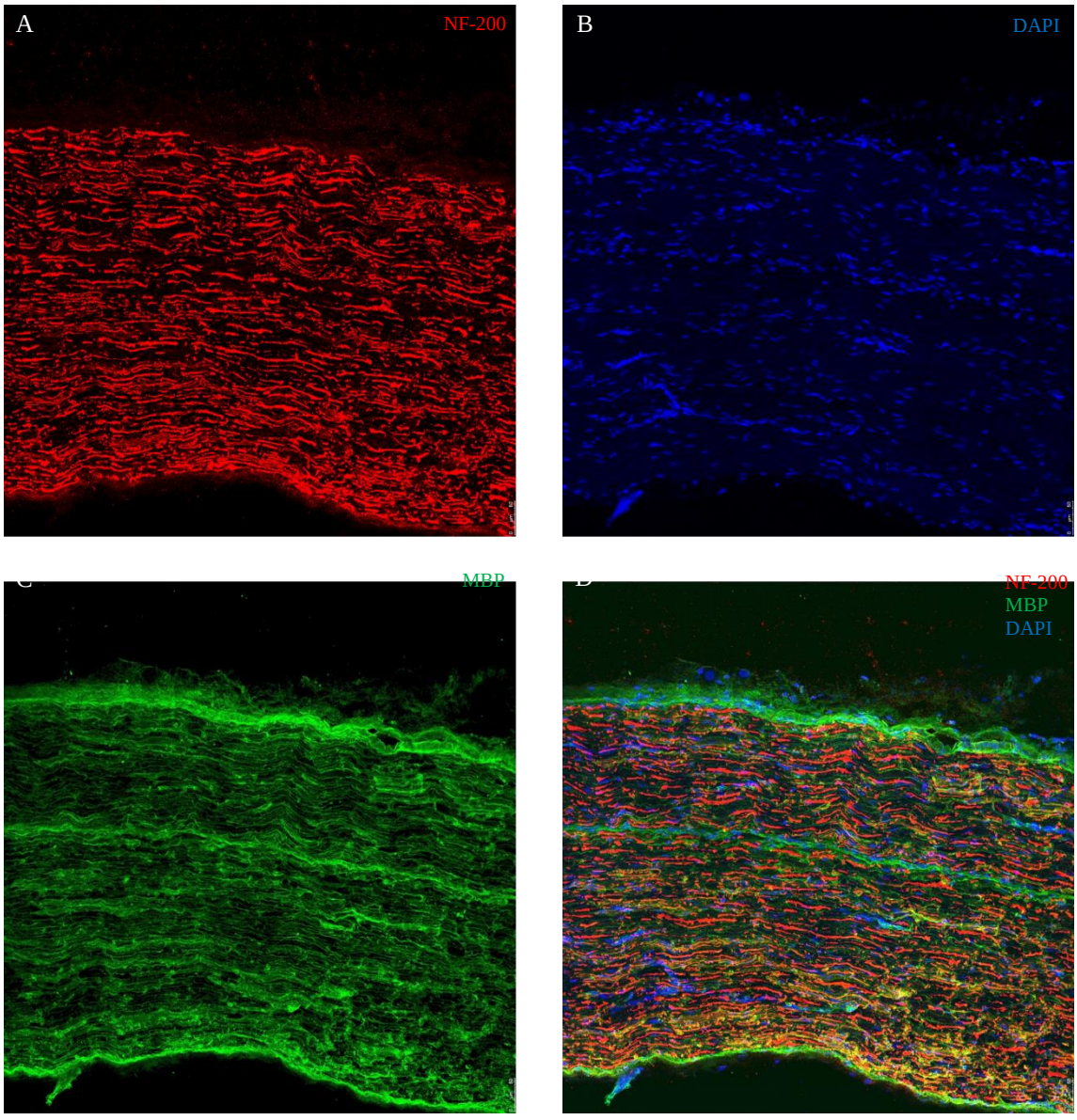

Figure 5.9. Immunostaining of horizontal sections of sciatic nerve which was dissected 3 months after LPC injections. Myelin sheath was stained with MBP in green, neurofilaments were stained with NF-200 and nuclei of Schwann cells were labelled with DAPI.

Transverse sections were also obtained at time points 1 month, 2 months and 3 months after LPC injections and controls. They were stained with anti MBP, NF-200 and DAPI to visualize the myelin sheath, neurofilaments and Schwann cells' nuclei, respectively. With the help of transverse sections, we are able to see each bundle of sciatic nerve that is surrounded by the myelin sheath. The myelin sheath should be in circular shape and the middle of it should have neurons that look like a dot. In Figure 5.10, neurofilaments in red color, formed bundle-like structures of the nerve side by side. Myelin sheaths surrounding each neurofilament bundle have normal round shape, in green. Schwann cells' nuclei are elongated and located around the neurofilaments as expected.

In Figure 5.11, myelin sheath of sciatic nerve dissected 1 month after LPC injection showed a disturbed round shape, seemed to be disorganized, and still lost to some extent. Neurofilaments did not seem to be finely structured compared to controls. Also, some of the Schwann cells' nuclei appeared rounded unlike elongated nuclei in control groups.

In Figure 5.12, myelin sheath seemed to be recovered more 2 month after LPC injection compared to samples harvested at 1 month. But it was still disorganized to some extent and some of myelin sheath did not have fine circular shape. However, Schwann cells' nuclei were elongated as it should be during remyelination.

In sciatic nerves harvested at 3 months after injection, the myelin sheath was finally in normal circular shape that surrounded neurofilaments as in control sections (Figure 5.13).

After LPC injections, the myelin sheath became disorganized during demyelination and was lost. Immunostaining of horizontal and transverse sections showed that 7 days after LPC injections the myelin sheath appeared damaged and mostly disappeared during demyelination. After that point, remyelination started and the recovery was still ongoing at 1 month after injections. The myelin sheath assumed its normal condition at 2 months and eventually it appeared fully recovered at 3 months after LPC injections.

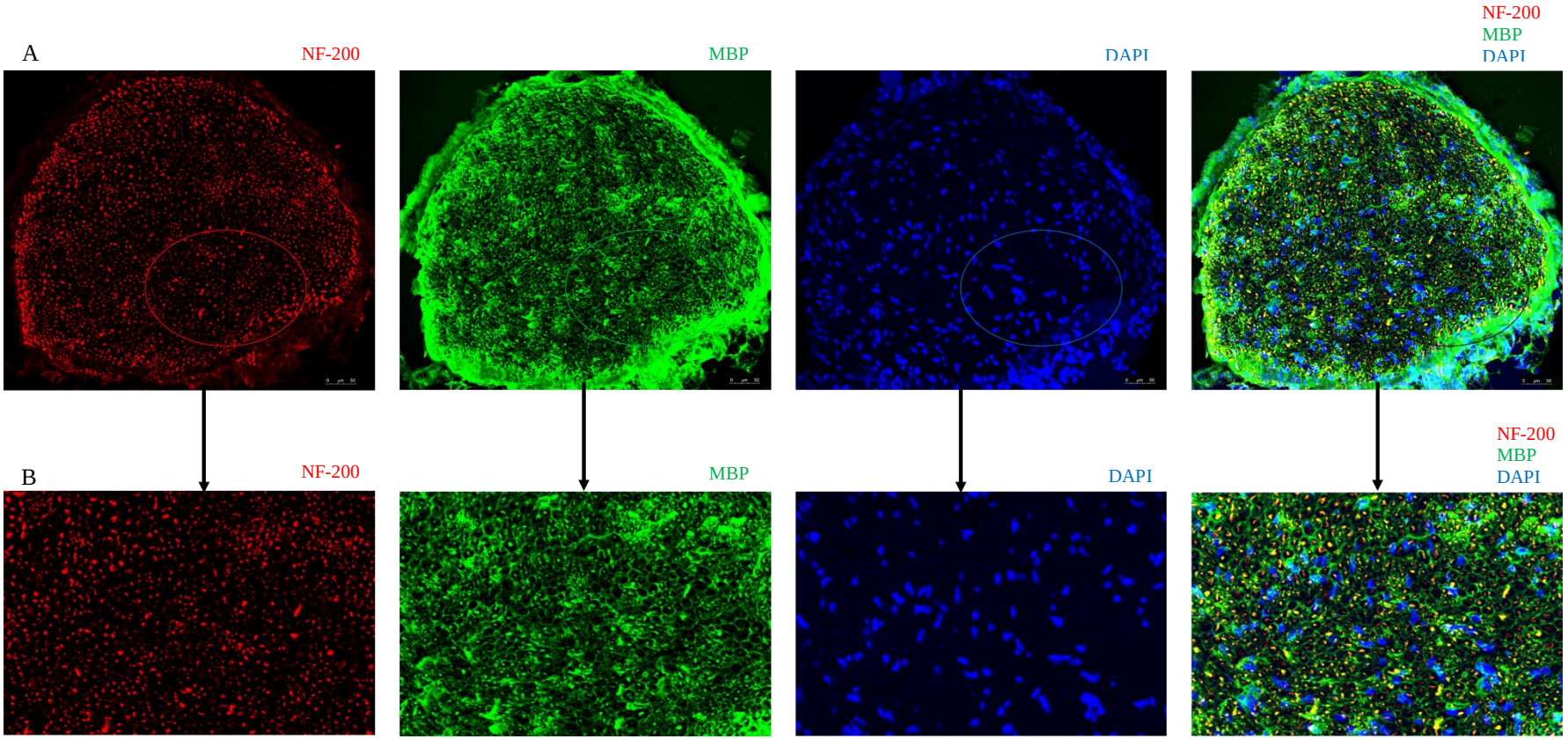

Figure 5.10. Immunostainings of transverse sections of sciatic nerve which was dissected 3 months after NaCl injections. Myelin sheath was stained with MBP (green), neurofilaments were stained with NF-200 (red) and nuclei of Schwann cells were labelled with DAPI (blue). A.10x magnification. B. 20x magnification.

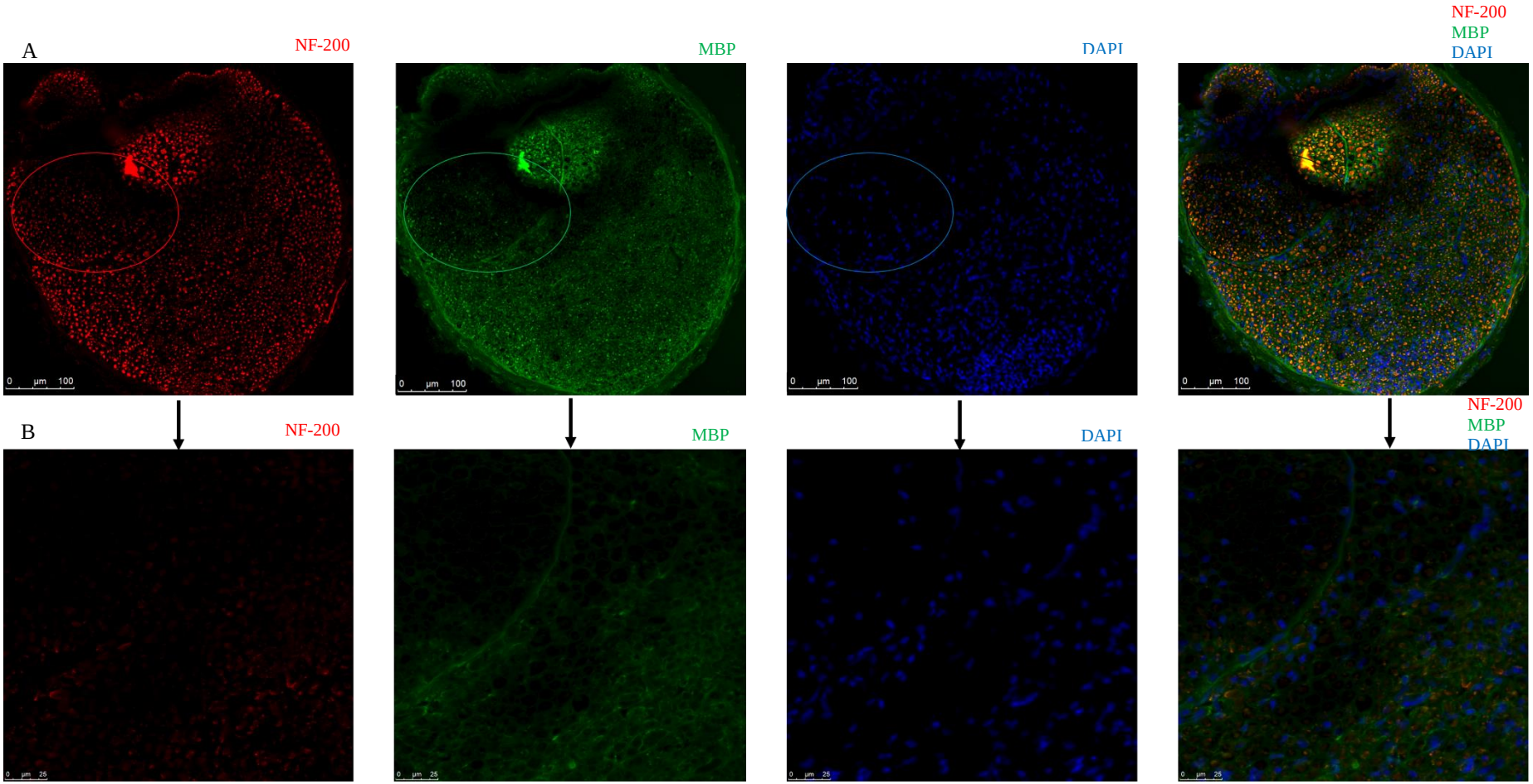

Figure 5.11. Immunostainings of transverse sections of sciatic nerve dissected 1 month after LPC injections. NF-200 in red, MBP in green, DAPI in blue. A. 10x magnification. B. 20x magnification.

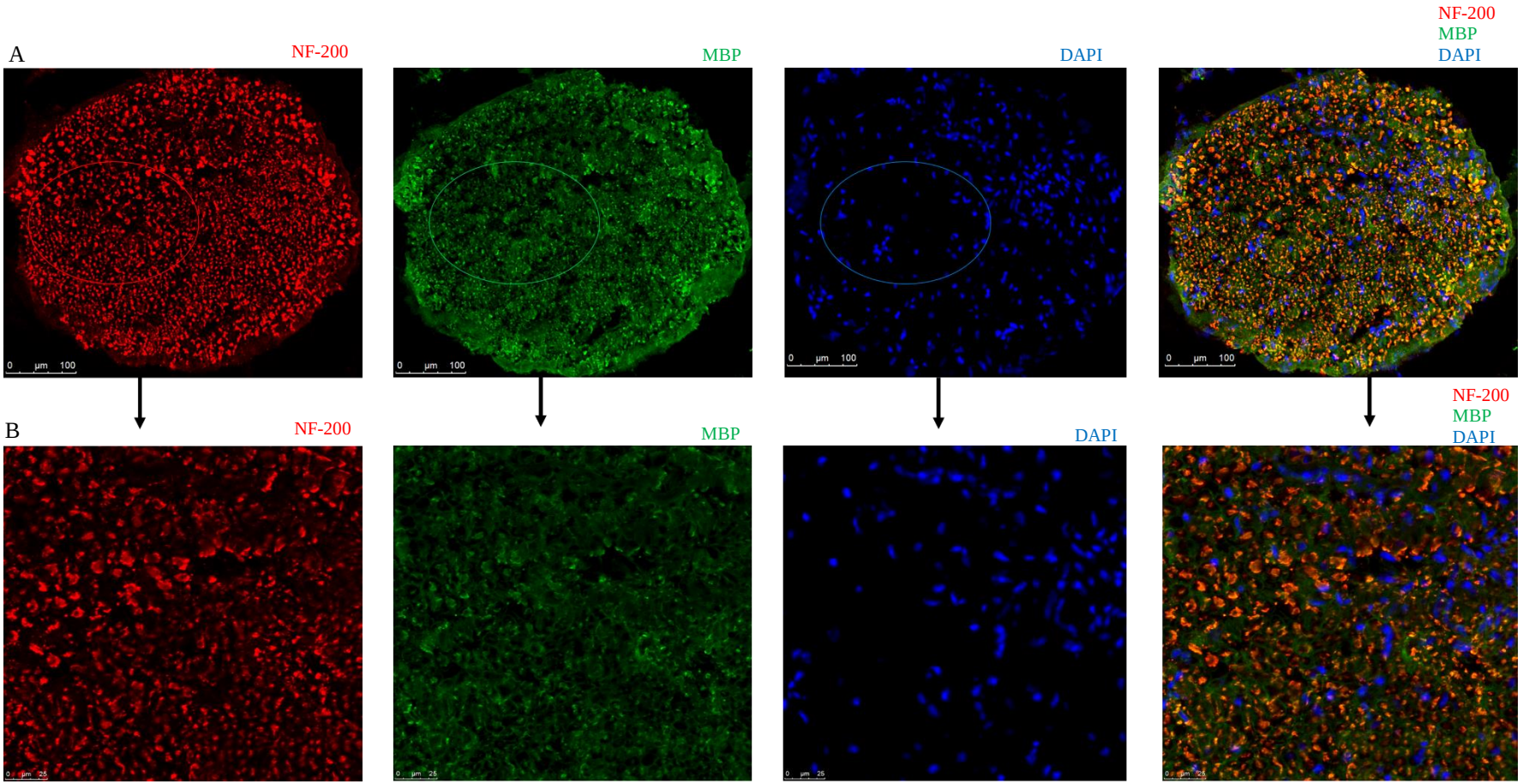

Figure 5.12. Immunostainings of transverse sections of sciatic nerve dissected 2 month after LPC injections. NF-200 in red, MBP in green, DAPI in blue. A. 10x magnification. B. 20x magnification.

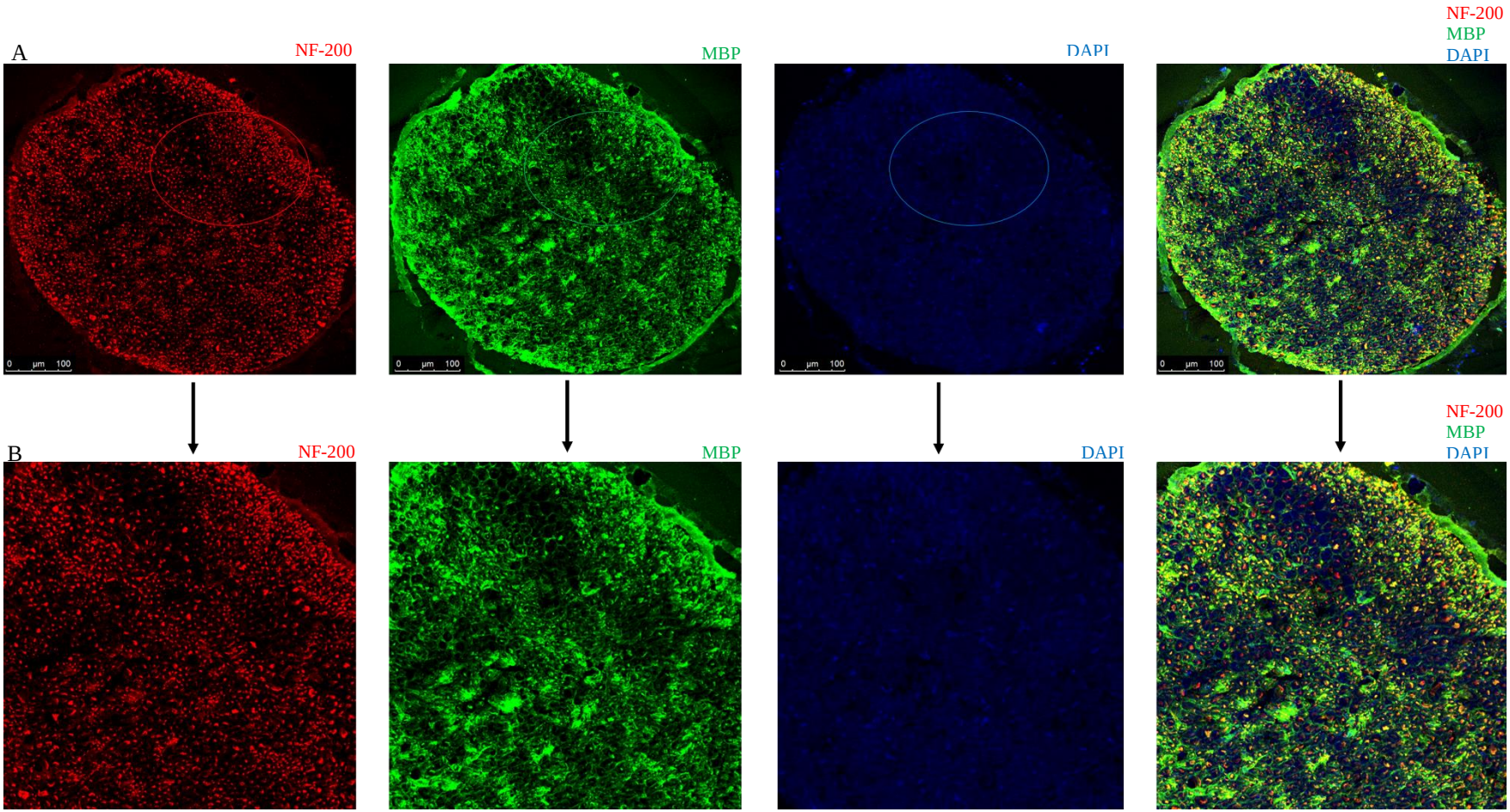

Figure 5.13. Immunostainings of transverse sections of sciatic nerve dissected 3 month after LPC injections. NF-200 in red, MBP in green, DAPI in blue. A. 10x magnification. B. 20x magnification.

5.1.3. Mouse Recombinant FGF1 Injections

To investigate possible FGF1 involvement in remyelination after LPC induced demyelination, FGF1 was directly injected to the sciatic nerve of mice.

Mice were initially injected with 2% LPC to induce demyelination. 7 days after LPC injection when remyelination started, mice were injected with 100 µg/ml of FGF1 or 0.09% NaCl for negative controls. Fifteen days after the injection of LPC, mice were sacrificed and the expression of myelin proteins were analyzed by western blot analysis (Figure 5.14).

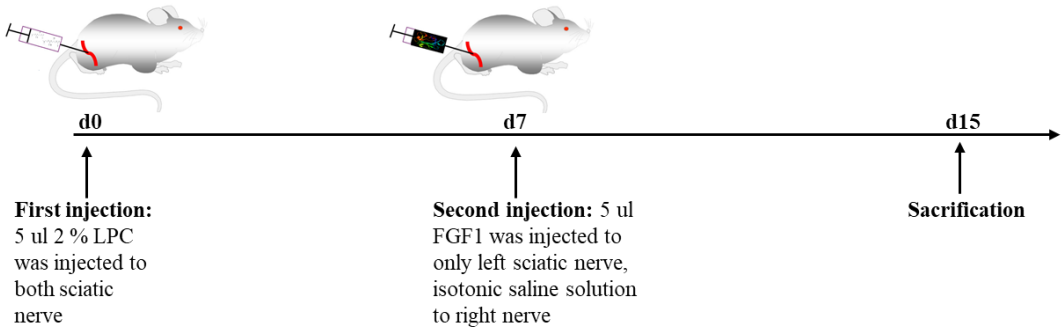

Figure 5.14. Timeline of injections of first experimental design.

MAG and MBP expression were analyzed. Expression of the MAG protein was increased slightly in FGF1 injected group compared to control groups that were injected with saline solution. When Student t-test was used for statistical evaluation of the results from three biological repeats and experimental repeats, the change in FGF was not found to be statistically significant. When expression of MBP was analyzed using the same methodology, there was a slight increase but it was not statistically significant, either (Figure 5.15 or Figure 5.16).

To check whether increasing the concentration of injected FGF would affect the expression of myelin proteins, the injected FGF1 concentration was increased to 200 µg/ml. Even at this higher FGF1 concentration, the expression of MAG was not affected (Figure 5.17).

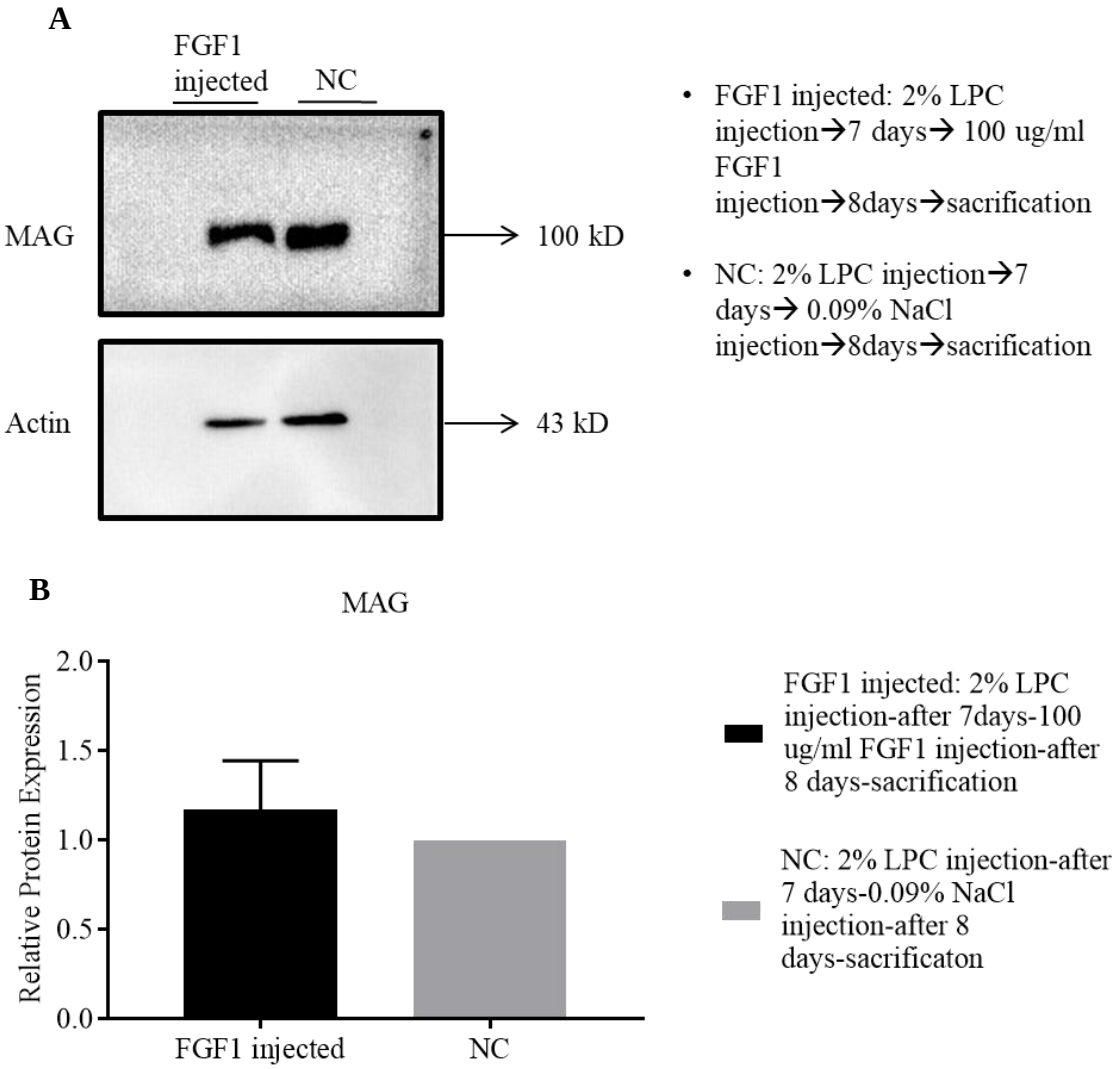

Figure 5.15. Western blot analysis of MAG levels after 100 µg/ml FGF1 injection. A. Expression in two experimental groups, FGF1 injected and NC. B. Analysis of relative protein expression to actin. P value= 0.1934. For analysis, three experimental and three biological repeats were performed. T-test was applied.

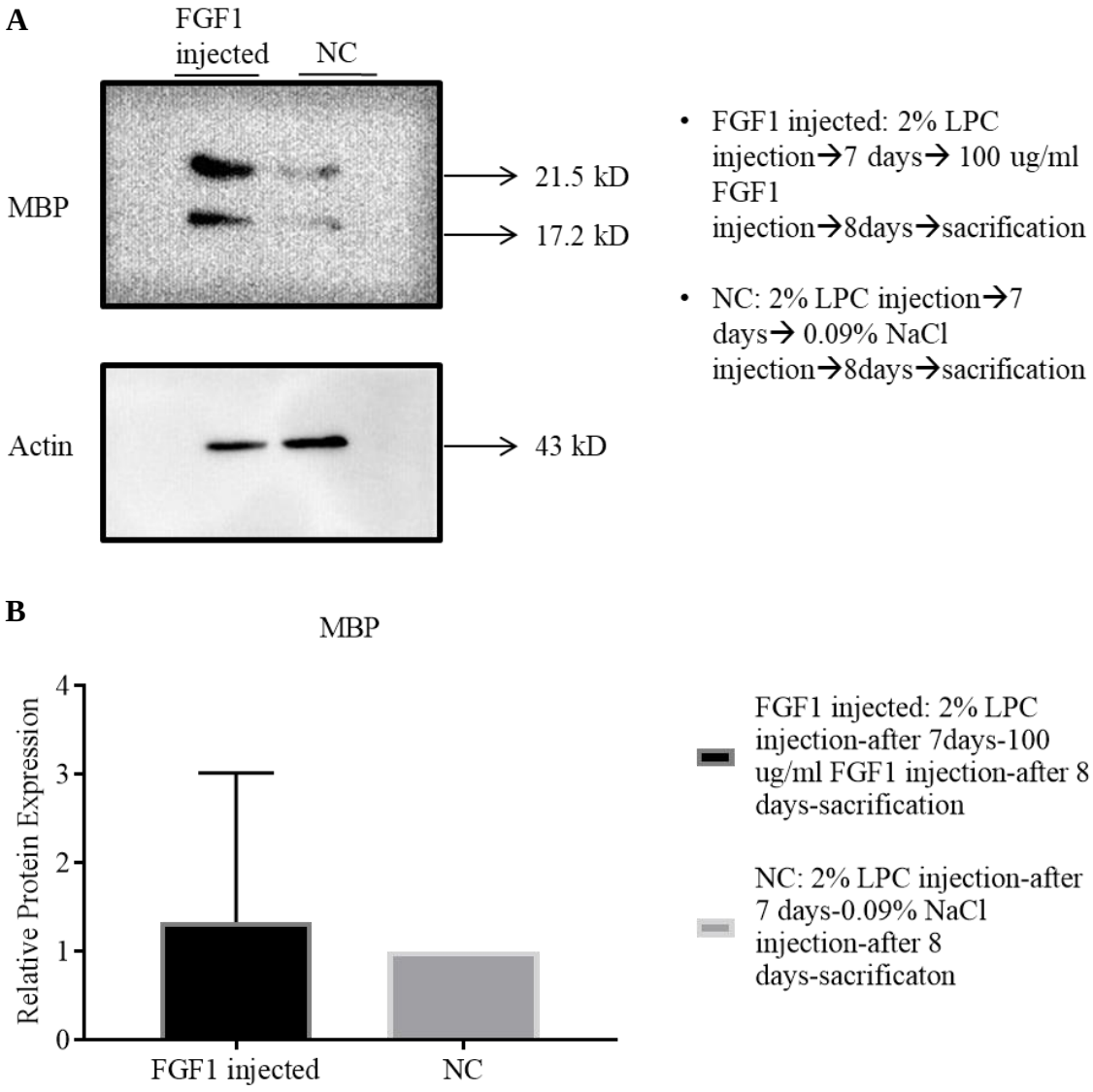

Figure 5.16. Western blot analysis of MBP levels after 100 μg/ml FGF1 injection. A. Expression in two experimental groups, FGF1 injected and NC. B. Analysis of relative protein expression to actin. P value= 0.8069. Experimental and biological repeats were performed. T-test was used.

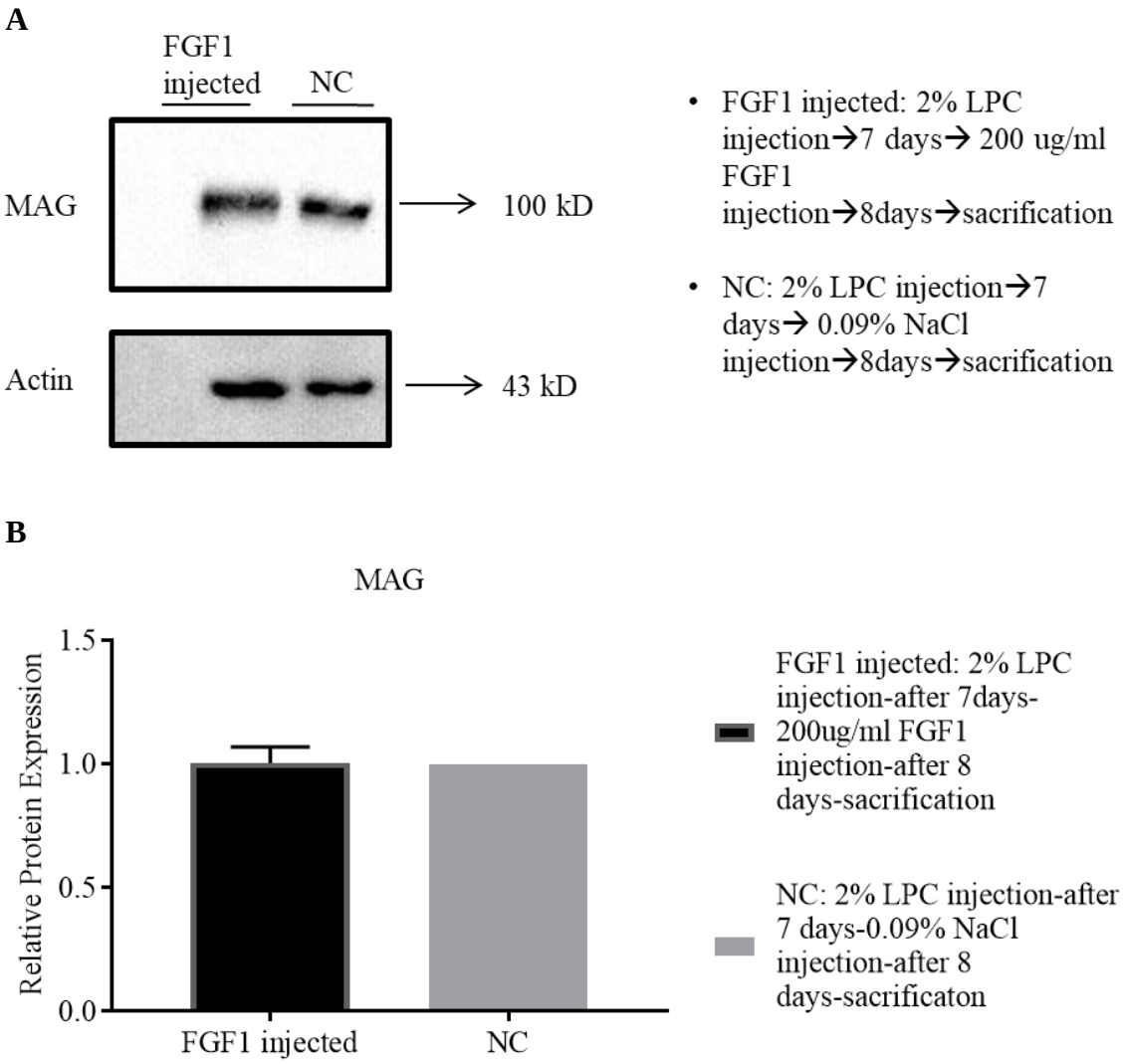

Figure 5.17. Western blot analysis of MAG levels after 200 µg/ml FGF1 injection. A. Expression in two experimental groups, FGF1 injected and NC. B. Analysis of relative protein expression to actin. Only experimental repeats were performed.

Since FGF is well known to exert its effects instantly and transiently, another experiment was designed in which mice were sacrificed in 30 minutes after FGF1 injection. The myelin protein expression was investigated by western analysis. The time table for this experiment was given in Figure 5.18.

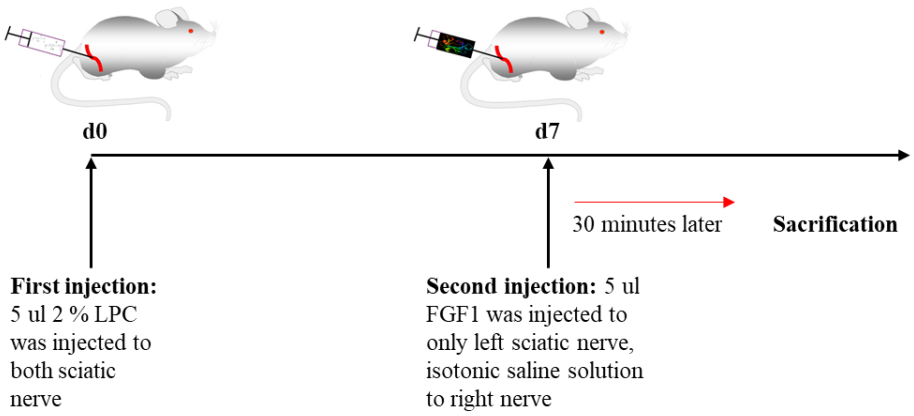

Figure 5.18. Timeline of injections of second experimental design.

To prove that FGF1 was injected to the nerves, the level of it was analyzed in FGF1 and NaCl injected sciatic lysate that followed the injection timeline in Figure 5.18. In Figure 5.19, FGF1 in FGF1 injected group was almost 7.5 fold increased as compared to the NaCl injected group. Figure 5.19 depicts two experimental repeats of one injection.

When myelin proteins were analyzed relative to actin in the second group of mice that were treated as in Figure 5.18, the MAG levels were found to be increased approximately 2.5 fold in the FGF1 injected group compared to that of the control group. Three experimental and biological repeats were performed and when t-test was used to analyze the results, the up-regulation of MAG was shown to be statistically significant with a p value of 0.0096 (Figure 5.20).

Using the same methodology, the MBP levels were also analyzed. We were able to observe only the 21.5 kD isoform of MBP on the western blots with the antibody used. MBP levels in FGF1 injected sciatic nerves was increased almost 2 fold as compared to the control groups. The difference between the expression of this isoform between two experimental groups was analyzed by t-test for 3 independent biological repeats and found to be statistically significant with a p value of 0.0134 (Figure 5.21).

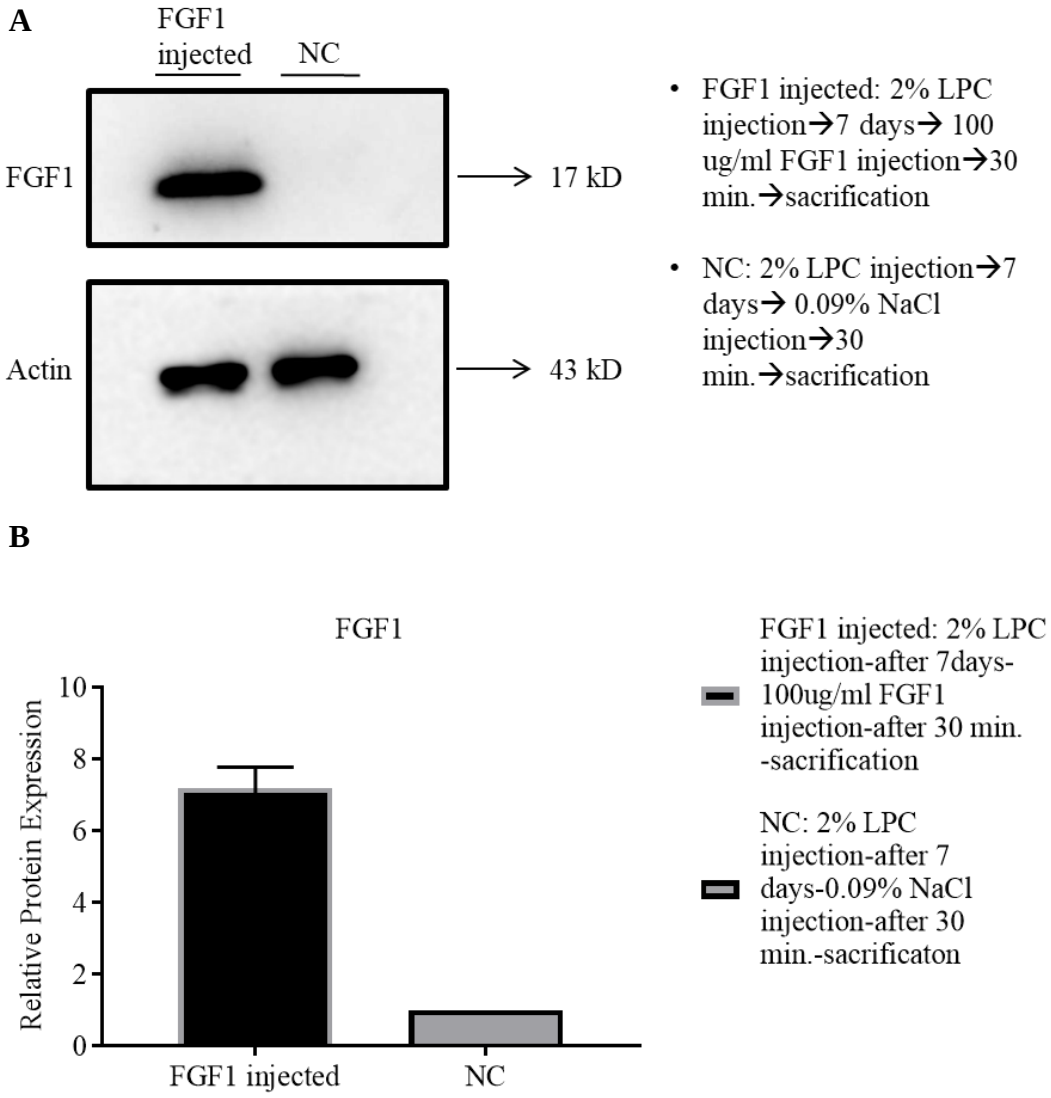

Figure 5.19. Analysis of FGF1 level in FGF1 injected and control groups. A. FGF1 expression of FGF1 injected and NC. B. The difference between two groups was depicted graphically.

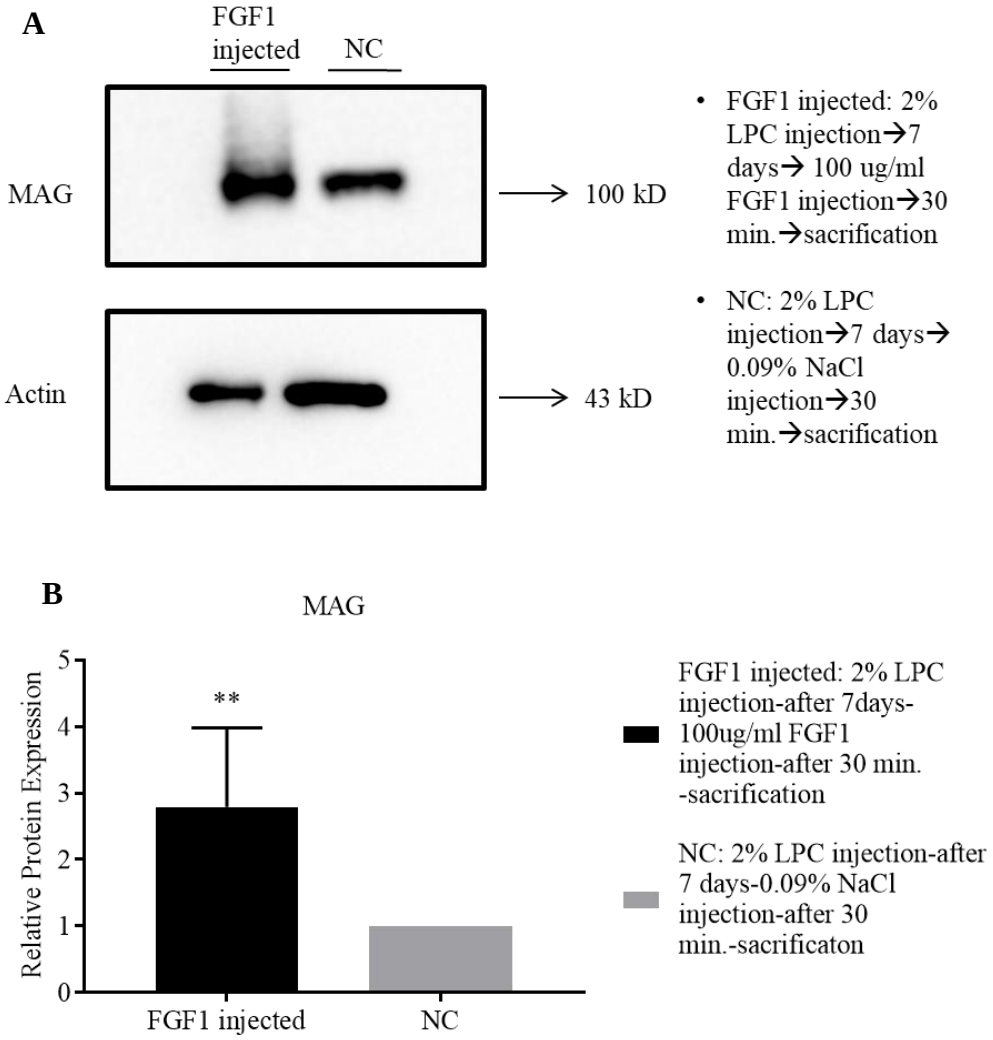

Figure 5.20. Western blot analysis of MAG levels after 100 µg/ml FGF1 injection. A. Expression in two experimental groups, FGF1 injected and NC. B. Analysis of relative protein expression of actin. Mean values of 3 independent experiments were graphically depicted, * $p < 0.05$ and ** $p < 0.01$. B. Timeline of the injections.

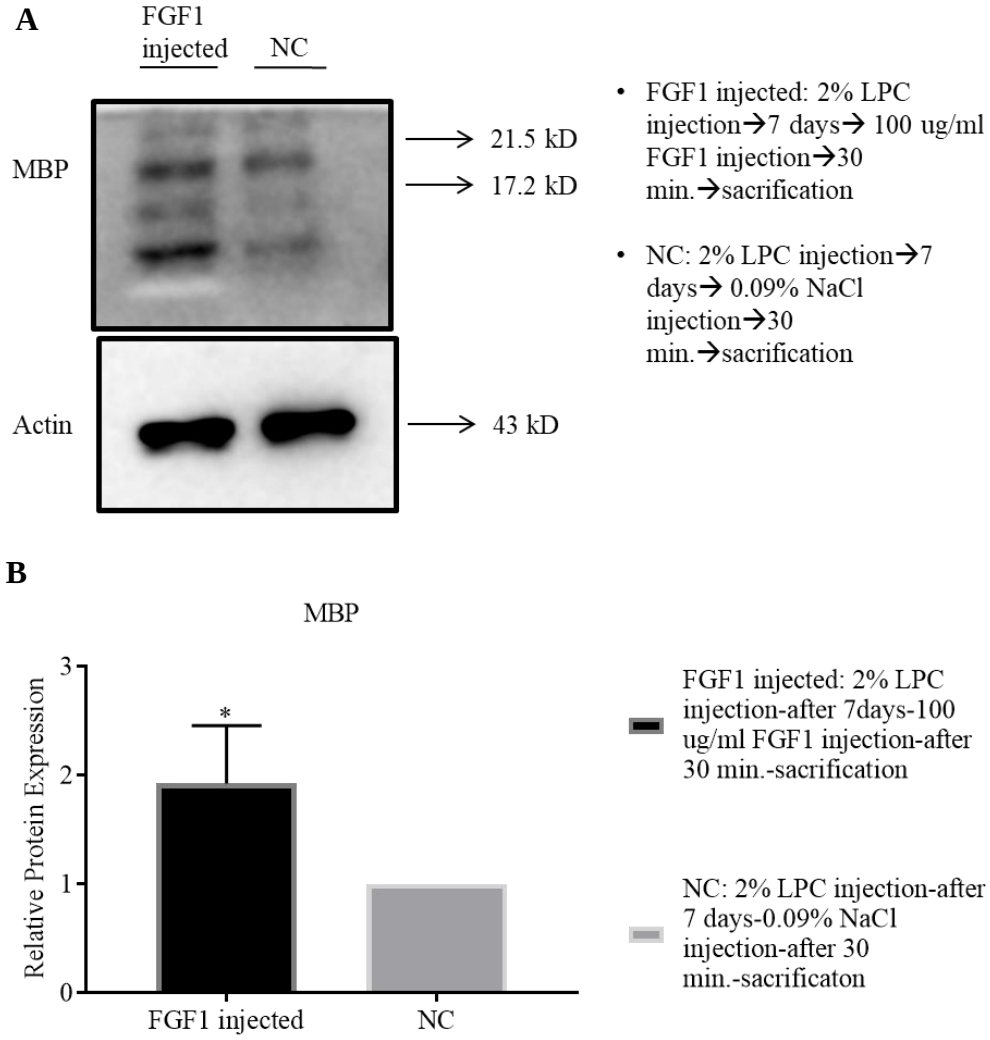

Figure 5.21. A. Western blot analysis of MBP levels after 100 µg/ml FGF1 injection. B. Analysis of relative protein expression of actin. Mean values of 3 independent experiments were graphically depicted, * $p < 0.05$ and ** $p < 0.01$.

When we analyze the FGF1 levels of two independent experiments, FGF1 level of FGF1 injected group of 1st and 2nd experiments was different even though both groups were injected with 100 µg/ml mouse recombinant FGF1. FGF1 level of FGF1 injected group of 2nd experiment was higher as almost two fold of FGF1 level of FGF1 injected group of 1st experiment (Figure 5.22). Also MAG and MBP levels were almost two fold more in 2nd experimental group than in 1st experimental group.

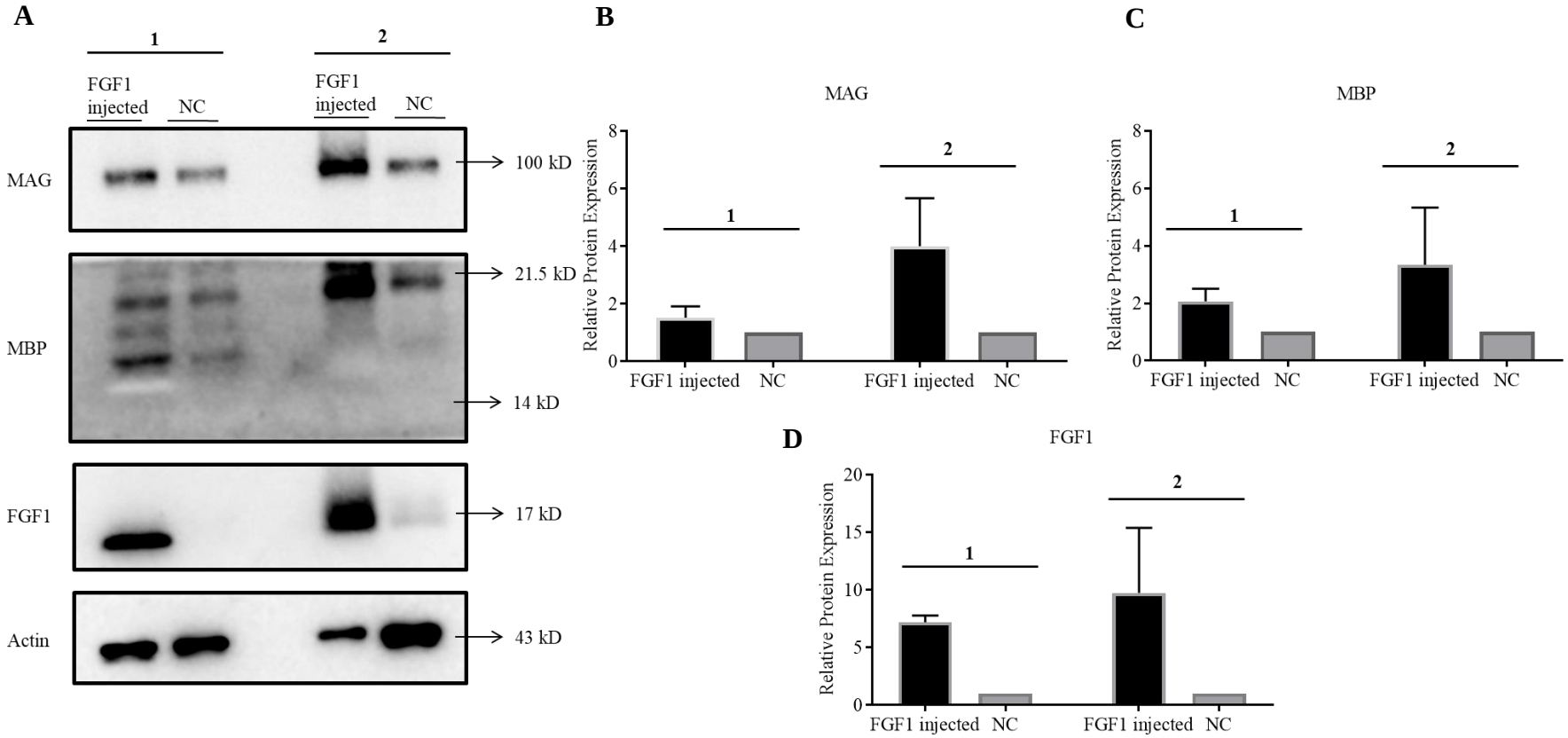

Figure 5.22. Analysis of FGF1 levels for two biological repeats. A. Expression of MAG, MBP and FGF1 in FGF1 injected and NC groups of two independent experiments depicted as 1st and 2nd. B. Relative protein expression of MAG of FGF1 injected and control groups of 1st and 2nd experiments. C. Relative protein expression of MBP of FGF1 injected and control groups of 1st and 2nd experiments. D. Relative protein expression of FGF1 of FGF1 injected and control groups of 1st and 2nd experiments. Two experimental repeats were performed.

5.2. Dorsal Root Ganglion (DRG) Co-culture and Protein Levels Analysis

To identify possible interaction partners of FGF1 in myelinating co-culture, DRG co-cultures were performed. After dissecting and seeding of DRGs of E14.5 embryos into 6-well plates, DRGs were exposed to nerve growth factor (NGF) to allow the development of neurons. After Schwann cells and neurons populated the culture, they were supplied with ascorbic acid to induce myelination. Ascorbic acid is very well known to help Schwann cells to produce a myelin sheath and wrap the neurons. The development of myelin sheath was monitored by light microscopy and according to their development rate the type of medium was changed to an appropriate one. Some DRG co-cultures showed tendency to detach after seeding and were supplied with further nerve growth factor. Some of them were supplied in myelinating co-culture more than 21 days to become healthier and produce a myelin sheath. When myelin production reached to a certain level in the co-culture, the cells were fixed and analyzed by immunocytochemistry. Both fluorescence and confocal images were captured for which examples are given in Figure 5.23 and Figure 5.24, respectively.

After observation of myelin sheath in DRG co-cultures, co-immunoprecipitation method was used to elute FGF1 and its possible interaction partners that may be involved in myelination. For this purpose, DRG co-cultures were supplied with myelinating medium for 21-29 days and then were ceased and lysed with Co-IP lysis buffer. For negative control of Co-IP, liver from E13.5 mice were dissected and lysed with Co-IP lysis buffer.

DRG co-cultures and liver from E13.5 mice were also lysed with a special lysis buffer that contains 2% SDS to determine the FGF1 level in those co-cultures and liver samples before precipitating FGF1 from those co-cultures. E13.5 liver was reported not to express FGF1 protein and we initially confirmed its absence in liver. It also allowed us to gain insight about the approximate FGF1 amount in our co-cultures. That information helped us to determine the concentration of antibody that was used to precipitate FGF1 from lysates. FGF1 level in sciatic lysates of untreated 2 months mice was also analyzed. FGF1 levels of myelinating DRG co-culture, untreated sciatic lysates and liver were demonstrated in Figure 5.25. FGF1 and MAG were not expressed by liver tissues as expected. FGF1 was present in 20 μg and 40 μg sciatic and DRG lysates. MAG was highly expressed by sciatic nerve and DRG co-cultures as expected.

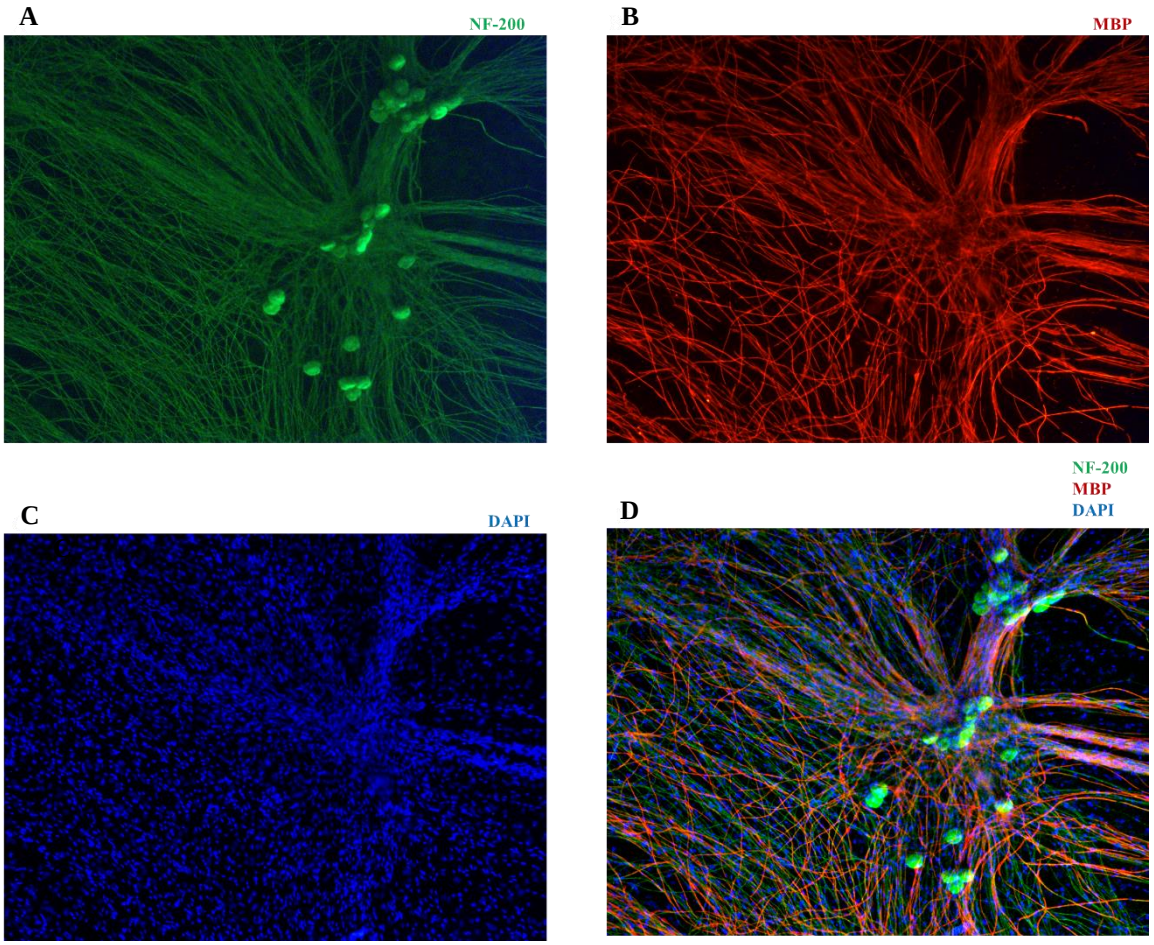

Figure 5.23. Myelin sheath of mouse DRG-Schwann cells co-culture by fluorescence microscopy. A. NF-200 in green. B. MBP in red. C. Nuclei of Schwann cells in blue. D. composition of images. 20x magnification.

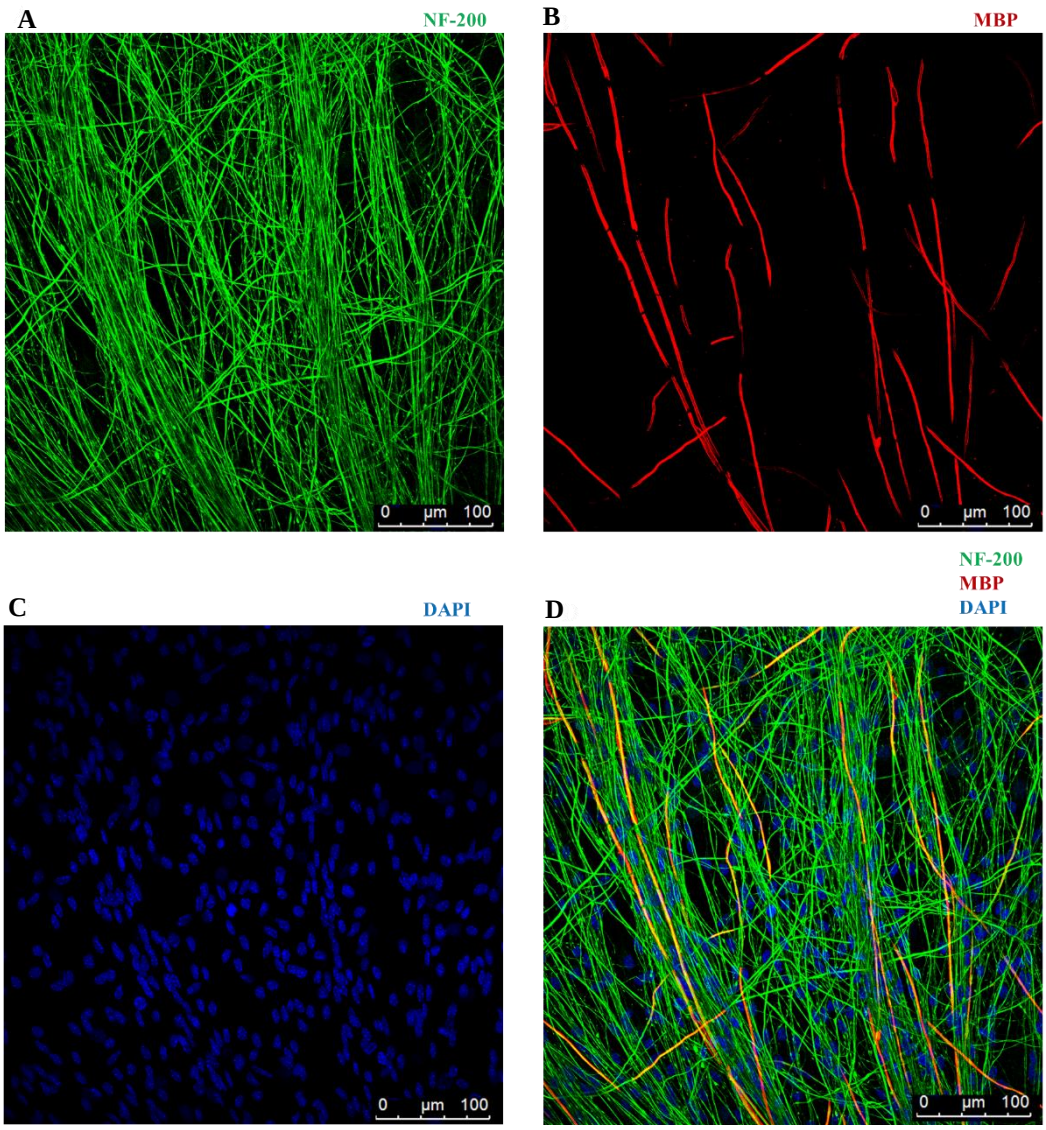

Figure 5.24. Myelin sheath of mouse DRG-Schwann cells co-culture by confocal microscopy. A. NF-200 in green. B. MBP in red. C. Nuclei of Schwann cells in blue. D. composition of images. 20x magnification.

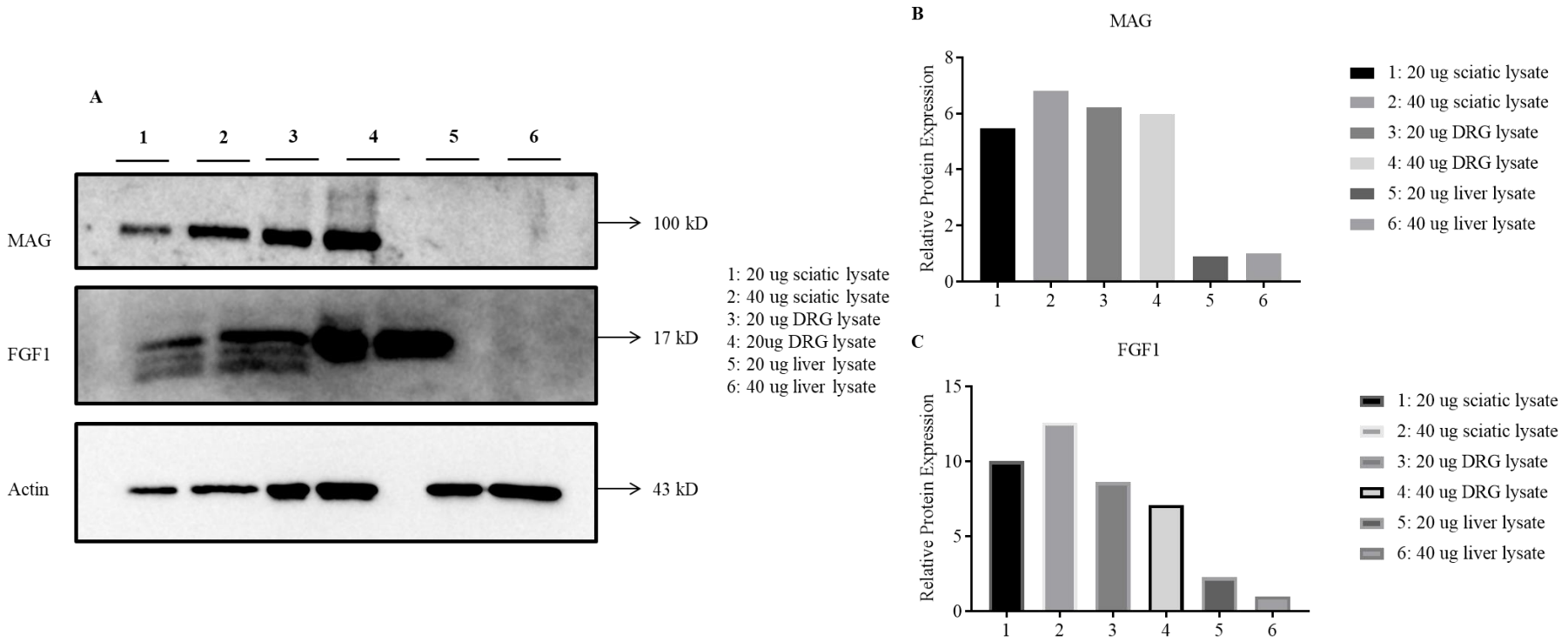

Figure 5.25. Analysis of FGF1 levels in 20 µg and 40 µg sciatic nerve lysates, 20 µg and 40 µg myelinating DRG co-cultures lysates, 20 µg and 40 µg E13.5 liver lysates. A. FGF1 and MAG levels. B. Relative protein expression of MAG to actin. C. Relative protein expression of FGF1 to actin. Only experimental repeats were performed for this analysis.

FGF1 and FGFR1 levels were analyzed for unmyelinated DRG co-cultures, myelinated DRG co-cultures, sciatic lysates from untreated 2 months mice, and E13.5 liver lysates (Figure 5.26).

FGF1 was not expressed by liver as expected that proved our literature survey. Therefore, it was shown that liver was a suitable negative control for further Co-IP experiments.

FGF1 and FGFR1 were expressed by sciatic nerve and myelinating DRG co-culture, in accordance with our previous data.

FGFR1 was also expressed by E13.5 liver that was known by literature survey.

When FGF1 levels of unmyelinated and myelinated cultures were analyzed, FGF1 expression was almost absent in unmyelinated DRG co-cultures while its expression was highly increased in myelinating DRG co-cultures.

Also, FGFR1 expression was abundant in myelinating DRG co-cultures while it was almost absent in unmyelinated DRG co-cultures, in accordance with our previous data.

The increase in FGF1 and FGFR1 levels during PNS developmental myelination was further confirmed with this study (Figure 5.26)

Also, our western blot analysis showed E13.5 liver does not express FGF1 while FGFR1 was shown to be expressed. This data provide further evidence for the literature knowledge.

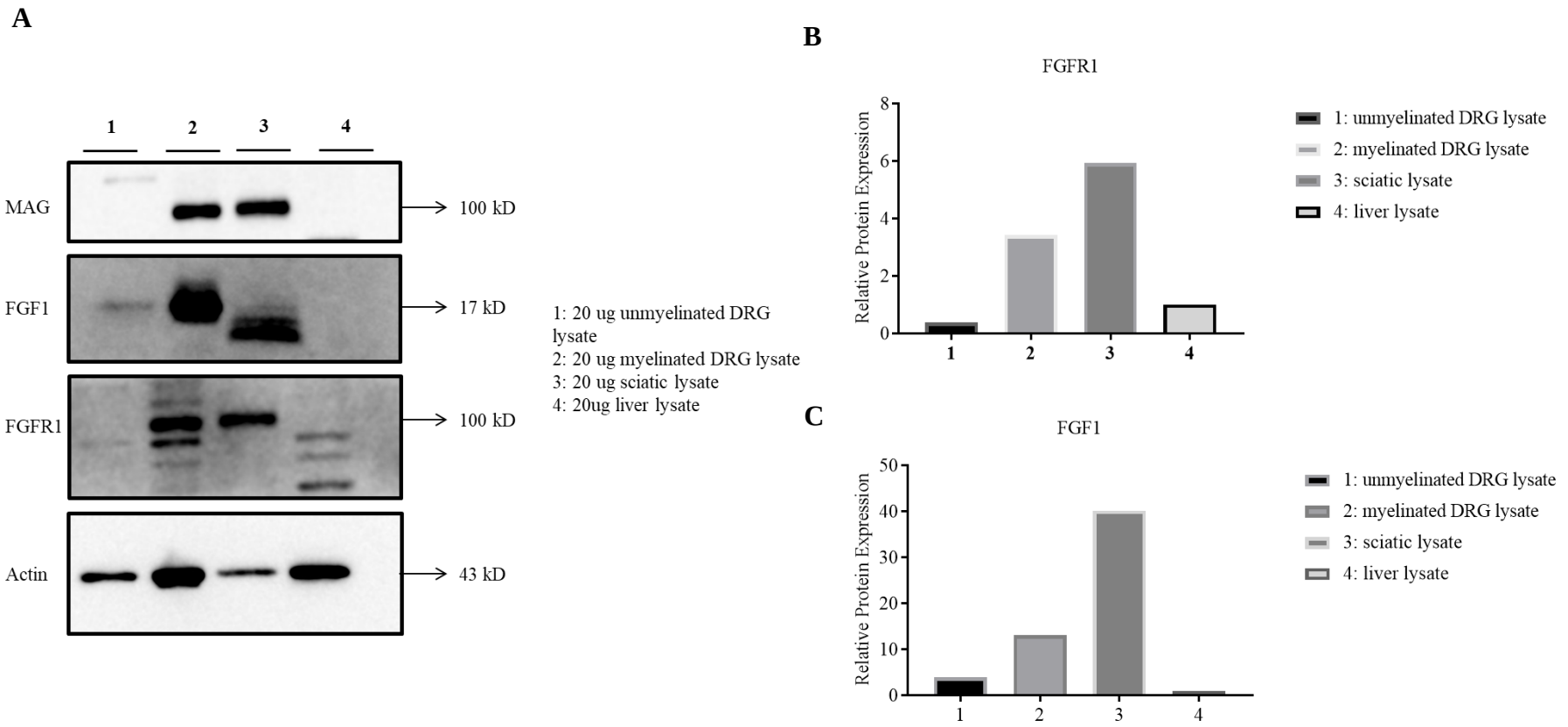

Figure 5.26. Analysis of FGF1 levels in unmyelinating DRG co-cultures lysates, myelinating DRG co-cultures lysates, sciatic nerve lysates, and E13.5 liver lysates. A. FGF1 and MAG levels. B. Relative protein expression of MAG to actin. C. Relative protein expression of FGF1 to actin. Only experimental repeats were performed for this analysis.

FGF1 levels of unmyelinated DRG co-cultures and myelinated co-cultures were analyzed statistically by 2 independent biological repeats. FGF1 expression was significantly increased in myelinating DRG co-cultures compared to unmyelinated DRG co-cultures (Figure 5.27).

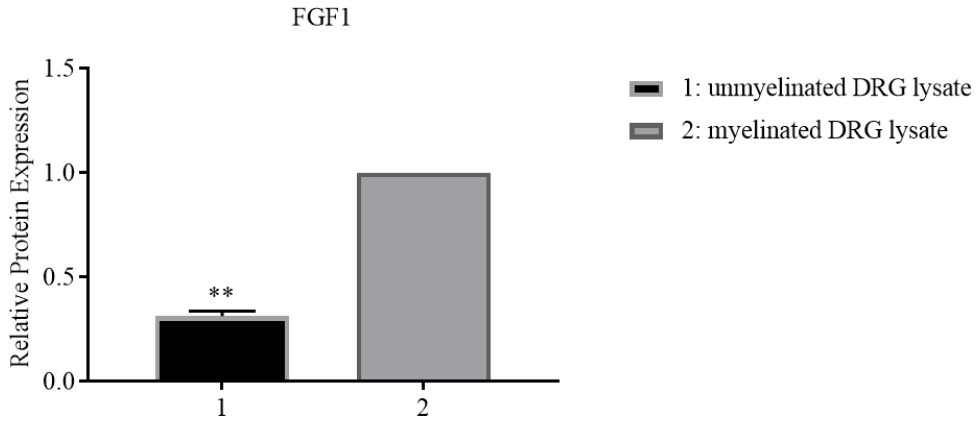

Figure 5.27. Relative Protein Expression of FGF1 to actin in unmyelinated (1) and myelinated (2) DRG lysates. Student t-test was applied for 2 biological repeats. **p<0.01

FGF1 levels of sciatic, myelinating DRG and liver lysates were also statistically analyzed in Figure 5.28.

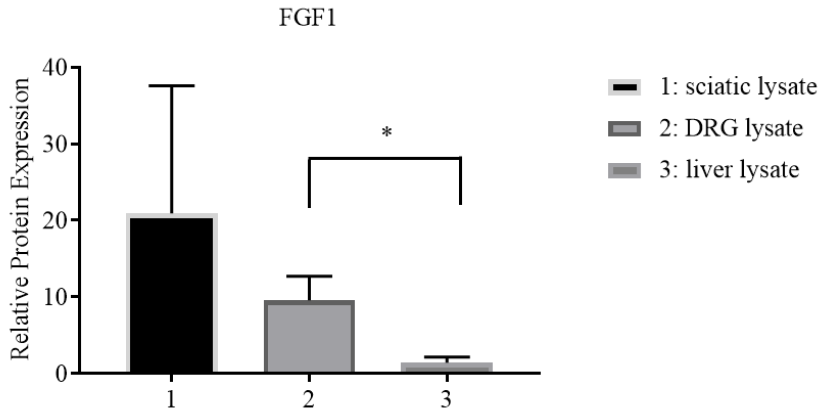

Figure 5.28. Relative Protein Expression of FGF1 to actin. 1: sciatic lysates, 2: myelinated DRG lysates, 3: liver lysates. t-test was applied for 2 biological repeats. *p<0.01

5.2.1. Co immunoprecipitation (Co-IP)

After FGF1 levels of DRG co-cultures were determined, Co-IP was performed in two different ways. Commercially available sepharose bead conjugated mouse FGF1 antibody was directly incubated with DRG lysates. Next day, bead conjugated FGF1 antibody bound and precipitated FGF1 and possible FGF1 bound proteins. For negative group of this experiment, sepharose beads that was not treated with an antibody was incubated with DRG lysates. After samples were run on SDS-PAGE, it was stained with Coomassie blue. A 17 kD band was observed that is expected with additional bands of 43, 55, and 72 kD. Some bands were common for both experimental and control lysates.

To confirm FGF1 precipitation, samples were run on SDS-PAGE and immunoblotted with sheep anti FGF1 antibody (Figure 5.29). The host of FGF1 antibody (Mouse) that was used for Co-IP was different than the host of FGF1 antibody (Sheep) that was used for Western blot, therefore, cross-reactivity was not expected. FGF1 was observed in experimental group implicating that FGF1 was precipitated successfully. Based on the assumption that the other bands are possible proteins that may interact with FGF1, the protein of interest was tested with its antibody on the immunoblot. One of the bands was around 95 kD that might be the FGFR1 that is widely expressed in PNS. Therefore, antibody against FGFR1 was used to check FGFR1 presence in our Co-IP lysates. However, FGFR1 antibody detected a smooth signal at 55 kD but not in 95 kD in experimental group while it detected smear like signals in control group. FGFR1 was known to have isoform 11- Gamma A2 that is 55 kD that was accepted as a biologically inactive in human but not have been identified in rodents yet. Also, MPZ was known to be involved in myelination, and the bands that were observed with Coomassie blue staining was around the same molecular weight of MPZ. Use of MPZ antibody revealed that MPZ was present in the control group but not in the experimental group.

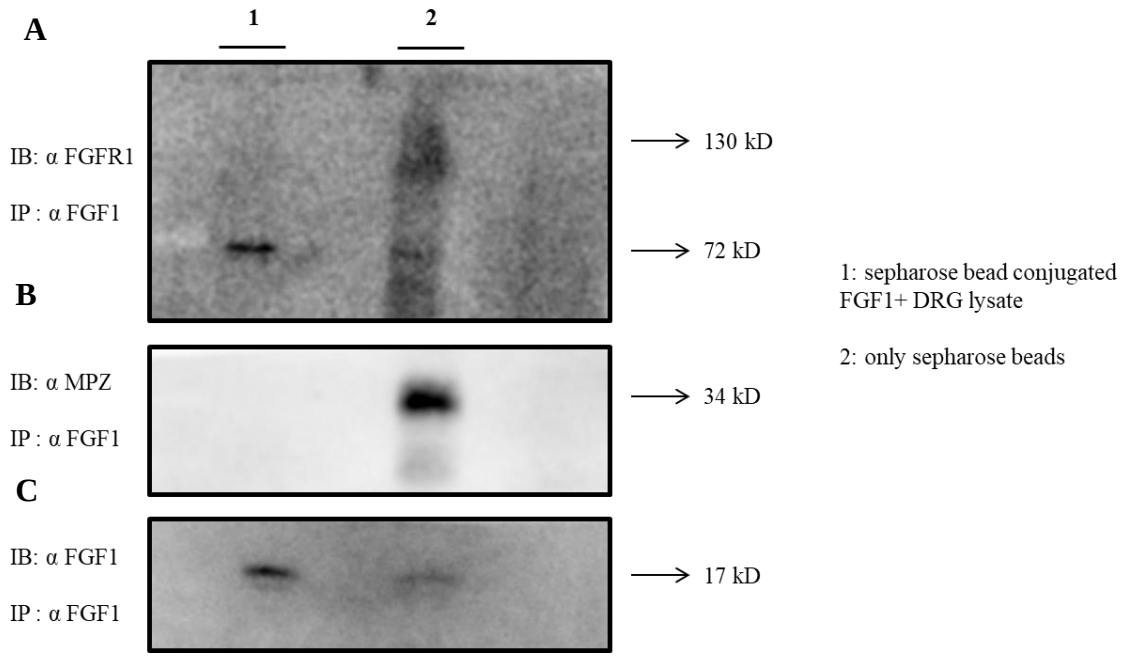

Figure 5.29. Immunoblot of DRG co-cultures that were immunoprecipitated with FGF1. A. Immunoblot with FGFR1 antibody, Co-IP with FGF1. B. Immunoblot with MPZ antibody, Co-IP with FGF1. C. Immunoblot with FGF1 antibody, Co-IP with FGF1.

In the second Co-IP analysis agarose beads were used. The beads were incubated with sc 7910 Rabbit anti FGF1 antibody to produce agarose bead-antibody bounded complex. Then, DRG lysates were incubated with antibody-bead complex overnight. Next day, FGF1 and possible proteins that interact with it were precipitated. For negative controls, agarose beads were incubated with DRG lysate without any incubation with antibody. Another negative control was the E13.5 liver lysate that was incubated with agarose bead-antibody complex. Co-IP samples were run on SDS-PAGE and stained with Coomassie blue. Signal was observed at 17 kD in the experimental group but not in the control groups. To check whether this band corresponds to FGF1, samples were run on SDS gel that was immunoblotted with Sheep anti FGF1 antibody. FGF1 was clearly precipitated in experimental group but not in controls (liver and only agarose) that was presented in Figure 5.30. Two different proteins- MPZ and FGFR1- were also assayed for western blot. FGFR1 gave a strong signal at 55 kD in 1st lane that harbors the agarose bead/ FGF1 antibody/DRG lysate group. It also gave a weak signal at 55 kD in 2nd lane that was our control group consisting of agarose bead/ FGF1 antibody/ E13.5 liver group. A signal was not recorded in

3rd group that was the second negative control consisting of only agarose beads/DRG lysates. When MPZ was checked with Rabbit anti MPZ, there was a signal that was not so strong in 1st lane but not 2nd and 3rd lane (Figure 5.30).

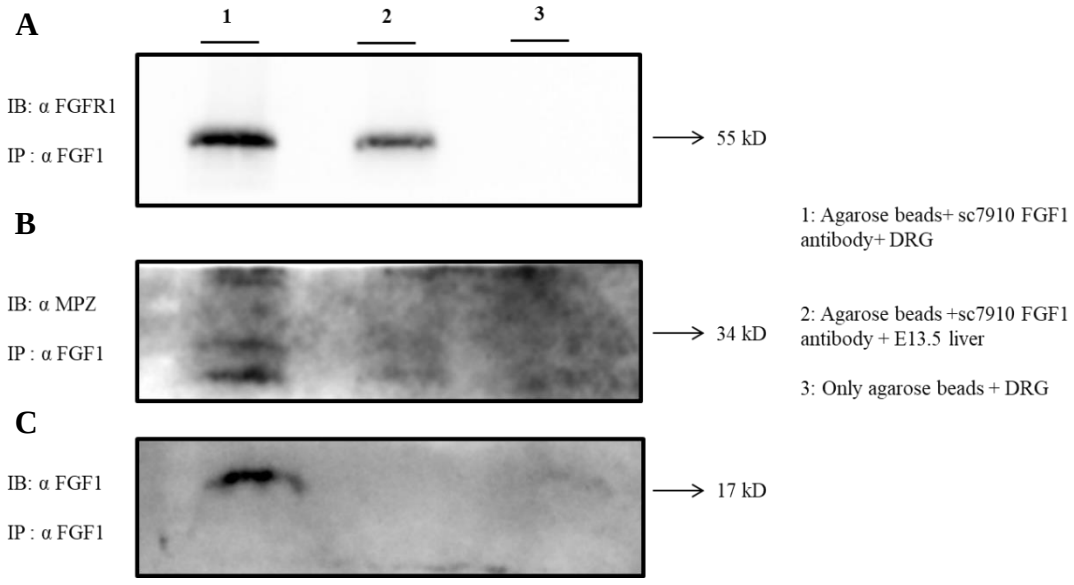

Figure 5.30. Immunoblot of DRG co-cultures that were immunoprecipitated with FGF1. A. Immunoblot with FGFR1 antibody, Co-IP with FGF1. B. Immunoblot with MPZ antibody, Co-IP with FGF1. C. Immunoblot with FGF1 antibody, Co-IP with FGF1.

Unfortunately, rabbit FGF1 antibody was used to produce agarose bead-antibody complex and the host of FGFR1 and MPZ antibodies were also rabbit. Therefore, a cross-reactivity was suspected since the secondary antibody- anti rabbit HRP- that were used to detect FGFR1 and MPZ antibodies in western analysis might have detected also FGF1 antibody that was used for Co-IP. To eliminate this possibility and to be sure that the signals were originally produced by proteins themselves and not from the antibody or cross-reactivity, samples and sc 7910 Rabbit anti FGF1 were run on SDS gel and incubated with anti-rabbit HRP (Figure 5.31).

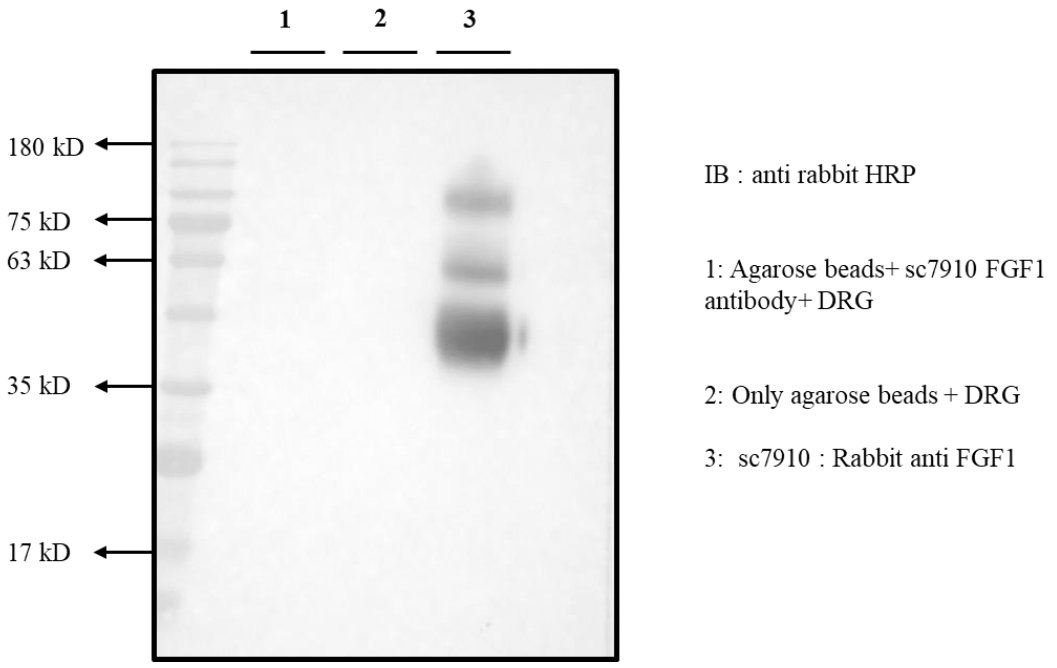

Figure 5.31. Immunoblot of Co-IP samples with anti rabbit- HRP. 1: experimental group-agarose bead FGF1 antibody complex incubated with DRG lysates. 2: only agarose beads were incubated with DRG lysates. 3: rabbit FGF1 antibody used for agarose bead antibody complex.

Incubating Co-IP samples- both control and experimental groups- with anti-rabbit HRP showed that signals that was observed from FGFR1 and MPZ were caused by real proteins not from the cross reactivity or FGF1 antibody. There were no signals from 1st and 2nd lane in Figure 5.31. Third lane showed the size of FGF1 antibody and it was not at the same molecular weight with FGFR1 and MPZ.

The results from Co-IP were inconclusive. FGF1 was surely precipitated from both agarose bead and sepharose bead experiments. FGFR1 was one of the proteins of interest, however, it was also found in negative control group- agarose bead/FGF1 antibody/liver complex although intensity of the band was more in experimental groups than in the control. MPZ was another protein of interest that gave a signal in experimental group when agarose bead was used for Co-IP. However, it gave strong signals in control groups when sepharose beads were used. Experimental repeats were performed for four times for each methods.

6. DISCUSSION

Bidirectional and continuous interactions between Schwann cells and axons are crucial for myelin during PNS development, maintenance and remyelination periods after injury. Disruption of this communication attributes to peripheral neuropathology, therefore, revealing the molecular pathways that underlie these bidirectional and continuous dialogs between Schwann cells and axon is fundamental for understanding the etiology of PNS disease. The aim of this project was to reveal the possible role of FGF1 that may be an axonal molecule and involved in both remyelination after LPC induced demyelination and peripheral myelination.

6.1. Optimization of 'LPC induced demyelination' model

Nerve transection and injury models are commonly used for PNS but they damage both axons and myelin. Therefore, it is crucial to optimize a model for PNS demyelinating disease for further analysis whereby myelin sheath is disrupted primarily while axons are preserved or degenerate secondarily due to loss of their protective myelin shield as in patients. 'LPC induced demyelination' is widely used and preferred model in CNS compared to other chemically induced demyelination models since it has a robust and rapid effect in myelin sheath. It also dissolves the myelin sheath primarily without disrupting axons. Therefore, in the scope of this thesis, this model is further optimized and the recovery of myelin sheath from LPC effect was demonstrated using mouse sciatic nerve. The effect of demyelination was still observable at day seven. The myelin sheath was partly dissolved and was highly disorganized. In CNS, LPC leads to complete disruption of myelin sheath and exerts this effect in a very short time period, about 24 hours after the injection. However, in our analysis, complete disruption of myelin sheath was not observed. Indeed, this observation was consistent with the myelin condition in CMT patients that present partial loss and disorganized myelin in their pathological samples. After injury, Remak SCs and myelinating SCs become elongated and give rise to repair SCs that are involved in axonal regeneration, removal of myelin debris and formation of regeneration track- bands of Bungner. Repair SCs express injury related genes like c-Jun and STAT3 unlike immature, Remak and myelinating SCs. During regeneration, repair SCs are transformed into re-myelinating SCs by shortening

(Gomez-Sanchez *et al.,* 2017). DAPI staining of sciatic nerve samples at day seven after LPC injections demonstrated some elongated nuclei and some shortened, rounded nuclei. Since remyelination was initiated around seven days after demyelination induced by LPC, these compressed nuclei may represent the re-myelinating SCs that were derived from the repair SCs. These nuclei may also represent fibroblast like cells, fibroblasts and macrophages that are known to be populated in peripheral nerves. To confirm that these nuclei belong to re-myelinating SCs, lineage tracing analysis that labels SCs during demyelination and remyelination periods should have been performed. The analysis of myelin sheath recovery at 14 days and a month after LPC injection demonstrated that myelin sheath was still partly missing and disorganized. Myelin sheath became more organized and recovered better at two months after LPC injection. Finally, it was recovered and strikingly organized in three months' time.

The effect of demyelination on myelin protein expression was shown to persist until 7 days after LPC injections. Both MAG and MBP levels were reduced compared to saline solution injected samples. After that point, the level myelin proteins started to increase and almost reached to normal at three months. Remyelination after injury is supposed to recover the myelin sheath to a certain extent that never reaches to the level of uninjured myelin. This conclusion was also confirmed in our model of 'LPC induced demyelination' by demonstrating that in three months' time myelin protein levels were almost close to that of uninjured sciatic nerves.

In this part of the project, the optimization of 'LPC induced demyelination' model was successfully performed and it was demonstrated that it can be used as PNS demyelinating disease model and to unravel the effect of different molecules on remyelination.

6.2. FGF1 Involvement in Remyelination after Demyelination Induced by LPC

The second aim of the study was to confirm the possible role of FGF1 in remyelination. This is achieved by injecting FGF1 to sciatic nerve during remyelination and studying its effect on expression of myelin proteins. When the sciatic nerves were first treated with LPC and then with 100 or even 200 μg/ml FGF1 and nerve samples were collected after eight

days, we observed that the level of myelin proteins were not affected compared to that of control group.

It is well known that FGF1 molecule has a transient and instant effect. Thus, by collecting samples after eight days, if there is any transient effect of FGF1 on myelin protein expression, we might not be able to observe that effect. In the light of this hypothesis, the experiments were repeated and this time the nerve samples were collected after 30 minutes of FGF1 injection. This approach demonstrated that the levels of myelin proteins were increased significantly almost by two folds upon injection of 100 μg/ml FGF1 compared to the controls. This finding suggested that FGF1 may have short term and immediate effect in myelin production during remyelination at 30 minutes after injection while its effect may cease during eight days period. Therefore, the levels of myelin proteins in both FGF1 and NaCl injected groups were observed similar after eight days.

Western analysis of FGF1 isolated after injections of LPC and FGF1 to the nerves showed that FGF1 injections were performed successfully and led to increase in FGF1 concentration. The level of FGF1 in FGF1 injected group was almost 7.5 fold more than in NaCl injected group when samples collected after 30 minutes of FGF1 injection were analyzed. When the FGF1 levels in two biological replicates were examined individually, we observed a difference even though both were injected with 100 μg/ml FGF1. The difference might be caused by differential amounts of FGF1 that reaches to the nerve during injections that can be accepted as an experimental error. The other possibility is that endogeneous FGF1 level may differ between these two experimental groups that might have affected the ultimate FGF1 level after injection. Another possibility is that LPC injection might have been more successful in one of the groups so that FGF1 level in that group was reduced more compared to the other group. In accordance with these suggestions, MAG and MBP expression were increased relative to FGF1 levels in each group of these two experiments. . The increase of MAG and MBP in the second group was also approximately 3.5 fold higher than the increase of those proteins in the first experimental group (Figure 5.22). For these analyses, only two experimental repeats were performed since these were assumed as biological repeats before FGF1 levels were determined.

The concentration of FGF1 to be injected to sciatic nerve to induce demyelination was determined by several injection trials of different concentration of FGF1 as 50, 100 and 200 μg/ml. The final concentration was chosen as 100 μg/ml for further analysis. It is also worth to mention that soluble NRG1 has concentration dependent bifunctional effect on myelination as it promotes myelination at lower doses and inhibits myelination at higher doses. Therefore, the effect of different concentrations of FGF1 on remyelination should be examined to see whether FGF1 may exert bifunctional effects depending on its concentration.

Several isoforms of MBP protein is known to be expressed in mouse PNS, however, only 21.5 kD isoform could be detected in FGF1 injection experiments and some of remyelination monitoring analysis. Absence of other isoforms might indicate the inefficiency of the antibody used in this analysis. Interestingly, recent studies in CNS demonstrated that the transcript level of 21.5 kD isoform of MBP is upregulated during early myelin development in human and mouse. The analysis in MS patient samples also showed that the expression of 21.5 kD isoform of MBP was increased during remyelination (Harauz *et al.*, 2013). In the light of these findings, it can be suggested that the expression of this isoform may be upregulated upon injury to myelin also in PNS. This isoform of MBP may have an active role in PNS remyelination as it has in CNS.

In the light of these findings we further confirmed that FGF1 may act as a promoter of remyelination after demyelination induced by LPC. Our findings that showed an increase in myelin proteins, namely MAG and MBP, upon FGF1 injections were in accordance with our previous findings which showed that FGF1 blockage during remyelination period reduced MAG and MBP levels.

6.3. DRG Co-culture and Co-IP

The third aim was to identify the possible proteins interacting with FGF1 during peripheral myelination. To reach this goal, DRG co-cultures were established and generated and FGF1 was immune-precipitated with its possible partners during myelination. Before Co-IP application, the presence of FGF1 in DRG co-cultures was confirmed with western blot analysis. The level of FGF1 in myelinated DRG lysates were significantly increased

compared to unmyelinated ones that further confirms the possible involvement of FGF1 in peripheral myelination.

E13.5 liver lysates were used as a negative control in Co-IP experiments since it was reported not to express FGF1. Accordingly, FGF1 was not detected in liver lysates incubated with bead-antibody complex. The second negative control was generated by incubating DRG lysates with agarose beads without FGF1 antibody and FGF1 was absent in Co-IP samples as expected. Since FGF1 may act through its receptors, possible FGFR-FGF1 interaction during peripheral myelination was suspected. When interaction between FGF1 and FGFR1 was tested, strong signals were observed in the experimental group. Unfortunately, we have also observed this signal in liver control groups though it was very weak. These experiments should be repeated for FGFR2 and FGFR3 receptors, too. Another protein that were suspected to interact with FGF1 during peripheral myelination was MPZ since it is known to be actively involved in myelination. MPZ was only detected in experimental groups not in negative controls for agarose bead experiments. On the other hand, in the experiments that is repeated with sepharose beads FGFR1 was found in only experimental group while MPZ was observed in only negative controls. Overall, because of presence of weak signals from negative controls, the results of Co-IP analysis remained inconclusive. However, the signals from FGFR1 was much stronger in experimental groups than in negative controls.

One interesting observation was that the FGFR1 molecular weight that was detected in our analysis was 55 kD although FGFR1 has 99 kD molecular weight. It is known that FGFR1 has a 55kD isoform in human but not in mouse from literature. Our findings suggest that 55 kD FGFR1 may also be expressed in mouse.

For further analysis, Co-IP experiment should be repeated for normal sciatic nerve in basal condition and LPC induced demyelination condition to check *in vivo* FGF1-protein interaction in peripheral myelination and in remyelination, respectively.

7. CONCLUSION

In the literature, reports were available that implicate the possible roles of FGFs in peripheral neuropathies. The role of FGF1 in CNS remyelination was more commonly elucidated than in PNS. To our knowledge, our laboratory is the first one that investigated the involvement of FGF1 in PNS myelination and remyelination. This study provided *in vivo* evidence for FGF1 to act in peripheral remyelination.

PNS does not have a model that can induce demyelination in short term without any disruption to axons. Optimization of 'LPC induced demyelination' model was successfully performed by monitoring its effect on myelin sheath for long time periods. Our study suggests that this model can be used for further analysis as a PNS demyelinating disease model.

FGF1 injection during remyelination helped recovery in the myelin protein expression that suggests this molecule as a therapeutical target in demyelinating disease. The study also contributed to identification of interacting partners of FGF1 during this process. The effect and the molecular pathways of these candidate partners, FGFR1 and MPZ, can be further investigated in future studies.

REFERENCES

Aguayo, A. J., J. Epps, L. Charron, G. M. Bray, 1976, *Multipotentiality of Schwann cells in cross-anastomosed and grafted myelinated and unmyelinated nerves: quantitative microscopy and radioautography*.

Armstrong, R. C., T. Q. Le, E. E. Frost, R. C. Borke, A. C. Vana, 2002, "Absence of fibroblast growth factor 2 promotes oligodendroglial repopulation of demyelinated white matter", *The Journal of neuroscience : the official journal of the Society for Neuroscience*, Vol. 22, No. 19, pp. 8574-8585.

Arter, J., M. Wegner, 2015, "Transcription factors Sox10 and Sox2 functionally interact with positive transcription elongation factor b in Schwann cells", *Journal of neurochemistry*, Vol. 132, No. 4, pp. 384-393.

Dong, Z., A. Brennan, N. Liu, Y. Yarden, G. Lefkowitz, R. Mirsky, K. R. Jessen, 1995, "Neu Differentiation Factor Is a Neuron-Glia Signal and Regulates Survival, Proliferation, and Maturation of Rat Schwann-Cell Precursors", *Neuron*, Vol. 15, No. 3, pp. 585-596.

Durso, D., P. J. Brophy, S. M. Staugaitis, C. S. Gillespie, A. B. Frey, J. G. Stempak, D. R. Colman, 1990, "Protein Zero of Peripheral-Nerve Myelin - Biosynthesis, Membrane Insertion, and Evidence for Homotypic Interaction", *Neuron*, Vol. 4, No. 3, pp. 449-460.

Eichberg, J., S. Iyer, 1996, "Phosphorylation of myelin protein: recent advances", *Neurochemical research*, Vol. 21, No. 4, pp. 527-535.

Filbin, M. T., F. S. Walsh, B. D. Trapp, J. A. Pizzey, G. I. Tennekoon, 1990, "Role of myelin P0 protein as a homophilic adhesion molecule", *Nature*, Vol. 344, No. 6269, pp. 871-872.

Galzie, Z., A. R. Kinsella, J. A. Smith, 1997, "Fibroblast growth factors and their receptors", *Biochem Cell Biol*, Vol. 75, No. 6, pp. 669-685.

Gardinier, M. V., P. Amiguet, C. Linington, J. M. Matthieu, 1992, "Myelin Oligodendrocyte Glycoprotein Is a Unique Member of the Immunoglobulin Superfamily", *J Neurosci Res*, Vol. 33, No. 1, pp. 177-187.

Gomez-Sanchez, J. A., K. S. Pilch, M. van der Lans, S. V. Fazal, C. Benito, L. J. Wagstaff, R. Mirsky, K. R. Jessen, 2017, "After Nerve Injury, Lineage Tracing Shows That Myelin and Remak Schwann Cells Elongate Extensively and Branch to Form Repair Schwann Cells, Which Shorten Radically on Remyelination", *Journal of Neuroscience*, Vol. 37, No. 37, pp. 9086-9099.

Haastert, K., E. Lipokatic, M. Fischer, M. Timmer, C. Grothe, 2006, "Differentially promoted peripheral nerve regeneration by grafted Schwann cells over-expressing different FGF-2 isoforms", *Neurobiology of Disease*, Vol. 21, No. 1, pp. 138-153.

Harauz, G., J. M. Boggs, 2013, "Myelin management by the 18.5-kDa and 21.5-kDa classic myelin basic protein isoforms", *Journal of neurochemistry*, Vol. 125, No. 3, pp. 334-361.

Jacob, C., P. Lotscher, S. Engler, A. Baggiolini, S. V. Tavares, V. Brugger, N. John, S. Buchmann-Moller, P. L. Snider, S. J. Conway *et al*, 2014, "HDAC1 and HDAC2 Control the Specification of Neural Crest Cells into Peripheral Glia", *Journal of Neuroscience*, Vol. 34, No. 17, pp. 6112-6122.

Jahn, O., S. Tenzer, H. B. Werner, 2009, "Myelin Proteomics: Molecular Anatomy of an Insulating Sheath", *Mol Neurobiol*, Vol. 40, No. 1, pp. 55-72.

Jessen, K. R., 2004, "Glial cells", *Int J Biochem Cell Biol*, Vol. 36, No. 10, pp. 1861-1867.

Jessen, K. R., R. Mirsky, 1999, "Schwann cells and their precursors emerge as major regulators of nerve development", *Trends in Neurosciences*, Vol. 22, No. 9, pp. 402-410.

Jessen, K. R., R. Mirsky, P. Arthur-Farraj, 2015, "The Role of Cell Plasticity in Tissue Repair: Adaptive Cellular Reprogramming", *Dev Cell*, Vol. 34, No. 6, pp. 613-620.

Kuroda, M., R. Muramatsu, N. Maedera, Y. Koyama, M. Hamaguchi, H. Fujimura, M. Yoshida, M. Konishi, N. Itoh, H. Mochizuki *et al*, 2017, "Peripherally derived FGF21 promotes remyelination in the central nervous system", *J Clin Invest*, Vol. 127, No. 9, pp. 3502-3515.

Ledouari.Nm, M. A. M. Teillet, 1974, "Experimental Analysis of Migration and Differentiation of Neuroblasts of Autonomic Nervous-System and of Neurectodermal Mesenchymal Derivatives, Using a Biological Cell Marking Technique", *Dev Biol*, Vol. 41, No. 1, pp. 162-184.

Love, S., 2006, "Demyelinating diseases", *J Clin Pathol*, Vol. 59, No. 11, pp. 1151-1159.

Lutz, A. B., W. S. Chung, S. A. Sloan, G. A. Carson, L. Zhou, E. Lovelett, S. Posada, J. B. Zuchero, B. A. Barres, 2017, "Schwann cells use TAM receptor-mediated phagocytosis in addition to autophagy to clear myelin in a mouse model of nerve injury", *Proceedings of the National Academy of Sciences of the United States of America*, Vol. 114, No. 38, pp. E8072-E8080.

Mehndiratta, M. M., N. S. Gulati, 2014, "Central and peripheral demyelination", *Journal of neurosciences in rural practice*, Vol. 5, No. 1, pp. 84-86.

Mierzwa, A. J., Y. X. Zhou, N. Hibbits, A. C. Vana, R. C. Armstrong, 2013, "FGF2 and FGFR1 signaling regulate functional recovery following cuprizone demyelination", *Neurosci Lett*, Vol. 548, No., pp. 280-285.

Mohan, H., A. Friese, S. Albrecht, M. Krumbholz, C. L. Elliott, A. Arthur, R. Menon, C. Farina, A. Junker, C. Stadelmann *et al*, 2014, "Transcript profiling of different types of multiple sclerosis lesions yields FGF1 as a promoter of remyelination", *Acta Neuropathol Com*, Vol. 2, No., pp.

Monk, K. R., M. L. Feltri, C. Taveggia, 2015, "New insights on schwann cell development", *Glia*, Vol. 63, No. 8, pp. 1376-1393.

Morell, P., H. Jurevics, 1996, "Origin of cholesterol in myelin", *Neurochemical research*, Vol. 21, No. 4, pp. 463-470.

Nave, K. A., H. B. Werner, 2014, "Myelination of the nervous system: mechanisms and functions", *Annual review of cell and developmental biology*, Vol. 30, No., pp. 503-533.

Newbern, J. M., 2015, "Molecular control of the neural crest and peripheral nervous system development", *Current topics in developmental biology*, Vol. 111, No., pp. 201-231.

Newbern, J., C. Birchmeier, 2010, "Nrg1/ErbB signaling networks in Schwann cell development and myelination", *Seminars in cell & developmental biology*, Vol. 21, No. 9, pp. 922-928.

Norton, W. T., S. E. Poduslo, 1973, "Myelination in rat brain: changes in myelin composition during brain maturation", *Journal of neurochemistry*, Vol. 21, No. 4, pp. 759-773.

Ooto, S., T. Akagi, R. Kageyama, J. Akita, M. Mandai, Y. Honda, M. Takahashi, 2004, "Potential for neural regeneration after neurotoxic injury in the adult mammalian retina", *Proceedings of the National Academy of Sciences of the United States of America*, Vol. 101, No. 37, pp. 13654-13659.

Parkinson, D. B., A. Bhaskaran, P. Arthur-Farraj, L. A. Noon, A. Woodhoo, A. C. Lloyd, M. L. Feltri, L. Wrabetz, A. Behrens, R. Mirsky *et al*, 2008, "c-Jun is a negative regulator of myelination", *Journal of Cell Biology*, Vol. 181, No. 4, pp. 625-637.

Parmantier, E., B. Lynn, D. Lawson, M. Turmaine, S. S. Namini, L. Chakrabarti, A. P. McMahon, K. R. Jessen, R. Mirsky, 1999, "Schwann cell-derived desert hedgehog controls the development of peripheral nerve sheaths", *Neuron*, Vol. 23, No. 4, pp. 713-724.

Pereira, J. A., F. Lebrun-Julien, U. Suter, 2012, "Molecular mechanisms regulating myelination in the peripheral nervous system", *Trends in Neurosciences*, Vol. 35, No. 2, pp. 123-134.

Quarles, R. H., 1997, "Glycoproteins of myelin sheaths", *J Mol Neurosci*, Vol. 8, No. 1, pp. 1-12.

Quintes, S., B. G. Brinkmann, 2017, "Transcriptional inhibition in Schwann cell development and nerve regeneration", *Neural Regen Res*, Vol. 12, No. 8, pp. 1241-+.

Raju, R., S. M. Palapetta, V. K. Sandhya, A. Sahu, A. Alipoor, L. Balakrishnan, J. Advani, B. George, K. R. Kini, N. P. Geetha *et al*, 2014, "A Network Map of FGF-1/FGFR Signaling System", *J Signal Transduct*, Vol. 2014, No., pp. 962962.

Rodriguez-Enfedaque, A., S. Bouleau, M. Laurent, Y. Courtois, B. Mignotte, J. L. Vayssiere, F. Renaud, 2009, "FGF1 nuclear translocation is required for both its neurotrophic activity and its p53-dependent apoptosis protection", *Bba-Mol Cell Res*, Vol. 1793, No. 11, pp. 1719-1727.

Shah, N. M., M. A. Marchionni, I. Isaacs, P. Stroobant, D. J. Anderson, 1994, "Glial Growth-Factor Restricts Mammalian Neural Crest Stem-Cells to a Glial Fate", *Cell*, Vol. 77, No. 3, pp. 349-360.

Smith, M. M., B. K. Hall, 1993, "A Developmental Model for Evolution of the Vertebrate Exoskeleton and Teeth - the Role of Cranial and Trunk Neural Crest", *Evol Biol*, Vol. 27, No., pp. 387-448.

Syed, N., K. Reddy, D. P. Yang, C. Taveggia, J. L. Salzer, P. Maurel, H. A. Kim, 2010, "Soluble Neuregulin-1 Has Bifunctional, Concentration-Dependent Effects on Schwann Cell Myelination", *Journal of Neuroscience*, Vol. 30, No. 17, pp. 6122-6131.

Taveggia, C., 2016, "Schwann cells-axon interaction in myelination", *Current opinion in neurobiology*, Vol. 39, No., pp. 24-29.

Taveggia, C., M. L. Feltri, L. Wrabetz, 2010, "Signals to promote myelin formation and repair", *Nat Rev Neurol*, Vol. 6, No. 5, pp. 276-287.

Theveneau, E., R. Mayor, 2012, "Neural crest delamination and migration: From epithelium-to-mesenchyme transition to collective cell migration", *Dev Biol*, Vol. 366, No. 1, pp. 34-54.

Waxman, S. G., J. M. Ritchie, 1993, "Molecular Dissection of the Myelinated Axon", *Ann Neurol*, Vol. 33, No. 2, pp. 121-136.

Weinberg, E. L., P. S. Spencer, 1979, "Studies on the Control of Myelinogenesis .3. Signaling of Oligodendrocyte Myelination by Regenerating Peripheral Axons", *Brain research*, Vol. 162, No. 2, pp. 273-279.

Woodhoo, A., M. B. D. Alonso, A. Droggiti, M. Turmaine, M. D'Antonio, D. B. Parkinson, D. K. Wilton, R. Al-Shawi, P. Simons, J. Shen *et al*, 2009, "Notch controls embryonic Schwann cell differentiation, postnatal myelination and adult plasticity", *Nat Neurosci*, Vol. 12, No. 7, pp. 839-U846.